DEVELOPMENT AND MECHANISTIC TRANSFORMATION OF
ANTIMICROBIAL AGENT-LOADED *IN-SITU* FORMING GEL AND
MICROPARTICLE USING EUDRAGIT RS AND ROSIN AS MATRIX FORMERS
FOR PERIODONTAL POCKET DELIVERY

By
MISS Tiraniti CHUENBARN

A Thesis Submitted in Partial Fulfillment of the Requirements
for Doctor of Philosophy PHARMACEUTICAL TECHNOLOGY
Department of PHARMACEUTICAL TECHNOLOGY
Graduate School, Silpakorn University
Academic Year 2021

การพัฒนาและกลไกการเปลี่ยนแปลงของตำรับเจลและไมโครพาร์ติเคิลก่อตัวเองบรรจุ
ยาต้านเชื้อแบคทีเรียโดยใช้ยูดราจิตอาร์เอสและยางสนเป็นสารก่อเมทริกซ์สำหรับนำส่ง
ยาทางร่องลึกปริทันต์

โดย
นางสาวถิรนิติ ชื่นบาล

วิทยานิพนธ์นี้เป็นส่วนหนึ่งของการศึกษาตามหลักสูตรปรัชญาดุษฎีบัณฑิต
สาขาวิชาเทคโนโลยีเภสัชกรรม แบบ 1.2 ปรัชญาดุษฎีบัณฑิต
ภาควิชาเทคโนโลยีเภสัชกรรม
บัณฑิตวิทยาลัย มหาวิทยาลัยศิลปากร
ปีการศึกษา 2564
ลิขสิทธิ์ของมหาวิทยาลัยศิลปากร

DEVELOPMENT AND MECHANISTIC TRANSFORMATION OF ANTIMICROBIAL AGENT-LOADED *IN-SITU* FORMING GEL AND MICROPARTICLE USING EUDRAGIT RS AND ROSIN AS MATRIX FORMERS FOR PERIODONTAL POCKET DELIVERY

By

MISS Tiraniti CHUENBARN

A Thesis Submitted in Partial Fulfillment of the Requirements
for Doctor of Philosophy PHARMACEUTICAL TECHNOLOGY
Department of PHARMACEUTICAL TECHNOLOGY
Graduate School, Silpakorn University
Academic Year 2021
Copyright of Silpakorn University

Title	Development and mechanistic transformation of antimicrobial agent-loaded *in-situ* forming gel and microparticle using Eudragit RS and rosin as matrix formers for periodontal pocket delivery
By	MISS Tiraniti CHUENBARN
Field of Study	PHARMACEUTICAL TECHNOLOGY
Advisor	Professor Thawatchai Phaechamud, Ph.D.

Graduate School Silpakorn University in Partial Fulfillment of the Requirements for the Doctor of Philosophy

....Dean of graduate school
(Associate Professor Jurairat Nunthanid, Ph.D.)

Approved by

....Chair person
(Professor Sontaya Limmatvapirat, Ph.D.)

....Advisor
(Professor Thawatchai Phaechamud, Ph.D.)

....Committee
(Associate Professor Prasert Akkaramongkolporn, Ph.D.)

....Committee
(Associate Professor GAYSORN CHANSIRI, Ph.D.)

....External Examiner
(Associate Professor Srisagul Sungthongjeen, Ph.D.)

58353801 : Major PHARMACEUTICAL TECHNOLOGY
Keyword : In-situ forming gel, In-situ forming microparticle, Phase separation,
Solvent exchange, Eudragit RS, Rosin

MISS TIRANITI CHUENBARN : DEVELOPMENT AND MECHANISTIC TRANSFORMATION OF ANTIMICROBIAL AGENT-LOADED *IN-SITU* FORMING GEL AND MICROPARTICLE USING EUDRAGIT RS AND ROSIN AS MATRIX FORMERS FOR PERIODONTAL POCKET DELIVERY THESIS ADVISOR : PROFESSOR THAWATCHAI PHAECHAMUD, Ph.D.

This research aimed to prepare and evaluate *in situ* forming gel (ISG) and *in situ* forming microparticle (ISM) containing antibiotics for periodontitis treatment employing Eudragit RS (ERS) and rosin (R) as the matrix forming agents. In addition, the underlying mechanism of the phase transformation of ISG and ISM were also investigated. Doxycycline hyclate (DH)-loaded ERS-based and vancomycin hydrochloride (V)-loaded R-based ISG and ISM were developed. ERS and R-based ISM showed advantages over ISG owing to its lower viscosity and ease of injection because of the lubricity effect from the external oil phase. Dimethyl sulfoxide (DMSO) was presented as a suitable solvent because of its higher polarity and less viscosity. Olive oil and camellia oil presented similar properties as the external phase of ISM and minimized the burst drug release with a lubricity effect promoting ease of injectability. Moreover, ISM presented a higher adhesion force than the ISG, indicating that ISM exhibited better attachment to the periodontal pocket. Furthermore, all of the R-based formulations exhibited plasticity properties; therefore, they could easily adapt to the specific shape of a patient's periodontal pocket. ISM exhibited a prolonged release of the antibiotic drug up to 20 hours for ERS-based and 7 days for R-based formulation using dialysis technique since the presence of outer oil phase retarded drug release. After contacting the aqueous environment, all formulas suddenly turned into solid-like. ERS-based ISG using 2-pyrrolidone (PYR) as solvent presented a smoother surface topography from SEM than that prepared using DMSO indicating that DMSO modified the structures of ERS matrix from its leakage and drug release thereafter generated more pores in a matrix structure. ISM appeared as a spherical shape with a smooth surface whereas cross-sectional topography revealed its porous structure. ERS and R-based ISG and ISM exhibited efficient antimicrobial activities against periodontal pathogens such as *Streptococcus mutans* and *Porphyromonas gingivalis*. Furthermore, computerized modeling using Gaussian software clarified these phase transitions and matrix formation. The molecule configuration of the matrix former and the drug were optimized, and binding energy was calculated molecularly in the gradient aqueous environment. R and ERS exhibited a similar trend of binding energy which was increased with the presence of water; thereafter, the complex molecules changed their position into more rigidity during the transformation process. V-loaded 40% w/w R-based ISM and DH-loaded 30%w/w ERS-based ISM exhibited the appropriate physicochemical properties and efficient antimicrobial activities as the localized antimicrobial periodontal pocket targeting. However, the safety of the developed ISMs should be further investigated such as cytotoxicity on gingival cells and the clinical study of their effectiveness should be also considered and tested.

ACKNOWLEDGEMENTS

TABLE OF CONTENTS

Page

LIST OF TABLES

LIST OF FIGURES

Page

LIST OF ABBREVIATIONS

%w/w	Percent weight by weight
%	Percent
®	Trademark
°	Degree
°C	Degree Celsius
±	Plus per minus
µg	Microgram(s)
µm	Micrometer(s)
A	Abeitic acid
cm	Centimeter(s)
cm^2	Square centimeter
cps	Centipoise
CO.,LTD.	Company Limited
DH	Doxycycline hyclate
DMSO, D	Dimethyl sulfoxide
ERS, E	Eudragit RS
$F_{adhesion}$	Adhesion force
$F_{max\ deformation}$	Maximum deformation force
$F_{remaining}$	Remaining force
g	Gram(s)
GMS	Glyceryl monostearate
h	Hour(s)
ISG	*In-situ* forming gel
ISM	*In-situ* forming microparicle
Log	Logarithm
Log P	Logarithm (base 10) of the partition coefficient (P)
mg	Miligram(s)
mm	Millimeter(s)
mN	Millinewton
min	Minute(s)
ml	Mililiter(s)
msc	Model selection criteria
N	Newton
NMP	*N*-methyl-pyrrolidone
PBS	Phosphate buffer solution
pH	Potetial hydrogenii (Latin); power of hydrogen
PYR	2-Pyrrolidone
r^2	Coefficient of detrmination
R	Rosin
rpm	Round per minute
sec	second(s)
SEM	Scanning electron microscope
S.D.	Standard deviation
UV/vis	Ultraviolet-visible
V	Vancomycin hydrochloride

CHAPTER 1
INTRODUCTION

1.1 Rational and problem statement

Nowadays, many humans suffer from chronic serious gum infections, especially periodontitis. The main pathogens of this disease are *Gram*-positive and *Gram*-negative bacteria including *Aggregatibacter actinomycetemcomitans, Porphyromonas gingivalis, Streptococcus sanguinis,* and *Streptococcus mutans* [1]. The effective treatment is mechanical cleaning teeth and oral antimicrobial therapy to stop periodontal ligament destruction [2]. However, systemic antibiotics have limited drug accessibility to the target site and various side effects. Therefore, local drug delivery systems have been developed [1]. *In-situ* forming gel (ISG) comprising 10 % doxycycline hyclate (DH) and 36.7 % poly-DL-lactide dissolved in 63.3 % *N*-methyl-2-pyrrolidone (NMP) in a pre-filled syringe is launched as a commercial product named Atridox® for eradication of bacteria in the periodontal cavity [3]. After injection at the target site, the phase separation caused by surrounding water leads to precipitation of polymer, and the drug is entrapped inside as a depot [4].

Nevertheless, ISG often shows an initial burst release [5]. To overcome this problem, *in-situ* forming microparticles (ISM) have been developed. The fabrication of the ISM system is obtained from the basic knowledge of non-aqueous emulsion. After contact with an aqueous environment, the internal phase of this emulsion becomes solid, forms into microparticles, and entraps the drug inside [6]. ISM shows more benefits in reducing the solvent toxicity owing to the presence of an external oil phase, easy injection through the needle, and retarding the drug release [6].

The crucial consideration for developing both ISG and ISM is the utilization of the material which forms into the aqueous insoluble matrix after exposing water. Eudragit RS (ERS) is a synthetic polymer used in pharmaceutical industries as a time-controlled coating material due to its aqueous insoluble property, low permeability, and pH-independent drug release [7]. In previous studies, ERS has been successfully formulated as a polymer of ISG comprising clove oil to deliver DH for periodontitis treatment [8]. Furthermore, increasing the amount of ERS showed a slow diffusion rate of both solvent and environmental water leading to retardation of the drug release [8]. Interestingly, rosin (R), a natural resin from pines, is composed of major abietic acid and minor nonacidic compounds [9] providing good encapsulating properties for controlled release drug delivery [10]. Furthermore, abietic acid exhibited antibacterial activities against *Gram*-positive bacteria such as *Staphylococcus aureus*, *Staphylococcus epidermidis* [11].

Nowadays, the mechanistic transformation of ISG and ISM into matrix and microparticles is described by the water-solvent exchange mechanism [6]. Upon injection into the target site, these systems become solidified by polymeric precipitation and encapsulation of the drug [12]. However, some parts of the solvent exchange mechanism are still unclear. There are no reports about the pathway of water diffusing through the external oil phase and inducing the solidification of the internal phase. Furthermore, the role of water and solvent on the polymeric precipitation process is inexplicit in which the computerized modeling of the transformation behavior of polymer/resin ISGs and the drug in the gradient amount of environment water for the researcher profoundly understanding of their mechanistic transformation after exposure to an aqueous phase.

The main aim of this present study is to develop of anti-microbial agent-loaded *in-situ* forming gel and microparticle using ERS and R as matrix formers for periodontal pocket delivery. Moreover, this investigation aims to study the mechanism of ISG and ISM transformation using computerized modeling for the behavior of polymer/resin which is the main component of both systems after contact with the environment water.

1.2 Objective of this research

1. To develop and evaluate doxycycline hyclate and vancomycin hydrochloride loaded ISG and ISM systems using ERS and R as the matrix formers for periodontitis treatment.

2. To investigate the mechanistic transformation of antimicrobial agent-loaded ISG and ISM using ERS and R as the matrix formers.

3. To apply the computerized modeling for investigating the transformation behavior of polymer/resin ISGs and the drug in the gradient aqueous environments.

1.3 The research hypothesis

1. ERS and R can be used as the matrix formers in local antimicrobial drug-loaded ISG and ISM systems for preparing local controlled-drug injection in periodontitis treatment.

2. Viscosity of internal and external phases is the crucial factor affecting the physicochemical properties and drug release of ERS and R ISG and ISM.

3. Both ISG and ISM prepared from ERS and R transform into the solid matrix by precipitation mechanism *via* phase separation and solvent exchange by pulling effect of the excess GMS in the oil.

CHAPTER 2
REVIEW OF RELATED LITERATURE

2.1 Periodontitis

2.1.1 Introduction to periodontitis

Periodontitis is a serious gum infection that damages the soft tissues and destroys the bone that supports the teeth which is a group of conditions with a multifactorial aetiology [13]. In the early stage, plaque accumulates in the area between the teeth, and the gums become inflamed and easily bleed during tooth brushing which are the signs of gingivitis [14]. Most of the patients diagnosed with gingivitis, which is the reversible stage of gum disease, with poor oral hygiene will easily progress to periodontitis. When periodontitis develops, the inner layer of the gum and bone pull away from the teeth and form pockets. These gaps between teeth and gums collect debris and bacteria which lead to infected [15]. At this advanced stage of gum disease, teeth are no longer anchored in the sockets and become lost. The symptoms of periodontitis include continued red, swollen, or bleeding gums, pain when chewing, poor tooth alignment, receding gums, and clear pockets between teeth and gums [13, 14, 16]. Normally, the severity of periodontitis disease was characterized by alveolar bone loss with the pocket formation and gingival recession [17] which has been classified into several categories including gingivitis, moderate periodontitis, advanced periodontitis, and periodontitis as a manifestation of systemic diseases [1, 17]. The periodontal pocket depth was measured in millimeters (mm) using a periodontal probe. The pocket with 1-3 mm depth is classified as normal and healthy gum, while a depth of more than 3 mm is revealed the gum disease[18, 19]. According to the risk of systemic infection from periodontitis disease, recent evidence suggests that periodontal infection may significantly enhance the risk for some systemic diseases including coronary heart diseases (CHD) and CHD-related events such as angina and infarction, atherosclerosis, stroke, diabetes mellitus, and respiratory conditions such as chronic obstructive pulmonary diseases [14].

The worldwide prevalence of periodontitis disease was reported by WHO that 15-20% of middle-aged adults (35-44 years) suffer from periodontitis and most children and adolescents showed signs of gingivitis [20]. Similar results were also found in Thailand from the survey of the department of health in 2012. Middle-aged and old adults suffer from periodontitis with a periodontal pocket depth of more than 6 mm [21] as shown in Figure 1. However, the exact mechanism underlying this disease is not clearly understood. It is hypothesized that the suspected periodontitis pathogens produce biologically active molecules, which directly attack the host tissue and/or that the immune response of the host to these pathogens results in tissue destruction [22].

Figure 1 Advanced periodontitis disease with a periodontal pocket depth of more than 6 mm [23]

2.1.2 Cause of periodontitis

The major cause of periodontitis is the plaque which is generated from the bacteria plus mucus and other particles in the mouth [1, 22]. These bacteria will constantly form a sticky colorless plaque on teeth. The plaque that is not removed can harden and form calculus which can only be cleaned by a dentist or dental hygienist. This tartar will be allowed the sore, gum bleeding, painful chewing problems, and even tooth loss [24]. Moreover, the toxins produced by the bacteria in plaque or tartar induced the immunogenic enzymes involved in fighting infections which results in weakening and breaking down bone and collective tissue that hold teeth in place. The pockets deepen and even more gum tissue and bone are destroyed [14, 16]. The bacteria which cause the periodontitis can be the gram-negative or gram-positive bacteria and most of them are anaerobe or facultative anaerobe bacteria owing to the depth of periodontal pocket such as *Aggregatibacter actinomycetemcomitans, Porphyromonas gingivalis, Streptococcus sanguinis, Streptococcus mutans* [1, 2, 4]. In addition, several risk factors caused gum disease, but smoking is the most significant. Cigarette smoking can make treatment for gum disease less successful and also suppressed the sign of gingivitis, because of the vasoconstriction and enhanced gingival tissue keratinization [13-16]. Other risk factors include diabetes, medications that lessen the flow of saliva, certain illnesses, such as AIDS, and their medications, and genetic susceptibility [13, 15, 16].

2.1.3 Treatment

To treat periodontitis, the removal of debridement from teeth by scaling and the reduction of risk factors, followed by daily home care are the first lines of treatment which can be classified into two groups.

2.1.3.1 Non-surgical therapy

This therapy consists of the removal of dental plaque and calculus with scaling and root planing by using hand scalers and/or ultrasonic instruments which required less time and cause less soft tissue trauma. To enhance treatment outcomes, several adjuncts to non-surgical therapy have been proposed. These include local drug delivery systems, systemic antibiotics, and systemic host modulation agents.

2.1.3.1.1 Local drug delivery

The drugs include antibiotics, such as minocycline and doxycycline, or antimicrobial such as chlorhexidine, that are delivered directly to the periodontal pocket using a powder, gel, chip, fiber, microspheres, and *in-situ* forming gels [2, 4, 25] delivery system for localized treatment.

2.1.3.1.2 Systemic antibiotics

Several regimens that vary in antibiotic type, dosage, duration, and timing of initiation have been proposed; typically, a broad-spectrum antibiotic is used either alone or in combination with antibiotic targeting such as tetracycline group, amoxicillin, macrolides group, and ciprofloxacin [26]

2.1.3.1.3 Systemic host response modulation

The sub antibiotics dose of doxycycline in the combination of scaling and root planning provided a defined but limited improvement in periodontitis status which is beneficial for patients with increased susceptibility. The drug inhibited the matrix metetalloproteinases with does not have systemic anti-microbial properties [16]. However, these non-surgical treatments have some limitations such as serious undesirable side effects from antibiotics, antibiotic resistance problems, local irritation, undesired burst release, and solvent toxicity [27].

2.1.3.2 Surgical therapy

The regenerative surgery using tissue regeneration was used to regenerate the lost tissue and reduce the depth of the periodontal pocket. Laser-assisted new attachment procedure (LANAP) has been recently introduced as a conservative alternative to surgical therapy. LANAP used a Nd:YAG laser for the initial pocket de-epithilialization and final fibrin clotting instead of a scalpel and sutures, and does not include extensive gingival flap elevation [16].

2.1.3.3 Others

Recently, vaccination against periodontal disease has been tested in mouse models. The results suggested that it could be possible to vaccinate against *P. gingivalis* infection and the immunological protection could manifest through alteration of the T_H17-T_{reg} cell balance [28]. Moreover, Tissue engineering using the novel periodontal therapies has incorporated gene-based, protein-based, and cell-based tissue regeneration approaches coupled with scaffolding and guiding biomaterial. 3D printing is used to approach on regenerating bone to stabilize teeth or implants [29, 30].

2.1.4 Gingival crevicular fluid (GCF)

Gingival crevicular fluid (GCF) is an exudate derived from the periodontal tissues. It is composed of substances derived from serum such as tissue breakdown products, inflammatory mediators, and immunomodulators against dental plaque bacteria, leukocytes, and structural cells of the periodontium and oral bacteria [31]. In the healthy gum sulcus, the amount of GCF is very less around 0.02-0.1 µl [32] and increases when the inflammation occurs [31]. The increased GCF flow contributes to host defense by flushing bacterial colonies and their metabolites away from the sulcus. Several factors can stimulate the flow of GCF, including pocket depth, gingival inflammation, mobility, periodontal surgery, enzymes, sex hormones, contraceptives, and smoking [31, 33]. This fluid can be used as a biomarker to identify the various stages of periodontal disease [33]. Numerous studies suggest that interleukin-1 beta (IL-1β), IL-2, IL-6, IL-8, IL-17, and tumor necrosis factor-alpha (TNF-α) are reliable inflammatory biomarkers in patients with periodontal disease [33].

2.2 *In-situ* biodegradable system

2.2.1 *In-situ* forming gel

In-situ forming gel (ISG), a liquid polymer formulation, will be transformed into solid or gel when contacted with the biological fluids *via* different mechanisms such as solvent exchange, thermally induction, and pH-induction [4, 34]. These systems contain biodegradable polymers including the drug dissolved in an organic solvent for example *N*-methyl-2-pyrrolidone (NMP), dimethyl sulfoxide (DMSO), 2-pyrrolidone (PYR), and ethyl acetate [2, 35]. After injection at the target site, the phase separation caused by surrounding water leads to the precipitation of polymer, and the drug is entrapped in a depot. Some research using ISGs to deliver the drug to the target site such as 5% w/w doxycycline hyclate (DH)-incorporated in Eudragit RS with clove oil (CO) dissolved in NMP was prepared as ISG system for periodontitis disease and evaluated for their fluid properties. The higher weight percentage of Eudragit RS and CO enhanced the viscosity of the prepared formulation. In addition, the presence of a high amount NMP leads to rapid transformation since the miscibility properties of NMP and water whereas higher CO amount retarded the phase transition. Moreover, ISG exhibited a plastic deformation which is suitable to adjust the shape to a specific periodontal pocket, and efficiently inhibited the test bacteria and fungi [36]. Borneol, which is low aqueous solubility and present as biological safety, was also used as the gel matrix for crevicular pocket targeting. The contact angles of the borneol ISGs increased after being in contact with the agarose gel or the bulging tissue of porcine due to the phase inversion. High concentration borneol rapidly formed a crystal matrix and sustained the drug release with a diffusion-controlled release mechanism. Moreover, the vancomycin HCl-loaded borneol-based ISM is a potentially effective local anti-solvent-based ISM for periodontitis treatment *via* crevicular pocket injection [37]. The DMSO removal-based ISGs of Eudragit®L (EL) transformed into an opaque gel after exposure to simulated crevicular fluid and modulated the DH release for longer than 3 days. Increasing the amount of EL resulted in a lower cumulative drug release owing to a thicker gel barrier. Thus, DH release depended on the amount of EL loading and corresponded with the polymeric matrix formation. The DH-loaded *in situ* solvent removal-based EL/ DMSO forming gels presented the efficient antimicrobial activities against *Staphylococcus aureus, Escherichia coli, Candida albicans and Porphyromonas gingivalis* [38]. ISG allows for reduced drug dose at the periodontal pocket and easily administers the drug to the target site. However, drug release from ISG often shows an initial burst release [2, 5]. To reduce unpredictable release patterns, increasing the polymer concentration results in more retardation of drug release owing to higher viscosity; nevertheless, leading to use the of large needle size for injection resulting increase in injection pain and decrease patient compliance [39]. Therefore, the recommended gauge needles used in dentistry are 25, 27, and 30 gauges [5], and the injection force is not more than 50 N [40].

2.2.2 *In-situ* forming microparticles

In-situ forming microparticles (ISM) is developed using the basic knowledge of non-aqueous emulsion consisting of non-aqueous droplets containing drug dissolved in

a polymeric solution dispersed in an external oil phase. After injection and contact with an aqueous environment of physiological fluid, the internal phase of an emulsion becomes to solidify, forms into ISM with solvent exchange mechanism, and entraps the drug inside [6]. ISM emulsions can be prepared by using the high shear forces of probe sonication to generate ready-to-inject formulation or by using the two-syringe connector method for preparing prior-to-inject formulation by back and forth movement of syringe plungers [34]. Due to the presence of the external oil phase, ISM shows the advantages over high viscous ISG in reducing the initial burst release and myotoxicity from solvent toxicity. Moreover, ISM exhibits an easy injection through the needle and retards the drug release [6]. However, ISM presents less stability owing to the high surface free energy of emulsion droplets. To stabilize the formulation, glyceryl monostearate (GMS) was obtained to improve the stability of poly(D,L-lactide-co-glycolide) (PLGA) solution in vegetable oil. GMS formed a birefringent layer at the interface between PLGA solution droplets and the oil phase which there was no phase separation over 1 hour while the other stabilizers did not inhibit the phase separation under 15 min[39]. Sucrose acetate isobutyrate (SAIB) and PLGA were used alone or in the combination to prepare long-acting injectable rivastigmine (RV) by using sesame oil containing sorbitan monostearate (2.5% w/w) as stabilizer. This ISMs can extend the rivastigmine in in-vitro drug release for a period of one month. Furthermore, the results in *in-vivo* revealed that subcutaneous (SC) and intramuscular (IM) injections of ISM formulations had a longer half-life than RV-solution and the C_{max} was also minimized owing to the decrease of burst release [41]. Bleached shellac (BS), a water-insoluble polyester resin, was dissolved in three different solvents such as *N*-methyl pyrrolidone (NMP), dimethyl sulfoxide (DMSO) and 2-pyrrolidone (PYR) as the internal phase of ISM. Olive oil comprising GMS was used as the external oil phase. All prepared emulsions exhibited pseudoplastic flow and low syringeability force. Moreover, PYR exhibited the slow transformation from emulsion into microparticles owing to the slower solvent exchange of this solvent which promoted a less porous structure of obtained BS matrix microparticles. The system containing PYR exhibited a higher degradability than that prepared with DMSO owing to the softness characteristics of the microparticles [42]. Beta-cyclodextrin (β-CD) was another substances which was studied as the matrix former for ISM system. The stable emulsion was obtained when the internal phase containing 5% w/w DH with 35% w/w β-CD dissolved in NMP and the external phase containing 7.5% w/w GMS dispersed in olive oil. The transformation from emulsion into a DH-loaded β-CD micro-particle was rapid after contact with a simulated crevicular fluid [43]. Meloxicam (Mex)-loaded-β-CD ISG and ISM were prepared using β-CD in DMSO as the internal phase and camellia oil comprising 5% GMS as the external phase. The highly concentrated β-CD in ISG

promoted the rapid phase inversion of β-CD aggregates into matrix-like. Upon exposure to aqueous phase, the ISM system comprising 40% β-CD transformed into microparticles and extended the drug release to 7 days with minimized an initial burst release following Fickian diffusion. The high viscous character of β-CD initiated the slow diffusion rate of the solvent from the ISM system [44].

Furthermore, the safety of ISG and ISM formulations was investigated by using the rodent skeleton muscle model in an *in-vitro* experiment to observe the level of creatinine kinase which is the muscle damage titer. Additionally, the *in-vivo* CK levels were also observed by the intramuscular injection (IM) of both ISG and ISM formula into male Sprague Dawley rats. In this research, PLA and PLGA were chosen as the matrix former, and three universal solvents which are usually in ISG and ISM systems (NMP, DMSO, and PYR) were studied as the internal solvents for the polymer and the drug since their LD_{50} was greater than 2ml/kg. The results of the effect of solvents presented the same trend in cumulative CK levels which PYR<DMSO<NMP. Additionally, increasing the amount of oil phase (peanut oil with pluronic 68 exhibited low CK levels, where the ratio 1:4 and 1:10 of internal phase: external phase showed a similar CK level which nearly presented the same CK level as 0.9% NaCl. The ISM revealed the significant advantages in myotoxicity over the ISG, the 1:2 ratio of ISM reduced the CK levels for 2 times compare to ISG [34]

2.3 Formulation parameters
2.3.1 Matrix former
2.3.1.1 Eudragit RS PO

Eudragit RS PO (ERS) is a powder of synthetic copolymer (Figure 2) prepared by polymerization of methyl acetate, methyl methacrylate, and low content of methacrylic acid ester with quaternary ammonium group. The presence of the quaternary ammonium group indicates as salts and makes the polymer permeable [7, 45]. In general, ERS is used as a time-controlled release of active ingredients due to insoluble properties, low permeability, and pH-independent drug release [7, 46, 47]. In previous studies, ERS has been formulated in microballoons by evaporation method of non-aqueous emulsion to deliver propranolol HCl. ERS microballoons showed a biphasic released pattern owing to initial burst release followed by retarded release [47]. The formulated ISG using ERS as a polymer comprising clove oil was developed to deliver DH for periodontitis treatment. Clove oil significantly reduced the burst release of the drug. Additionally, increasing the amount of ERS can reduce the diffusion rate of organic solvent and environmental water leading to minimizing the initial burst drug release [8]. Increasing the amount of ibuprofen in pellet containing ERS decreased the elastic modulus. Nevertheless, the types of Eudragit did not affect the elastic properties [48].
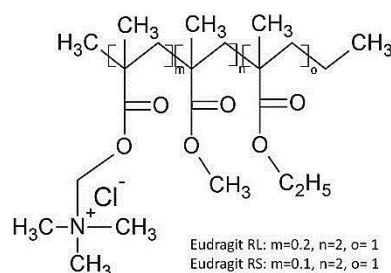
Figure 2 Structure of Eudragit RS

2.3.1.2 Rosin

Rosin (R) or colophony is a natural product obtained from pines (*Pinus palustris* or *Pinnus line*) which contains abietic acid as the main structure and a small number of nonacidic compounds (Figure 3) [9]. In pharmaceutical applications, rosin showed good film-forming and coating properties for enteric-coated drug delivery systems due to its ester bonds [9]. Being a natural material, rosin provides biodegradable properties, and non-toxic and biocompatibility features [49]. Furthermore, abietic acid presents the antibacterial activity against gram-positive bacteria such as *S. aureus*, and *Staphylococcus epidermidis* and provides a low effective antibacterial against the resistant streptococci and enterococci. However, it has no antibacterial effect against gram-negative bacteria [11]. Rosin exhibits good encapsulating property for controlled release drug delivery of tablets thus various drugs should be incorporated [10].
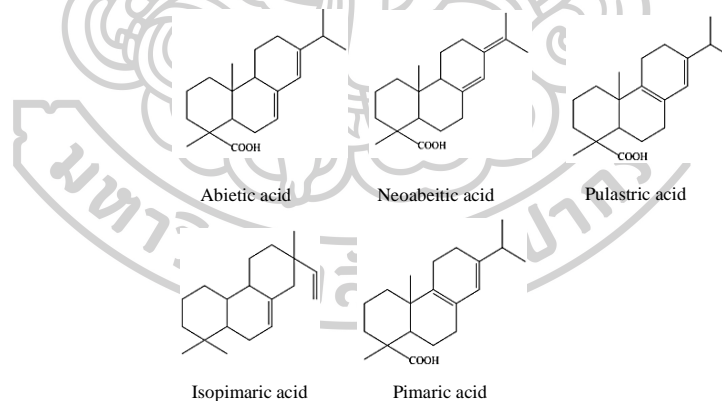
Figure 3 Compounds typically found in rosin

2.3.2 Solvents

2.3.2.1 Dimethyl sulfoxide (DMSO)

Dimethyl sulfoxide (DMSO), $(CH_3)_2SO$ as shown in Figure 4, is an organosulfur compound that is miscible to water and organic solvents. It is a polar aprotic solvent with a high boiling point and a melting point of 189°C and 19°C, respectively. At room temperature, DMSO generally presents a colorless liquid [50, 51]. It is safe for humans with LD50 of 14,500 mg/kg in rats [52]. In pharmaceutical applications, DMSO was used as a topical penetration enhancer without destroying the integrity membranes [53] which is not rapidly penetrate either the nail or the enamel of

the tooth [54]. It has been reported that DMSO is bacteriostatic in 20 percent concentration against *Escherichia coli*, *Staphylococcus aureus,* and *Pseudomonas* spp [55]. Moreover, various research use DMSO as the vehicle in *in-situ* forming implant formulation such as the solvent for PLGA [39], bleached shellac [25], and poly(d,L-lactide) (PLA) [34].
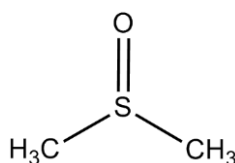
Figure 4 Dimethyl sulfoxide (DMSO)

2.3.2.2 *N*-methyl1-2 pyrrolidone (NMP)

N-methyl1-2 pyrrolidone (NMP) is an organic compound with a 5-membered lactam structure (C_2H_9NO) as shown in Figure 5. This chemical structure presents a planar non-polar region which possibly leads to hydrophobic interactions [56]. NMP is miscible to various organic compounds such as ethyl acetate, chloroform, and benzene and also high polar solvent such as water. The melting point and boiling point of NMP are -24˚C and 202-204˚C, respectively. It is colorless to slightly yellow with a faint amine odor. Other properties of this organic vehicle include low volatility, low flammability, and low toxicity (LD50 3,914 mg/kg in rats) [57]. According to biodegradability, NMP was widely used in pharmaceutical applications as a penetration enhancer in transdermal products [58] and a polymer-solvent in *in-situ* forming implants [5, 34].
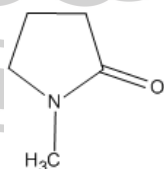
Figure 5 *N*-methyl1-2 pyrrolidone (NMP)

2.3.2.3 2-pyrrolidone (PYR)

2-pyrrolidone (PYR), C_4H_7NO is a chemical compound with five-membered ring lactam as shown in Figure 6 that presents a high-polar property, allowing it to be miscible with a variety of solvents such as water and common organic solvents, but not with aliphatic or cycloaliphatic hydrocarbons [59]. 2-Pyrrolidone has amphoteric properties, it forms salts with hydrogen chloride, hydrogen bromide, and alkalis [59] The melting point and the boiling point of this solvent are at 25˚C and 245˚C respectively, Its apparent is a colorless to slightly yellow liquid with an unpleasant ammonia-like odor above 25˚C. It has no teratogenic effect, no carcinogenicity, low

toxicity (LD50 3,288 mg/kg in rat), low acute toxicity in mammals with oral, and slight irritation at injection sites, Nevertheless, the derivative of PYR has been reported the skin irritation is low [60]. In pharmaceutical research, PYR is used as a solubilizing enhancer, penetration enhancer on transdermal drug delivery [61], and solvent in ISG and ISM [5].
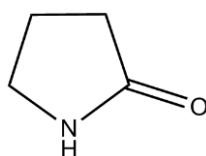
Figure 6 2-pyrrolidone (PYR)

2.3.3 Drug

2.3.3.1 Doxycycline hyclate (DH)

Doxycycline hyclate (DH), broad-spectrum antibiotic in the tetracycline group, is an effective drug for use in periodontitis disease to get rid of bacteria after treatment of scaling or root planing (SRP). The structure of DH is shown in Figure 7. Furthermore, oral low dose DH can dramatically reduce the inflammation of the gum [62]. Although DH is active against a range of both gram-positive and gram-negative aerobic and anaerobic bacteria, this drug should be considered first-line therapy for odontogenic infections. Gastrointestinal disturbances are common side effects of the use of the tetracycline group, and hypersensitivity reactions such as skin rash and drug fever can occur. The use of tetracyclines in children under 13 years of age and pregnant women is contraindicated due to the risk of tooth discoloration and interference with bone development [63]. To overcome this problem, the local DH delivery has been developed. It has been launched in the market as a commercial product such as Atridox® which contains DH in a pre-filled syringe *in-situ* forming gel (ISG) system [3]. Atridox® containing 10 % DH in 36.7 % poly-DL-lactide dissolved in 63.3 % *N*-methyl-2-pyrrolidone (NMP) allows for controlled release of DH for 7 days [3, 62]. Moreover, it has been reported that treatment of periodontitis using a DH-loaded delivery system for 4 months can significantly reduce the depth of the periodontal pocket which is equally effective as SRP [64].
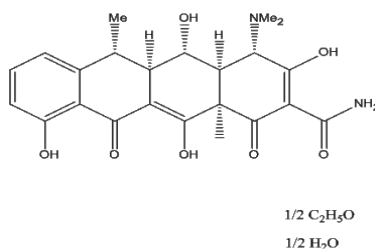
Figure 7 Structure of doxycycline hyclate

2.3.3.2 Vancomycin hydrochloride (V)

Vancomycin hydrochloride (V), a glycopeptide antibiotic, as shown in Figure 8 is used to eradicate methicillin-resistant *Streptococcus aurues* (MRSA), multidrug-resistant *Streptococcus epidermidis* (MRSE). Systemic vancomycin has potentially serious side effects but topical formulation has no adverse effects [65, 66]. It has been reported that 1% vancomycin oral paste applied to periodontal patients after the removal of periodontal dressing can reduce plaque scores and gingivitis [65]. Moreover, vancomycin ointment significantly reduced the redness of the gum and also reduced the amount of plaque when compared to placebo [66]. In contrast, some studies have reported that there is no significant reduction of the inflammation in gingivitis in patients with non-oral hygiene [67]. Vancomycin also has a good effect against *Enterococcus faecalis* which is the facultative gram-positive pathogen found in the subgingival tooth of chronic periodontits patients [68]. In addition, the 3% vancomycin gel was applied as the local oral treatment to the children aged 9-11 years for treating the *Streptococcus mutans* infection since the drug cannot absorb through the alimentary mucosa; thus, the systemic side effects are precluded [69].
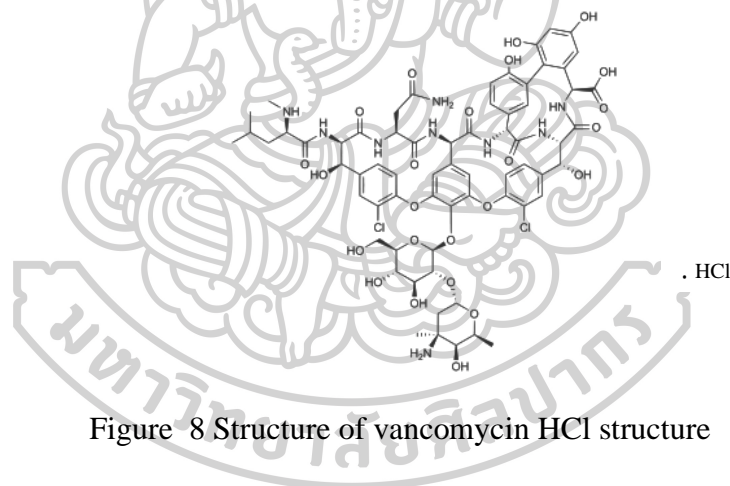
Figure 8 Structure of vancomycin HCl structure

2.3.4 Oils

2.3.4.1 Olive oil

Olive oil (O) (Figure 9) is a nutrient vegetable oil obtained from pressing the whole olives. Normally, it is used in Mediterranean foods with many health benefits such as reducing cholesterol, anticancer and antioxidant activities [70]. Owing to strong antioxidant activity, topically olive oil can reduce skin tumors from UV-B and DNA damage in mice [71]. Additionally, olive oil has been used as traditional medicine for the treatment of gum disease by using one tablespoon for 15-20 min as a mouth rinse to reduce the plaque and prevent the gum bleeding because of nourishing and anti-inflammatory activities [72]. Furthermore, some studies reported that olive oil pulling minimized *S. mutans,* and oil massage disrupted the bacterial biofilms in the oral cavity [73]. In pharmaceutical research, olive oil has a lubricating effect which benefits the

injected formulations. Olive oil comprising GMS was used as an external oil phase of ISM which exhibited more advantages than ISG for reducing viscosity and being suitable for local injections due to pseudoplastic flow [74].
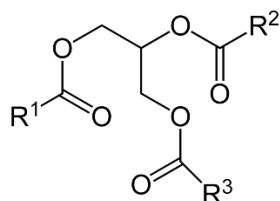
Figure 9 The structure of olive oil, R1 = oleic acid, R2= linoleic acid, and R3= palmitic acid

2.3.4.2 Camellia oil

Camellia oil (C) or tea seed oil is edible oil achieved from cold-pressed *Camellia oleifera* fruit. This natural oil contains unsaturated oleic acid and high vitamin E with health promotion such as lowering blood pressure, cholesterol and triglyceride levels. It has been widely used as anti-aging in skincare products owing to its high antioxidant activity [75, 76]. C presents rich oleic acid indicating effective inhibition of a spontaneous metastasis of melanoma cells in mice through intraperitoneal injection [77]. Additionally, C also showed antimicrobial activities against *Escherichia coli, Bacillus cereus*, and *Candida albicans* [78] and anti-inflammatory *via* reducing the production of prostaglandin E_2 and nitric oxide [79].

2.3.5. Glyceryl monostearate (GMS)

Glyceryl monostearate (GMS) (Figure 10) is an organic molecule. The physical appearance of GMS includes colorless, odorless, and sweet-tasting flaky powder. It has been used in food additive, cosmetics, and controlled drug delivery system. GMS is lipophilic non-ionic surfactant with HLB 3.6-4.2 that can improve the physical stability and injectability of ISM based on PLGA to be stable for 12 h [39].
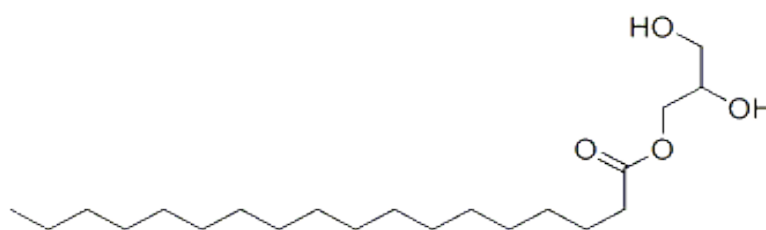
Figure 10 Glyceryl monostearate (GMS)

2.4 Evaluations

The concept of evaluation methods in this research had been introduced in chapter 4 before describing the result and discussion, However, some particular characterizations such as mechanical properties and computer modeling require intensive basic knowledge to interpret the complicated data efficiently.

2.4.1 Mechanical analysis

2.4.1.1 Injectability test

Injectability property is investigated by using texture analyzer (TA.XT plus, Stable micro system, UK) in compression mode to simulate the force which humans use for expelling the formulation through the needle at room temperature. The maximum force (N) is selected for analysis and area under the curve (AUC) is used for determining the work of expulsion. The force less than 50N is acceptable as an injectable formulation [40].

2.4.1.2. Adhesion properties studies

The adhesion properties is used to describe the attachment force of the formulation with the surface. This property is investigated by using agarose gel with the well simulating a human periodontal pocket. The formulation is filled in the well and let it transform completely into solid. The transformed formulation is evaluated by using a texture analyzer (TA.XT plus, Stable micro system, UK) in compression mode with hold until time. The probe moves downward and penetrates through the transformed formulation. The applied force and displacement of the probe is determined as a function of time. This position is held for 60s, after that the probe is driven upwards. The maximum deformation force ($F_{max\ deformation}$) is measured at maximum force when the probe penetrates into the transformed formulation, The force after holding for 60s is remaining force ($F_{remaining}$) and the adhesion force is defined as the maximum force measured during the upward movement of the probe, which is negative direction of the force ($F_{adhesion}$). The ratio $F_{remaining}/F_{max\ deformation}$ is used as the measured of elasticity/plasticity. High value indicates high elasticity whereas low value indicates high plasticity. Each experiment is conducted in triplicate and the results are presented in mean value ± S.D [80].
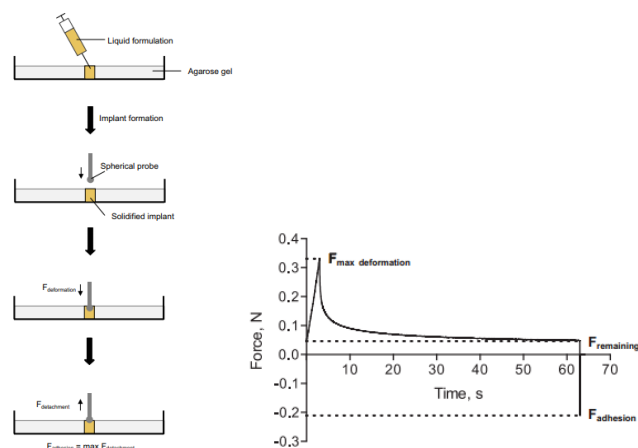
Figure 11 Adhesion properties study (A) Preparation of the transformation matrix (B) Graphical of deformation force, remaining force, and adhesion force [81]

2.4.2 Computer modeling

Computer modeling is the use of the computer to simulate and study complex systems using computer programs, mathematics models, physics, and computer sciences [81]. Gaussian is a computer program that utilizes the fundamental law of quantum mechanics to predict the energies, molecular structure, spectroscopic data, and much more advanced calculations [82]. It has been continuously updated since the Gaussian 16 is the latest version in the Gaussian series programs. It provides state-of-art capabilities for electronic structure modeling. Gaussian is licensed for a variety of computer systems (Windows, Linux/UNIX/Intel Mac, Mac OS X). To design the graphical input data for submission to Gaussian, the GaussView program provides for open files from the protein data bank (PDB). The user can manipulate, modify the structure and examine the results of the calculation from Gaussian.

2.4.2.1 Geometry optimization

Geometry optimization is a procedure that attempts to find the configuration of the minimum energy of the molecule. The procedure calculates the wave function and the energy is starting geometry and then proceed to search a new geometry of lower energy. This is repeated until the lowest energy geometry is found. This process is necessary for searching the optimized position of the initial molecule before calculating the binding energy [83].

2.4.2.2 Binding energy

Binding energy is the lowest energy requires to separate the drug from the binding site. The procedure calculates to predict the appropriate molecular position of the drug and binding site in the surrounding environments. When more bond energy in a different molecule is taken into consideration, the average energy is calculated [84].
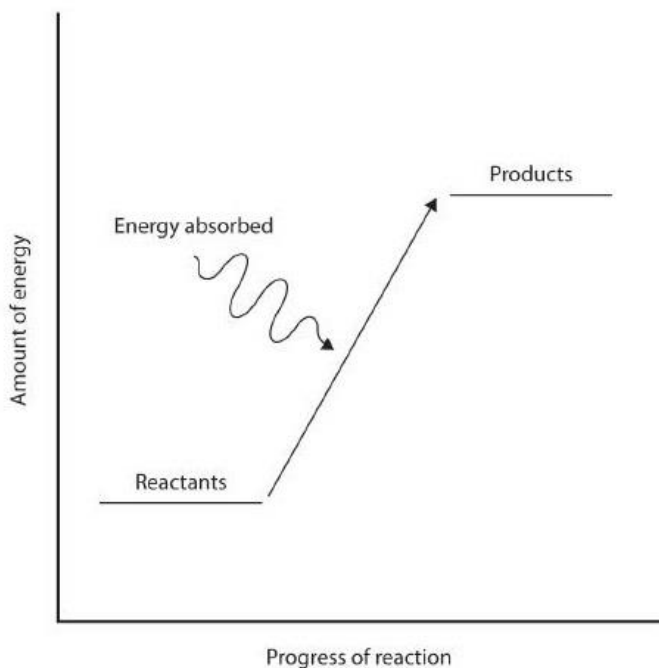
Figure 12 (left) Exothermic Reactions. For an exothermic chemical reaction, energy is given off as reactants are converted to products. (right) Endothermic Reactions. For an endothermic chemical reaction, energy is absorbed as reactants are converted to products.

2.4.3 Release kinetics

Over the past few decades, the development of controlled drug release to maintain the drug concentration in the blood or the target tissue at the desired value for as long as possible was widely studied to increase the therapeutic effectiveness of the drug and patient compliance [85]. The mathematics modeling was highly employed to identify the phenomena ruling release kinetics by measuring the physical parameters, such as the drug diffusion coefficient, and resorting to model fitting on experimental release data [85, 86]. The fundamental principle for the evaluation of the kinetics of drug release was offered by Noyes and Whitney in 1897 as the equation

$$dM/dt = KS (Cs ñ Ct) \tag{1}$$

where M, is the mass transferred with respect to time (t) by dissolution from the solid particle of instantaneous surface (S) under the effect of the prevailing concentration driving force (Cs ñ Ct), where Ct is the concentration at the time and Cs is the equilibrium solubility of the solute at the experimental temperature. The rate of dissolution dM/dt is the amount dissolved per unit area per unit time [85, 86].

The methods of approach to investigate the kinetics of drug release from controlled release formulation can be classified into three categories:

2.4.3.1 Statistical methods

Statistical methods using the exploratory data analysis which is useful in obtaining an improved understanding of the dissolution data of controlled release formulation. This method can be used in the first step to compare dissolution profile data in both a graphical and numerical manner. The dissolution profile data are plotted as the average dissolution profile data for each formulation with error bars at each time point. Then, the data of the dissolution profiles are summarized numerically and 95% confidence intervals for the differences in the mean dissolution profiles at each dissolution time point are evaluated. [85]

2.4.3.2 Model dependent methods

Model-dependent methods are based on different mathematical functions, which describe the dissolution profile. Once a suitable function has been selected, the dissolution profiles are evaluated depending on the derived model parameters to determine the release kinetics of the formulation. Several models have been widely used such as zero order, first order, Higuchi, Korsmeyer-Peppas model, Hixson Crowell, Baker-Lonsdale model, Weibull model, etc.

2.4.3.2.1 Zero order model

Drug dissolution from dosage forms that do not disaggregate and release the drug slowly can be represented by the equation:

$$Q_t = Q_0 + K_0 t \tag{2}$$

where Q_t is the amount of drug dissolved in time (t), Q_0 is the initial amount of drug in the solution (most times, $Q_0 = 0$) and K_0 is the zero order release constant expressed in units of concentration/time [85, 86].

2.4.3.2.2. First order model

This model has also been used to describe absorption and/or elimination of some drugs. The release of the drug which followed first order kinetics can be expressed by the equation:

$$\log C = \log C_0 - nKt / 2.303 \tag{3}$$

where C_0 is the initial concentration of drug, K is the first order rate constant, and t is the time. The data obtained are plotted as log cumulative percentage of drug remaining against time which would yield a straight line with a slope of nK/2.303 [85, 86].

2.4.3.2.3. Higuchi model

The first attempt is to create this model for describing the drug dissolution from the matrix system. Then it was extended to different geometrics and porous systems. This model has based on the hypothesis that

(i)   Initial drug concentration in the matrix is much higher than drug solubility.
(ii)   Drug diffusion takes place only in one dimension.
(iii)   Drug particles are much smaller than system thickness.
(iv)   Matrix swelling and dissolution are negligible.
(v)   Drug diffusivity is constant.
(vi)   Perfect sink conditions are always attained in the release environment.

Accordingly, model expression is given by the equation:

$$Q = K_H \times t^{1/2} \tag{4}$$

where Q is the amount of drug released in time t per unit area, K_H is the Higuchi dissolution constant and t is the time. The data obtained were plotted as cumulative percentage drug release versus square root of time [85-87].

2.4.3.2.4 Korsmeyer-Peppas model

To find out the mechanism of drug release from polymeric system, first 60% drug release data were fitted in Korsmeyern-Peppas model

$$M_t / M_\infty = Kt^n \tag{5}$$

where M_t / M_∞ is a fraction of drug released at time (t), k is the release rate constant and n is the release exponent. The n value is used to characterize different release for cylindrical shaped matrices. In this model, the value of n characterizes the release mechanism of drug as described in Table 1. [85]

Table 1 Interpretation of diffusional release mechanisms from Korsmeyern-Peppas model.

Release exponent (n)	Drug transport mechanism	Rate as function of time
0.5	Fickian diffusion	$t^{-0.5}$
$0.45 < n = 0.89$	Non -Fickian transport	t^{n-1}
0.89	Case II transport	Zero order release
Higher than 0.89	Super case II transport	t^{n-1}

2.4.3.3 Model independent methods

Model independent method using the difference factor (f1) and similarity factor (f2) to analyst the suitable for dissolution profile comparison when three to four or more dissolution time points are available. The difference factor calculates the percent difference between the two curves at each time point and is a measurement of the relative error between the two curves. Whereas the similarity factor is used to describe the similarity in the percent dissolution between the two curves [85].

For the easy calculation of the release kinetics, several programs have been available for analysts of the dissolution data such as DDSolver which is a free calculation and/or statistic program to fit drug release data. It can aid in reducing calculation errors and calculation time and is suitable to compare the dissolution data [88].

CHAPTER 3
MATERIALS AND METHODS

3.1 Materials

1. 2-Pyrrolidone (lot no.BCBG8182V, Sigma-Aldrich, Steinheim, Germany)

2. Agarose (Lot no. C7031-17, Vivantia Inc., California, USA)

3. Dimethylsulfoxide (DMSO) (lot no. 453035, Fluka, Basel, Switzerland)

4. Doxycycline hyclate (Bangkok lab and cosmetics Co. Ltd., Ratchaburi, Thailand)

5. Eudragit RS (ERS) (lot no. G140338039, Evonik Rohm GmbH, Kirschenallee, Germany)

6. *Escherichia coli* ATCC 25922

7. Glyceryl monostearate (GMS) (PC Drug, Bangkok, Thailand)

8. N-methyl-2-pyrrolidone (NMP) (lot no. A0251390, Fluka, New Jersey, USA)

9. Olive oil (Bertolli®, Florence, Italy)

10. Organic camellia tea oil (Naturel®, Samutprakarn, Thailand)

11. *Porphylomonas gingivalis* ATCC 33277

12. Potassium dihydrogen orthophosphate (lot no. E23W60, Ajax Finechem, Sydney, Australia)

13. Rosin (R) (Karnchanapon Co. Ltd., Nakhon Pathom, Thailand)

14. Sodium fluorescence (lot no. MKCG7851, Sigma-Aldrich, Missouri, USA)

15. Sodium hydroxide (lot no. AF310204, Ajax Finechem, Australia)

16. *Staphylococcus aureus* ATCC 25923

17. *Streptococcus mutans* ATCC 25175

18. Vancomycin HCl (V) (lot no. WXBB5169V, Sigma-Aldrich, Missouri, USA)

3.2 Equipments

1. Dialysis bag (Spectra/Por®membrane molecular weight cut off: 6000–8000, lot no. 32644, Spectrum Laboratories,Inc., California, USA)

2. Filter set and filter membrane 0.45 μm (Whatman®, Massachusetts, USA)

3. Micropipette 0.1-2 μL, 2-20 μL, 10-100 μL, 20-100 μL, 100-1000 μL, 1-5 mL (Masterpette®; Bio-Active Co., Ltd., Bangkok, Thailand) and micropipette tip

4. Pipette aid (Powerpette Plus; Bio-Active Co., Ltd., Bangkok, Thailand)

5. Disposible syringe (1 mL, 3 mL, 5 ml, 10 mL) (Nipro®, Ayutthaya, Thailand)

6. Female to female luer lock with wings (Qosina, New York, USA)

7. Analytical balance (Satorius CP224S, Scientific promotion Co., Ltd., Bangkok, Thailand)

8. Automatic autoclave (Model: LS-2D; Scientific promotion Co., Ltd., Bangkok, Thailand)

9. Desiccator
10. pH meter (Ultra Basic UB-10, Denver instrument, New york, USA)
11. Refrigerator, Freezer -20°C, Freezer 4°C
12. UV/Visible spectrophotometer (Scilogex, Ottawa, Canada)
13. Vortex mixer (Vortex-Genie® 2 mixer, Scientific industries. Inc., New York, USA)
14. Roller tube mixer (Scilogex MX-T6-S analog tube roller, Scilogex, Connecticut, USA)
15. Needle (18 and 27 guage) (Nipro®, Ayutthaya, Thailand)
16. Brookefield DV-III Ultra programmable rheometer (Brookefield Engineering Laboratory Inc., Massachusettes, USA.)
17. Texture analyzer (TA.XT plus, Stable Micro Systems, Godalming, UK)
18. Plastic petri-dish (6 cm)
19. Glass petri- dish (9 cm)
20. Stainless cylinder cup (6 mm)
21. Stereomicroscope (Miotic SMZ-171 Series, Hongkong, China)
22. Drop shape analyzer (FTA 1000, First Ten Angstroms, Cambridge, UK)
23. Glass slide
24. Glass syringe with 18 guage blunt tip
25. Quartz cuvette
26. Inverted microscope (Eclipse TE 2000-U, Nikon DXM 1200, Tokyo, Japan)
27. Fluorescence inverted microscope (GFP-B, wavelengths : excitation filter 480/40 and Emission filter 535/50, Nikon DXM 1200, Tokyo, Japan)
28. Dropper
29. Brain heart infusion (BHI, lot no. 0270845, Bacto™, Massachusettes, USA)
30. Brain heart minfusion agar (BHA, lot no. 0298038, Bacto™, Massachusettes, USA)
31. Tryptic soy agar (TSA, lot no. 7341698, Difco™, Massachusettes, USA)
32. Tryptic soy broth (TSB, lot no. 8091999, Difco™, Massachusettes, USA)
33. Sheep blood agar (Department of medical science, Ministry of public health, Nonthaburi, Thailand)
34. Incubator (Biocotek, Zhejiang, China)
35. Anaerobe incubator (Forma Anaerobic System, Thermo Scientific, Ohio, USA)
36. Hot air oven (Herareus UT 6760, Kendro laboratory, Berlin, Germany)
37. Glove (Sri Trang Gloves (Thailand) Plc., Bangkok, Thailand)
38. Sterile cotton stick
39. 70% Alcohol (Siribuncha Corp., Nonthaburi, Thailand)
40. Alcohol burner
41. L-shape glass rod
42. Lighter

43. Eppendorf centrifuge tube (15 ml) (Thermofisher Scientific, Massachusettes, USA)
44. Freeze dryer (Triad^{TM} Lanconco, Missouri, USA)
45. Scanning electron microscope (Tescan mira3, Kohoutovice, Czech Republic)
46. Gaussview 05 software (Gaussian Inc., Connecticut, USA)
47. Gaussian 09 software (Gaussian Inc., Connecticut, USA)

3.3 Methods

3.3.1 Development of ISG and ISM using ERS and R as matrix formers

3.3.1.1 Solvent screening for ISG and internal phase of ISM preparation

This study determined the possible solubility of 30%w/w ERS and 30%w/w R which were hydrophobic polymers and model drugs which were 10%w/w DH and 1% w/w V in selected organic solvents (NMP, DMSO, and PYR). The mixtures were rotated with a roller tube mixer (Scilogex MX-T6-S analog tube roller, Scilogex, Connecticut, USA) for 24 h. The organic solvent which can dissolve both polymers and drugs was selected for testing the miscibility with the external oil.

The external oil (olive oil : O and camellia oil : C) miscible testing was determined by filling 3 ml of each solvent in the test tube followed by 3 ml of O and C. Then observation of the miscibility of solvent and oil was performed visually. The immiscible solvent was chosen for formulating ISM in further study.

3.3.2 Preparation of ISG and ISM systems

3.3.2.1 ISG preparation using ERS as matrix former

Free-drug loaded solutions were prepared by dissolving 10, 20, and 30% w/w ERS in NMP, DMSO, and PYR as presented in Table 2. The mixtures were rotated for 48 h or until obtained the clear solutions by using roller tube mixer. To prepare drug-loaded systems, 10% w/w DH was added to the selected polymeric solutions then the mixtures were rotated using the roller tube mixer for 24 h or until obtained the clear solutions.

3.3.2.2 ISM preparation using ERS as matrix former

The internal phase of free-drug loaded ISM was prepared by dissolving 10, 20, and 30% w/w ERS in a selected organic solvent. The mixtures were rotated for 48 h or until obtained the clear solution using roller tube mixer to formulate polymeric solutions. 7.5% w/w of GMS was incorporated in oils including O and C as presented in Table 3 stirring with heat by magnetic stirrer (Hotplate and magnetic stirrer C-MAG HS7, IKA®, Staufen, Germany) until obtained the clear solution to generate the external oil phase. Two phases were merged into emulsion form with ratio 1:1 using 3 ml disposable syringe connected with butterfly luer lock then pressing forward and backward at the rate of 2 cycles/sec for 60 sec.

DH-loaded formulation was prepared by adding 10% w/w DH in an internal polymeric phase and the mixture was rotated using roller tube mixer for 24 h or until

clear solution formed. Then, the external oil phase was merged into emulsion form with ratio 1:1 using 3 ml disposable syringe connected with butterfly luer lock then pressed forward and backward at the rate 2 cycles/sec for 60 sec.

Table 2 Composition of ISG formula generated from ERS containing different solvents.

Formulation	ERS	DMSO	PYR	NMP
10ED	10	90		
20ED	20	80		
30ED	30	70		
10EP	10		90	
20EP	20		80	
30EP	30		70	
10EN	10			90
20EN	20			80
30EN	30			70

Table 3 Composition of ISG and ISM formula generated from ERS containing selected solvent, oils, GMS and DH.

Formulation	DH	ERS	Solvent	O	C	GMS
10% ERS						
F1		10	90			
F2	10	10	80			
F3		5	45	42.5		7.5
F4		5	45		42.5	7.5
F5	5	5	40	42.5		7.5
F6	5	5	40		42.5	7.5
20% ERS						
F7		20	80			
F8	10	20	70			
F9		10	40	42.5		7.5
F10		10	40		42.5	7.5
F11	5	10	35	42.5		7.5
F12	5	10	35		42.5	7.5
30% ERS						
F13		30	70			
F14	10	30	60			
F15		15	35	42.5		7.5
F16		15	35		42.5	7.5
F17	5	15	30	42.5		7.5
F18	5	15	30		42.5	7.5

3.3.2.3. ISG preparation using R as matrix former

Free-drug loaded solutions were prepared by dissolving 20, 30, 40, 50, and 60% w/w R in selected organic solvent and the mixtures were rotated for 48 h or until obtained the clear solution by using roller tube mixer. To prepare drug-loaded systems, 1% w/w V was incorporated in polymeric solutions then the mixtures were rotated using the roller tube mixer for 24 h or until the clear solution formed as shown in Table 4.

3.3.2.4. ISM preparation using R as matrix former

The internal phase of free-drug loaded ISM was prepared by dissolving 20, 30, 40, 50, and 60% w/w R in selected organic solvent. The mixtures were rotated for 48 h or until obtained the clear solution using roller tube mixer to formulate polymeric solutions. 7.5% w/w of GMS was incorporated in olive oil mixing with heat by magnetic stirrer until obtained the clear solution to generate external oil phase. Two phases were merged with ratio 1:1 using 3 ml disposable syringe connected with butterfly luer lock then pressed forward and backward at the rate of 2 cycles/sec for 60 sec.

V-loaded formulations were prepared by adding 1% w/w V in an internal phase and the mixtures were rotated using roller tube mixer for 24 h or until clear solutions were formed. Then, the external oil phase was merged with ratio 1:1 using 3 ml disposable syringe connected with butterfly luer lock then pressed forward and backward at the rate of 2 cycles/sec for 60 sec as presented in Table 5.

Table 4 Composition of ISG formula generated from R containing different solvents.

Formulation	R	DMSO	PYR	NMP
20RD	20	80		
30RD	30	70		
40RD	40	60		
50RD	50	50		
60RD	60	40		
20RP	20		80	
30RP	30		70	
40RP	40		60	
50RP	50		50	
60RP	60		40	
20RN	20			80
30RN	30			70
40RN	40			60
50RN	50			50
60RN	60			40

Table 5 Composition of ISM formula generated from R containing selected solvent, O, GMS and V

Formulation	V	R	Solvent	O	GMS
20R		20	80		
30R		30	70		
40R		40	60		
50R		50	50		
60R		60	40		
20RV	1	20	79		
30RV	1	30	69		
40RV	1	40	59		
50RV	1	50	49		
60RV	1	60	39		
20RISM		10	40	42.5	7.5
30RISM		15	35	42.5	7.5
40RISM		20	30	42.5	7.5
50RISM		25	25	42.5	7.5
60RISM		30	20	42.5	7.5
20RVISM	0.5	10	39.5	42.5	7.5
30RVISM	0.5	15	34.5	42.5	7.5
40RVISM	0.5	20	29.5	42.5	7.5
50RVISM	0.5	25	24.5	42.5	7.5
60RVISM	0.5	30	19.5	42.5	7.5

3.3.3 Evaluation ISG and ISM physicochemical properties

3.3.3.1. pH measurement

pH value of free-drug loaded and drug-loaded ISG and ISM prepared with each polymer were determined using pH meter (Ultra basic UB-10, Denver instrument, Bohemia, New York) (n=3).

3.3.3.2. *In-vitro* gel and micropaticle appearance

The prepared ISG and ISM were filled in 1 ml disposable syringe and then injected through a 27 gauge needle into a test tube containing 6 ml PBS. The formulations were observed by visual observation.

3.3.3.3. ISM stability studies

The phase separation of prepared ISM was investigated in a disposable syringe at room temperature. The formulation was filled in 1 ml syringe then put the syringe in the vertical position and observed by visual observation within 1 hour. The separation time was recorded and phase separation was calculated *via* the following equation:

$$\% \text{ phase separation} = \frac{\text{Separted oil height}}{\text{Height of formula}} \times 100 \qquad (6)$$

3.3.3.4. Viscosity and rheology behavior

The viscosity and rheology of prepared ISG and ISM were investigated using Brookfield DV-III Ultra programmable rheometer (Brookefield Engineering Laboratory Inc., Massachusettes, USA.) with spindles (CP40 and CP52) (n=3). Viscosity was measured at room temperature and the viscosity parameters were determined at different shear rates with 15 sec equilibration time at every shear rate (n=3). The flow parameter was calculated using the exponential formula as the following equations:

$$F^N = \eta G \hspace{10cm} (7)$$

$$\text{Log } G = N \text{ Log } F - \text{Log } \eta \hspace{8cm} (8)$$

where F is shear stress, G is shear rate, N is an exponential constant and η is a viscosity coefficient.

3.3.3.5. Injectability test

Prepared ISG and ISM were evaluated by using a texture analyzer (TA.XT plus, Stable Micro Systems, Godalming, UK) (n=3) in compression mode. The formula was filled in 1 ml syringe which was fixed with the stand. Then pressed the syringe plunger by a flat face cylindrical probe with a constant speed of 1.0 mm.s^{-1} and a constant force of 0.1 N for expelling the formulation through a 27 gauge needle for a barrel length of 20 mm at room temperature (n=3). The maximum force (N) was selected for analysis and the area under the curve (AUC) was used to determine the work of expulsion.

3.3.3.6 Adhesion properties studies

The agarose gel was prepared by dissolving 0.6% agarose powder in PBS with heat until obtaining a clear solution. Agarose solution was filled in 6 cm plastic petri-dish and waited until it set into a gel then the well was built at the center of the plate using a cylindrical stainless cup to simulate a human periodontal pocket. 200 μl of prepared ISG and ISM were filled in the well and let transformed completely into solid upon solvent exchanged for 1 week. The transformed formulation will be evaluated by using a texture analyzer in compression mode with hold until time. The spherical probe moved downward at a constant speed of 0.5 mm/sec and penetrated the transformed formulation. The applied force and displacement of the probe were determined as a function of time. When the penetration depth was 2 mm, this position was held for 60 sec, after that, the probe was driven upwards at the speed of 10 mm/sec. The maximum deformation force ($F_{max\ deformation}$) was measured at maximum force when the probe penetrated the transformed formulation, The force after holding for the 60 sec was the remaining force ($F_{remaining}$), and the adhesion force (the maximum attachment force) was measured during the upward movement of the probe, which was the negative direction of the force ($F_{adhesion}$). The ratio $F_{remaining}/F_{max\ deformation}$ was used as the measure of elasticity/plasticity. High value indicated high elasticity whereas low value indicated high plasticity. Each experiment was conducted in triplicate and the results were presented in mean value ± S.D.

3.3.3.7. Matrix formation rate of ISG and ISM

The agarose gel was prepared by adding 0.6% agarose powder in PBS, then the mixture was stirred with heat until a clear solution was obtained. After that, agarose solution was poured in a 9 cm plastic petri-dish and waited until it set into gel then built the hole by using a 6 mm diameter cylindrical stainless cup. 150μl of the prepared formulation was filled in the cylindrical hole and then observed under a stereomicroscope (Miotic SMZ-171 Series, Hongkong, China). The diffusion length of the gel was measured for 5 positions, the results were presented in mean ± S.D. and calculated into diffusion rate (n=3).

3.3.3.8. Contact angle

Contact angel of ISG and ISM were determined by a drop shape analyzer (FTA 1000, First Ten Angstroms, Cambridge, UK). The selected formula was filled in 1 ml syringe and expelled through an 18 gauge blunt needle to form the drop on a glass slide. The drop which contacted glass slide after 5 sec was selected for measuring the contact angle (n=3).

3.3.3.9. Surface tension and interfacial tension

Surface tension was determined by drop shape analyzer by filling the selected formula in 1 ml glass syringe and expelling it through 18 gauge blunt needle to form the drop. Then measured the surface tension between the biggest drop of formulation and the air (n=3).

Interfacial tension was measured by drop shape analyzer. The selected formula was filled in 1 ml glass syringe with 18 gauge blunt needle. Oils including, O and C were filled into a quartz cuvette as the outer phase of an emulsion. The tip of the needle was put into the oil and pressed syringe plunger to expel the formulation. Then measured interfacial tension between the biggest drop of formulation and the oil (n=3).

3.3.3.10 *In-vitro* drug release

Drug release was used dialysis method for checking the released amount of antibiotic drug from ISG and ISM in PBS by filling 1 g formulation in a dialysis bag (Spectra/Por® membrane molecular weight cut off: 6000-8000, lot no. 9200006, Spectrum laboratory, Inc., Fluka, Switzerland), then placed the bag in 100 ml PBS bottle. The bottle was swirled in an incubator (biocotek, Zhejiang, China) with 37 ± 0.5 ºC and 25 rpm. The medium was sampled for 10 ml at 5, 10, 15, 30, 45, 60, 120, 180, 240, 360, 480, 720, 960, 1440, and 2880 min or until completely released, then measured with UV-VIS spectrophotometry at 379 nm for DH and 280 nm for V (n=3). The mean of cumulative drug release ± S.D. was calculated. The data obtained from *in-vitro* drug released were analyzed by adding on Microsoft word program, DDsolver [88]. The cumulative release profile was fitted with different mathematical release equations. The least-square fitting the experimental dissolution data to the mathematical equations (power law, zero order, first order, and Higuchi's) were carried out. The high value of the coefficient of determination (r^2) or model selection criteria (msc) indicated the superiority of the release profile fitting to mathematical equations.

3.3.3.11. Weight loss study

The weight loss of the prepared ISG and ISM were evaluated by injection of 1 g. sample in dialysis tube and incubating in 10 ml PBS pH 6.8. Each sample was shaken with 50 rpm at 37.0±0.2ºC. Fresh PBS was replaced every week for 1 month. Then the sample was dried in a hot air oven at 65 ºC for 72 hours and kept in a desiccator. The percent of weight loss was carried out as the following equation :

$$\% \text{ Weight loss} = \frac{\text{Initial weight} - \text{Final weight}}{\text{Initial weight}} \times 100 \qquad (9)$$

3.3.3.12. Mechanism of transformation

The mechanism of transformation of ISG and ISM was investigated under the inverted microscope with 40x and 100x. PBS pH 6.8 was dropped on the center of glass slide, after that 50 μl of the formulation was dropped beside PBS and let the drop contact each other. Then observed the transformation at 1, 2, 3, 4, 5, 10, 15, 20, and 30 min. For a more clear understanding, 0.6% agarose gel including 0.003% sodium fluorescein was coated on the glass slide to simulate the human gum. The prepared formula of ISG and ISM was dropped beside the gel then observed the transformation under the inverted fluorescence microscope (Eclipse TE 2000-U; Model: T-DH Nikon®, Tokyo, Japan) with 40x and 100x and recorded with time-lapse mode every 10 sec for 180 sec.

In addition, the mechanism of water diffusion through the external oil phase of ISM was investigated. The prepared ISMs were dropped beside the 0.6% agarose gel including 0.003% sodium fluorescein and observed the transformation behavior under the inverted fluorescence microscope with 40x and 100x was recorded with time-lapse mode every 10 sec for 180sec.

3.3.3.13. Computational modeling of drug and matrix former
3.3.3.13.1. The preparation of the model drug and matrix former structure

The structure of abietic acid, the main component of rosin, and Eudragit RS were constructed by GuassView 5.0 program (Gaussian Inc. CT, USA). The structure of doxycycline (PubChem CID 54685920) [89] was obtained from National Center for Biotechnology Information and vancomycin (PDB ID: 1aa5) was obtained from RCSB protein data bank [90]. The model structure, physical and chemical properties data of dimethyl sulfoxide (DMSO) (PubChem CID 679) [91] and water (PubChem CID 962) [92] as the environmental solvent were obtained from National Center for Biotechnology Information. The computer and Gaussian 09 program (Gaussian Inc. CT, USA) were supported form the faculty of sciences, Silpakorn University. Nakorn Pathom Thailand.

3.3.3.13.2. The optimization of the configuration between molecules of matrix former and the model drug

The molecule of matrix former and the model drug were optimized in the air environment to predict the initial configuration of each structure by using the Gaussian 09 program. Then the combined structure of abietic acid and vancomycin (AV) and the combined structure of Eudragit RS and Doxycycline (ED) were optimized in the air

environment to predict the position of the initial configuration. After that, the combined structure was optimized in 3 different solvents such as dimethyl sulfoxide (DMSO), the mixture of water and DMSO with the ratio of 1:1, and pure water to simulate the transformation state of the matrix former which can form the matrix owing to the presence of water. The configuration which required the minimum energy were collected for calculating the binding energy.

3.3.3.13.3. The binding energy calculation

The minimum energy of the drug, matrix former, and combined structure was calculated in the different solvents to simulate the mechanism of transformation by using the Gaussian 09 program, then calculated the binding energy as the following equation:

$$\text{Binding energy AB} = AB - (A+B) \tag{10}$$

A is the minimum energy of the drug

B is the minimum energy of the matrix former

AB is the minimum energy of the combined form

3.3.3.14. Size of ISM emulsions and microparticles

The formulation was dropped on glass slide then the size of ISM emulsions were determined under the inverted microscope (Eclipse TE 2000-U, Nikon DXM 1200, Tokyo, Japan) at 40x by measuring the diameter of each droplet using the Miotic program (n=150). Then calculated the mean of diameter ± S.D. evaluation for the size of the formulation. For ISM microparticles, the formulation was dropped on glass slide and adding the drop of PBS pH 6.8 for observing the solid microparticles after being contacted with buffer and measuring the diameter of microparticles using the Miotic program (n=150) as mean of diameter ± S.D.

3.3.3.15. Antimicrobial activities

Antimicrobial activities of ISG and ISM of both drug-loaded and free drug formulations were evaluated against the standard microbes (*S. aureus* ATCC 6538P and *E. coli* ATCC 25922) and anaerobic microbes (*S. mutans* ATCC 27175 and *P. gingivalis* ATCC 33277) using agar cup diffusion method. The growth of both cultures of microbes was prepared with a turbidity of approximately 10^8 cells/ml. Then the microbes were swabbed on an agar plate and dried. The sterilized cylinder cups were carefully placed on the surface of swabbed agar. The 200μl of prepared ISG and ISM were separately filled in the cups and the plates were incubated at 37 ºC for 24-48 hours. For the anaerobic bacteria, the test was conducted in an anaerobic incubator (Forma Anaerobic System, Thermo Scientific, Ohio, USA.). The antimicrobial activities were measured as diameters (mm) of inhibition zones (n=3).

3.3.3.16. Topography study

For a clear understanding of both ISM and ISG structures after the drug release, the remnants were tested, The released formulation was moved through filter paper and was completely dried with a freeze dryer (Triad^{TM} Lanconco, Missouri, USA). Then the surface and cross-section of the remnants were observed under the SEM (Tescan mira3, Kohoutovice, Czech Republic) at a magnification of 1,000 and 10,000.

3.3.4. Statistical analysis

All experimental measurements were collected and their statistically significant measurements were analyzed using a one-way analysis of variance (ANOVA) followed by the least significant difference (LSD) post-hoc test or Duncan. The significant level was set at $p < 0.05$. Moreover, paired T-test was obtained to analyze the dependent data with a 95% confidential interval.
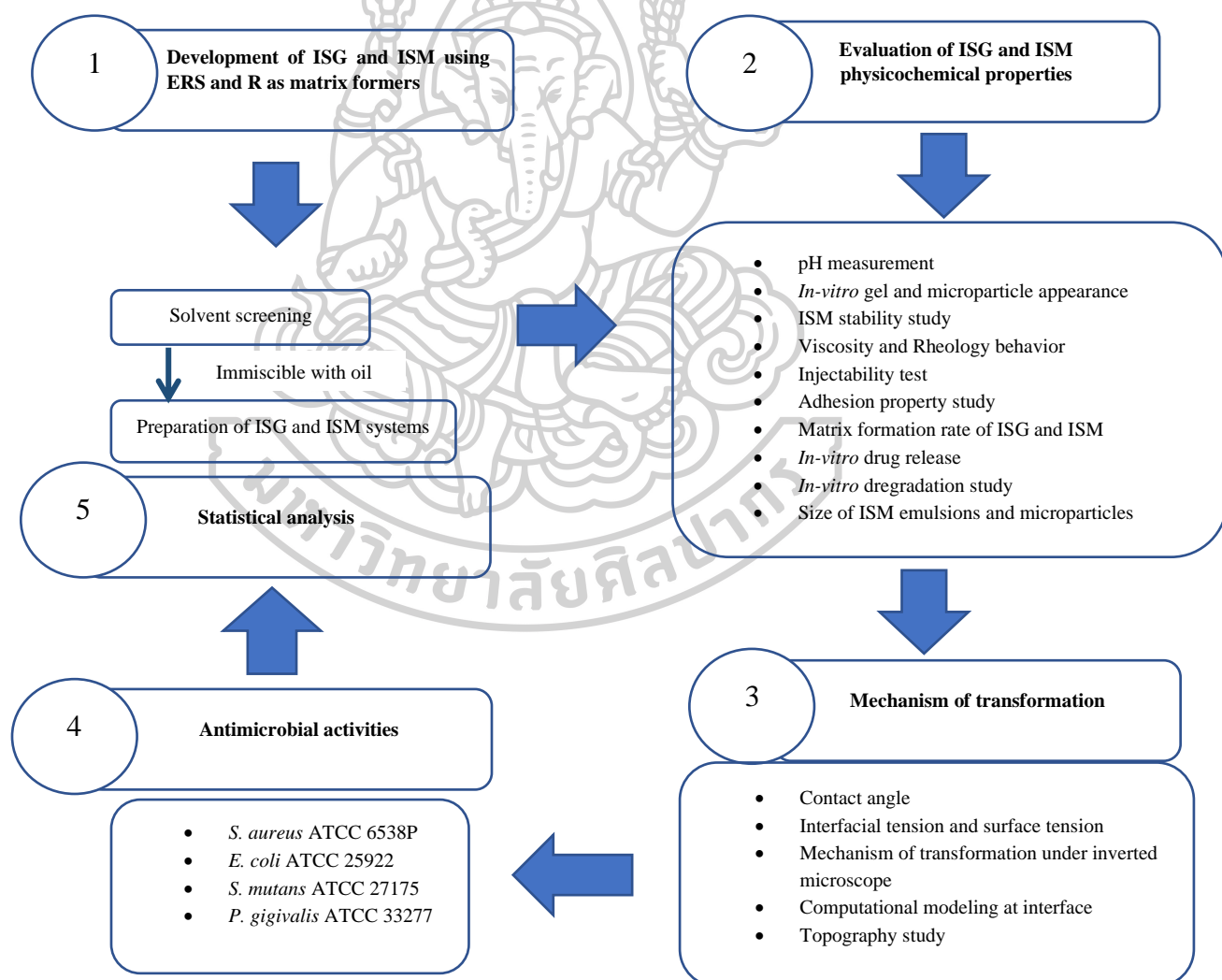
Figure 13 Schematic diagram of overall research

CHAPTER 4
RESULTS AND DISCUSSION
Part 1
Antimicrobial agent-loaded *in-situ* forming gel and microparticle using Eudragit® RS and rosin as a matrix former for periodontal pocket delivery

4.1 Eudragit RS

4.1.1 Solvent screening

In this study, 10% w/w DH with 30%w/w ERS (DHE) and 1%w/w V with 30%w/w R (VR) were dissolved in three different organic solvents (NMP, DMSO, and PYR). All solvents dissolved both DHE and VR within 24 hours and all of them presented as the clear solutions. From the miscibility study, only NMP was miscible with both O and C which cannot be prepared into the emulsion form of the ISM systems; thus, the DMSO and PYR were chosen for formulating ISM in further study.

4.1.2 Appearance of ERS-based liquid formulations

The ERS-based ISG formulations in DMSO or PYR presented a clear with the slightly viscous solution. After mixing with the DH for 48 hours, the DH-loaded ISGs illustrated as a clear yellowish system due to color from DH. To prepare the ISM formulations, the ISGs solutions were used as the internal phase emulsified with the external oil dispersed in GMS using the two-syringe connector method. All of the ISM formulations presented as the yellowish emulsions. However, the phase separation between the solvent and the oil occurred within 40 min in both systems comprising 10% w/w and 20% w/w ERS. Only emulsion containing 30%w/w ERS as the internal phase showed good stability for longer than 60 min (data not shown).

According to the solvent screening test and the stability testing of ERS-based formulations, DMSO and PYR were selected as the solvents for the drug and matrix former, and 30% w/w ERS was the proper concentration using in the further study. The composition of ERS-based ISG and ISM formulations using the different solvents and the oils were shown in Table 6.

Table 6 Composition of free-drug and DH-loaded ERS ISG and ISM formulations containing different solvents and oils (total 100%).

Formulation	DH	ERS	DMSO	PYR	Olive oil	Camellia oil	GMS
F1		30	70				
F2	10	30	60				
F3		30		70			
F4	10	30		60			
F5		15	35		42.5		7.5
F6		15	35			42.5	7.5
F7	5	15	30		42.5		7.5
F8	5	15	30			42.5	7.5
F9		15		35	42.5		7.5
F10		15		35		42.5	7.5
F11	5	15		30	42.5		7.5
F12	5	15		30		42.5	7.5

*F1 and F3 as control groups of ISG; F2 and F4 as DH-loaded ISGs and F5, F6, F9, F10 as control groups of ISMs; F7, F8, F11, F12 as DH-loaded ISM

4.1.3 Evaluation of formulation composition

4.1.3.1 pH measurement

pH is the parameter used to specify the acidity and alkalinity of a solution. It is an important factor that affects the stability of the drug which refers to the hydrogen ion concentration in an aqueous solution [93]. To consider formulating the ERS-based ISG and ISM for periodontal patient, pH value of gingival crevicular fluid (GCF) at periodontal pocket should be considered. In healthy resting oral cavity, the pH is between 5-9 which varies in different sites in the mouth whereas the GCF from the pockets of periodontitis patients were ranging from 2-9 owing to the debridement and bacteria [94, 95]. In this study, the pH of pure solvent, drug, and the free drug-loaded ERS formula was measured as presented in Table 7. Both DMSO and PYR showed alkaline properties as pH values of 11.40 and 11.20, respectively, and all of the free-drug loaded ERS formulas also presented pH values between 7.50-9.82 owing to alkaline properties of the solvents. The ISG and ISM formulation using DMSO as solvents (F1, F2, F5, F6, F7, and F8) exhibited slightly alkaline than PYR (F3, F4, F9, F10, F11, and F12) since DMSO has a high pH value. In addition, the pH of DH-loaded formulas was dramatically decreased ($p<0.05$) because of the acidic properties of DH which reached the pH value that improve the stability of DH and prevented the decomposition [96, 97] The pH value as 2.6 of acidified reverse-osmosis water revealed the DH recovery 93.8% and 84% after filling in untinted and tinted bottle respectively for 14 days[97]. Moreover, the formulations with pH value above 2 were acceptable to use in periodontal pockets of periodontitis patients [94, 95]. ERS also acceptable using as matrix former in acidic pH owing to the pH-independent dissolving property [7, 98]

Table 7 The pH of solvent, free-drug loaded ERS based formulation and DH-loaded ERS based formulation (n = 3)

Formulation	pH ± S.D.
DMSO	$11.40 \pm 0.09^{a,b}$
PYR	$11.20 \pm 0.22^{a,b}$
Free-drug loaded ERS based formulation	
F1	8.82 ± 0.01^{a}
F3	7.91 ± 0.00^{a}
F5	9.21 ± 0.01^{b}
F6	9.82 ± 0.00^{b}
F9	8.46 ± 0.01^{b}
F10	7.50 ± 0.01^{b}
DH-loaded ERS based formulation	
F2	3.35 ± 0.00^{a}
F4	3.21 ± 0.00^{a}
F7	3.30 ± 0.00^{b}
F8	3.24 ± 0.02^{b}
F11	3.14 ± 0.01^{b}
F12	3.18 ± 0.00^{b}

The superscripts a,b indicate a significant different ($p<0.05$) by using one-way ANOVA followed by LSD post-hoc test.

4.1.3.2 Viscosity and Rheology

Viscosity is an internal properties of a fluid that offers the resistance to flow affecting the *in-situ* forming systems, especially in the injection properties and the character of diffusion rate of solvent exchange mechanism. In this study DMSO and PYR which are the pure solvents exhibited low viscosity (less than 20 cPs) as 2.26 and 15.72, respectively while both olive oil and camelia oil presented the higher viscosity as 112.80 and 86.42, respectively as shown in Table 8. The free-drug loaded ERS based ISM formula such as F5, F6, F9, and F10 demonstrated significantly lower viscosity than ISG formulas (F1 and F3) (p<0.05) due to the lubricity effect of the oil in ISM [74, 99]. The ISG and ISM formulation comprising DMSO exhibited a lower viscosity than PYR revealed that DMSO is a good solvent for the systems in which polymer-solvent interactions prevail over polymer-polymer interactions whereas PYR presented a high viscosity especially in the ISG formula which is 6936.00 ± 75.62 cps. indicated that polymer-polymer interaction was obtained. Therefore, the aggregation of polymer occurred to result in increasing the viscosity of the formula [100]. Moreover, the formula which contains camellia oil showed lower viscosity than the olive oil formula owing to the less viscous of camellia oil.

The formula containing DH presented significant increasing in viscosity (P<0.05) because the amount of drug replaced some of the solvents in the systems [101]. Furthermore, the viscosity of ISG and ISM formulas which contained different oil as the external phase also showed the same trend with the free drug-loaded formula. Moreover, all formulas presented a Newtonian flow in rheology behavior which the viscosity is independent of shear rate except F11 and F12 which presented the non-Newtonian shear thinning behavior as presented in Figure 14. According to high viscosity of F4 formulation, the rheology behavior cannot be detected when using shear rate above 50 s^{-1}. However, F4 also presented a Newtonian flow in low shear rate as shown in Figure 15.

Table 8 The viscosity of solvent, oils, free-drug loaded ERS based formulation and DH-loaded ERS based formulation (n = 3)

Formulation	Viscosity ± S.D. (cPs)
DMSO	2.26 ± 0.15^c
PYR	15.72 ± 0.03^c
Olive oil	112.80 ± 0.17
Camelia oil	86.42 ± 0.15
Free-drug loaded ERS based formulation	
F1	862.57 ± 4.56^c
F3	6936.00 ± 75.62^c
F5	513.30 ± 9.18^c
F6	460.40 ± 6.96^c
F9	677.33 ± 16.54^c
F10	621.10 ± 5.29^c
DH-loaded ERS based formulation	
F2	2435.00 ± 23.79^c
F4	18812.00 ± 1274.63^c
F7	1714.30 ± 206.47^c
F8	1261.00 ± 42.14^c
F11	10782.00 ± 601.02^c
F12	9679.30 ± 479.75^c

The superscripts c indicate a significant different (p<0.05) by using one-way ANOVA followed by LSD post-hoc test.
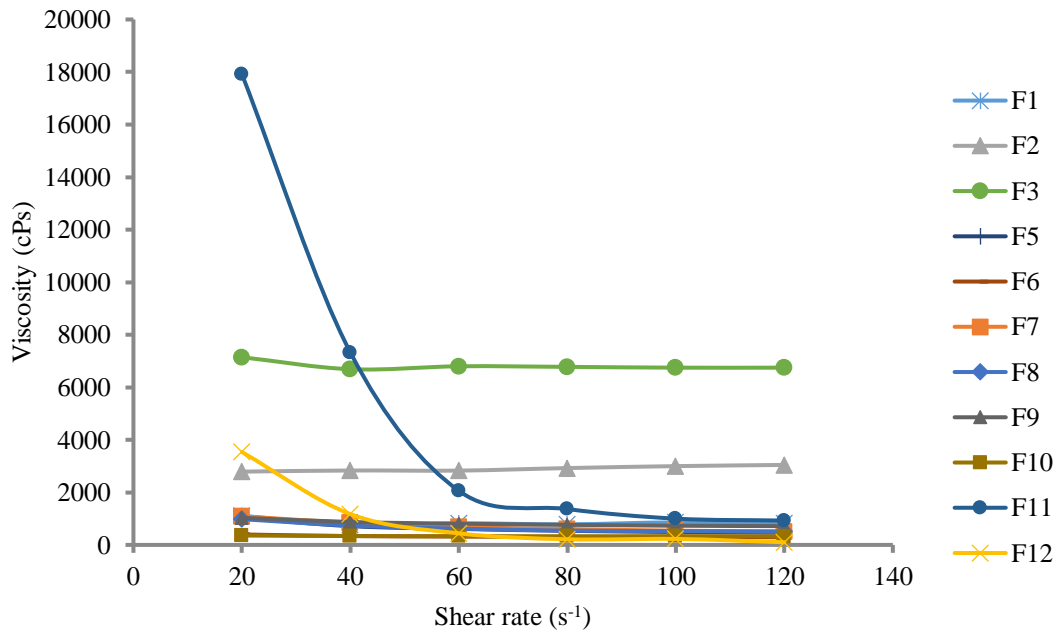
Figure 14 Rheology behavior of ERS based formulations
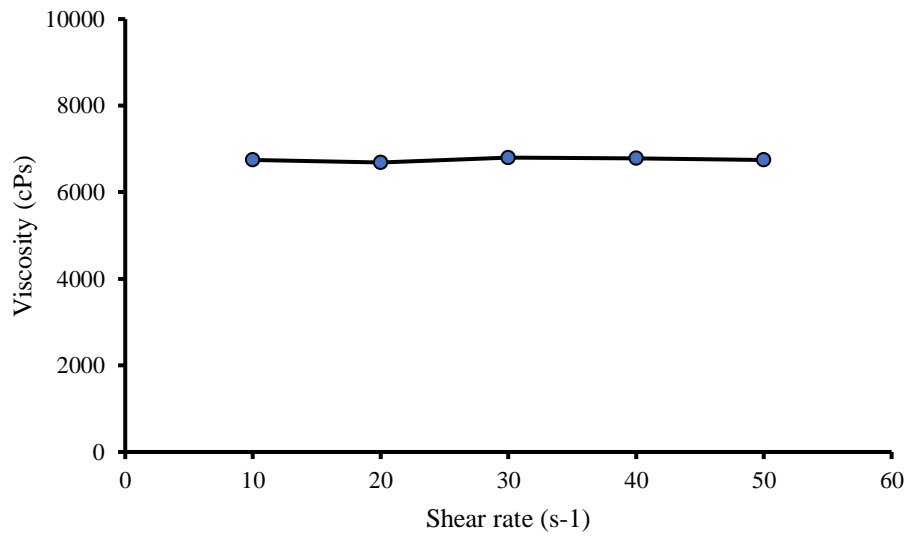
Figure 15 Rheology behavior of F4 formulation

4.1.3.3. Injectability test

In general, the most common size gauge needles in dentistry are 25, 27, and 30 gauges with bevel sharpness to generate less trauma in the gum tissue, reduce the pain, and easy to deliver the formula into gum cavity [101]. In this study, 27 gauge was selected to investigate the injectability force and injectability area under the curve (AUC) which required expelling the formula from prepared syringes whereof the low injectability force and work indicated the ease of injections during clinical administration [40]. The bare solvents and oils showed low injectability force (less than 20N) and low injectability with AUC value which DMSO presented the lowest in both results as shown in Table 9 related to the viscosity experiment. Surprisingly, camellia oil showed a higher injectability force and AUC than olive oil which contrast to their viscosity because camellia oil and olive oil contains unsaturated fatty acid for 88.2%, 86.3%, respectively [102] which has many bending structures resulting in the high friction force. Moreover, there has been reported that trans-unsaturated fatty acid revealed higher friction force than cis-forms [102]. Free-drug loaded formula containing DMSO in both ISG and ISM showed lower injection force and AUC than PYR, and ISM using camellia oil as dispersing phase also showed lower injection force and AUC than that using olive oil which conformed to previous results. The DH-loaded formula showed significantly increasing both injection parameters than the free drug-loaded formula (p <0.05) which related to the viscosity results. Moreover, olive oil exhibited better lubricity effects than camellia oil [102]. Thus, the ISM formula significantly reduced the injection force and AUC. Nevertheless, F3 containing ERS and PYR and the DH-loaded formula comprising PYR as the solvent could not be measured both of the injectability force and AUC since the needle detached from the syringe during the experiment owing to the high viscosity of the PYR formula.

Table 9 The Injectability properties of solvents, oils, free-drug loaded ERS based formulation and DH-loaded ERS based formulation (n = 3)

Formulation	Injectability Force± S.D. (N)	Injectability AUC ± S.D. (N.sec)
DMSO	$1.28 \pm 0.17^{d,e,i,j}$	$2.65 \pm 0.47^{l,m,p,q}$
PYR	$2.38 \pm 0.06^{d,e,i,j}$	$39.92 \pm 0.21^{l,m,p,q}$
Olive oil	$15.7 \pm 0.36^{f,g,i,j}$	$118.49 \pm 10.50^{n,p,q}$
Camelia oil	$10.26 \pm 0.39^{f,g,i,j}$	$98.79 \pm 13.41^{n,p,q}$
Free-drug loaded ERS based formulation		
F1	$51.63 \pm 4.28^{d,f,h,i,k}$	$331.68 \pm 16.42^{l,o,p}$
F3	N/A	N/A
F5	$29.45 \pm 3.86^{d,f,h,j,k}$	$195.98 \pm 11.34^{l,o,q}$
F6	$32.07 \pm 4.86^{d,f,h,j,k}$	$250.46 \pm 9.33^{l,o,q}$
F9	$42.90 \pm 7.71^{d,f,h,j,k}$	$323.31 \pm 16.18^{l,o,q}$
F10	$47.78 \pm 3.53^{d,f,h,j,k}$	$367.12 \pm 14.37^{l,o,q}$
DH-loaded ERS based formulation		
F2	$82.92 \pm 4.46^{e,g,h,i,k}$	$732.97 \pm 25.63^{m,n,o,p}$
F4	N/A	N/A
F7	$48.65 \pm 3.43^{e,g,h,j,k}$	$388.91 \pm 18.91^{m,n,o,q}$
F8	$54.11 \pm 2.93^{e,g,h,j,k}$	$486.36 \pm 30.66^{m,n,o,q}$
F11	N/A	N/A
F12	N/A	N/A

N/A = not available

The superscripts d-q indicate a significant different (p<0.05) by using one-way ANOVA followed by LSD post-hoc test.

4.1.3.4. Size of microparticles

Practically, ISM systems have been generated to reduce the burst release and viscosity of the injectable implants. To evade the inconvenience of large implant insertion, the ISM size should be less than 250 μm or ideally less than 125 μm in diameter [5]. In this study, the diameter of emulsion droplets and the microparticles after contacted with distilled water and transformed into solid particles were measured under the inverted microscope as shown in Table 10. For free drug-loaded formula, the size of emulsion droplets of F9 and F10 were 88.34 and 144.33 μm in diameter, respectively, which systems containing PYR as the internal phase presented the smaller size than F5 and F6 containing DMSO which were186.19 and 234.26 μm in diameter since high viscosity of PYR maintained the stability of formula better than less viscous solvent. The use of olive oil as dispersed phase decreased the size of the droplets due to its high viscosity which reduced the velocity of coalescent phenomena between the droplets and maintained the small size of the particle [103]. Moreover, the DH-loaded formula also showed the same trend as the free drug-loaded formula. The presence of DH reduced the size of both emulsion and microparticle related to the viscosity results since the DH-loaded formula illustrated higher viscosity than the free-drug formula. Notably, microparticles significantly exhibited smaller sizes than emulsion forms (95% confidential interval) by the reason of the solvent exchange mechanism which the drug and solvents leaking from the internal phase thereafter diffused out to the environments more than the adversative diffusing water leading to shrinking of the microparticle size [25].

Table 10 The diameter of free-drug loaded ERS based formulation and DH-loaded ERS based formulation in emulsion and microparticle form (n = 150)

Formulation	Diameter ± S.D. (μm)	
	Emulsion form	Microparticle form
Free-drug loaded ERS based formulation		
F5	186.19 ± 17.83*	159.08 ± 10.68*
F6	234.26 ± 20.74*	198.07 ± 14.93*
F9	88.34 ± 12.67*	81.72 ± 14.35*
F10	144.33 ± 15.36*	85.00 ± 13.69*
DH-loaded ERS based formulation		
F7	158.01 ± 14.21*	115.82 ± 13.75*
F8	86.99 ± 8.52*	76.94 ± 8.31*
F11	67.85 ± 7.59*	69.11 ± 9.38*
F12	81.12 ± 6.41*	78.43 ± 4.36*

*Indicate a significant different at 95% confidential interval between the size of ISM emulsion and microparticle form by using paired T-test analysis.

4.1.3.5 Drug release

In this experiment, all PYR formula were cut out since the formula containing PYR exhibited high viscosity, hard injection through 27 guage needle and retarded in transformations and that not proper for use in dentistry as an injectable local drug for periodontitis, thus F7 and F8 which were ISM containing DMSO in different external oil were selected for further study. The drug release study was performed by using the dialysis method employing 10% w/w DH in DMSO and PYR as control groups. DH from both control formula was completely released within 8 h with the burst release at the initial phase of the drug whereas F7 and F8 showed more retardation of drug release

up to 20 hr and the initial burst drug release was disappeared as presented in Figure 16 due to phase separation into matrix of ERS which is the well-known as controlled release polymer [104] and the outer oil phase performed as the barrier for drug liberation. However, F7 and F8 containing different external oil phases exhibited nearly identical released patterns which revealed that olive oil and camellia oil insignificantly influenced on DH released. ISM formula was fitted to mathematical release models in which the estimated r^2 and msc are shown in Table 11. The high value of these parameters determined the superiority of the release profile fitting to the mathematical release model. F7 and F8 also fitted well with first-order model and both of them are Fickian diffusion which the rate of drug release is independent of the drug concentration.
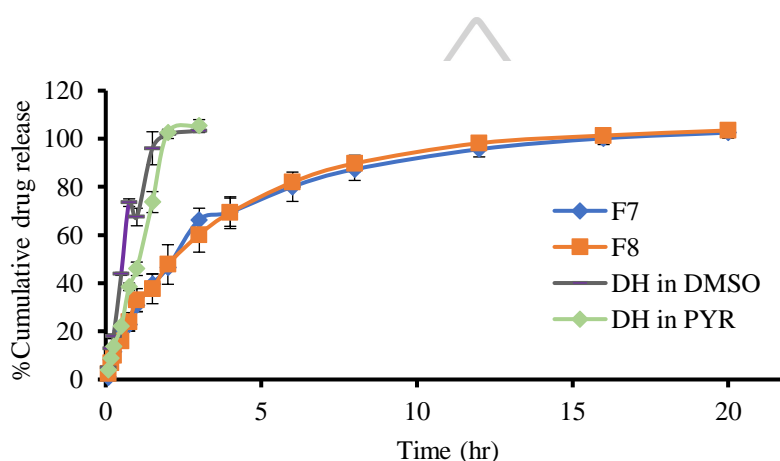
Figure 16 Release of DH from ISM dissolved in DMSO in different oil (n = 3)

Table 11 Comparison of degrees of goodness-of-fit from curve fitting of release profiles of DH released from ISM in PBS pH 6.8 using the dialysis membrane method for different release models.

Formula (%w/w)	First order		Higuchi's		Zero order		Power law			Release mechanism
	cd	msc	cd	msc	cd	msc	cd	msc	n± S.D.	
F7	0.9965	5.39	0.9268	2.35	0.7650	1.18	0.9645	2.91	0.3549 ± 0.0305	Fickian
F8	0.9920	4.56	0.9163	2.21	0.7559	1.14	0.9634	2.88	0.3428 ± 0.0305	Fickian

4.1.3.6 *In-vitro* weight loss

The *in-vitro* weight loss test usually measured the weight before and after drug release to observe the weight loss and the degradation of the formulation which related to the release kinetics and also the safety of the formulation. The free-drug-loaded ERS based formula presented greater weight loss than the drug-loaded formula, as illustrated in Table 12, owing to the lower viscosity of the formula, in which the molecular bond between the polymer was easily broken [105]. Moreover, the ISM formula exhibited less weight loss than the ISG since the outer oil phase prevented the formula from

dissipating [5]. The different solvents presented no significant difference in weight loss of both ISG and ISM.

Table 12 The degradation of free-drug loaded ERS based formulation and DH-loaded ERS based formulation after drug release (n = 3)

Formulation	Weight loss (%)
Free-drug loaded ERS based formulation	
F1	12.36 ± 0.35
F3	10.78 ± 1.55
F5	8.62 ± 0.27
F6	8.87 ± 0.75
F9	5.41 ± 0.33
F10	5.21 ± 0.12
DH-loaded ERS based formulation	
F2	2.11 ± 0.32
F4	2.15 ± 0.40
F7	1.98 ± 0.41
F8	1.88 ± 0.33
F11	1.87 ± 0.46
F12	1.85 ± 0.67

4.1.3.7. Antimicrobial test

The inhibition zone diameter of the pure solvent, DH dissolved in a different solvent and ISM formula against *S. aureus*, *E. coli*, *S. mutans*, and *P. gingivalis* are shown in Table 13 and Figure 17A-B. Pure solvents presented no inhibition zone that occurred against *Streptococcus* spp. and both solvents showed the inhibition zone against *E.coli* because high concentration of DMSO induces the cell shrinkage which can lead to cell death [106] and PYR compose of 5-membered lactam ring similar to *N*-methyl pyrrolidone (NMP) which enhanced the permeability of antimicrobial drug into microbe *via* interfering the RND type efflux pump of multidrug resistance *E.coli* . Only PYR presented the inhibition zone against *P. gingivalis* which is an anaerobic pathogen. The positive control which is DH in DMSO and PYR showed the inhibition zone against all bacteria which inhibited *E. coli* > *P. gingivalis* >*S. aureus* >*S. mutans* as following especially *E. coli* [107] which DH in PYR exhibited the most effective inhibition in microbes. In the case of ISM, all formula showed the inhibition zone against all bacteria in which the DMSO formula exhibited effectiveness over PYR against *S. mutans* and *P. gingivalis* whereas PYR showed better inhibition in the others which related to the control group results.

Table 13 Inhibition zone diameter of DH-loaded ISM containing different solvent and oil against *S. aureus*, *S. mutans*, *P. gingivalis* and *E. coli* (n=3)

Formula	Inhibition zone (mm)			
	S. aureus	*S. mutans*	*P. gingivalis*	*E. coli*
F7	14.67 ± 0.33^a	11.22 ± 0.38^c	17.00 ± 0.33	18.11 ± 0.19
F8	15.89 ± 0.19^b	11.11 ± 0.19^d	17.33 ± 0.33	15.11 ± 0.19
F11	13.67 ± 0.33^a	4.00 ± 0.67^c	20.78 ± 0.19	18.70 ± 0.33
F12	13.89 ± 0.19^b	9.22 ± 0.38^d	13.00 ± 0.33	14.78 ± 0.19
DMSO	-	-	-	12.00 ± 0.00
PYR	-	-	19.00 ± 0.00	17.33 ± 0.00
DH in DMSO	$42.33 \pm 0.67^{a,b}$	$30.00 \pm 0.92^{c,d}$	52.33 ± 0.14	52.33 ± 0.67
DH in PYR	$45.67 \pm 0.67^{a,b}$	$31.00 \pm 0.23^{c,d}$	48.33 ± 0.21	53.67 ± 1.40

- No clear zone

The superscripts a, b, c and d indicate a significant different ($p<0.05$) by using one-way ANOVA followed by LSD post-hoc test.

A)

Formula	Inhibition zone			
	S. aureus	*S. mutans*	*P. gingivalis*	*E. coli*
F7				
F8				
F11				
F12				

B)

S. aureus

S. mutans
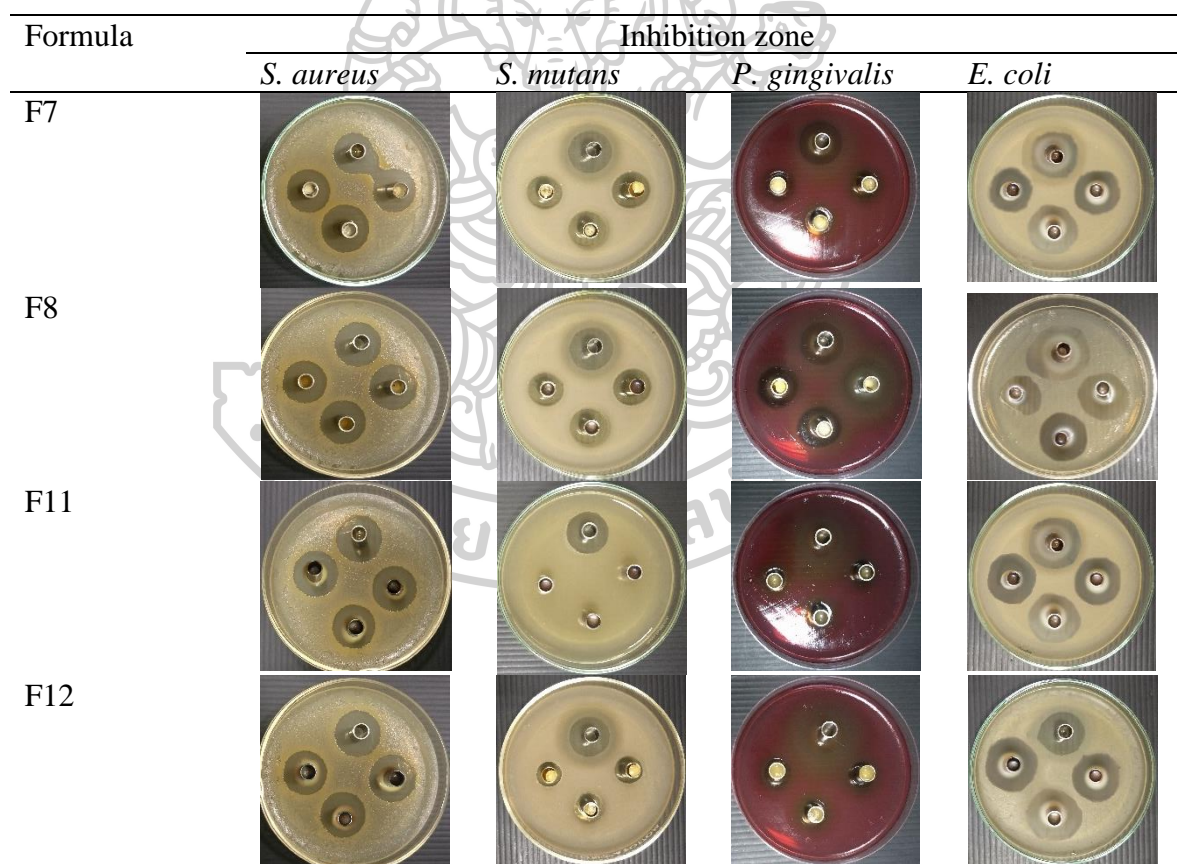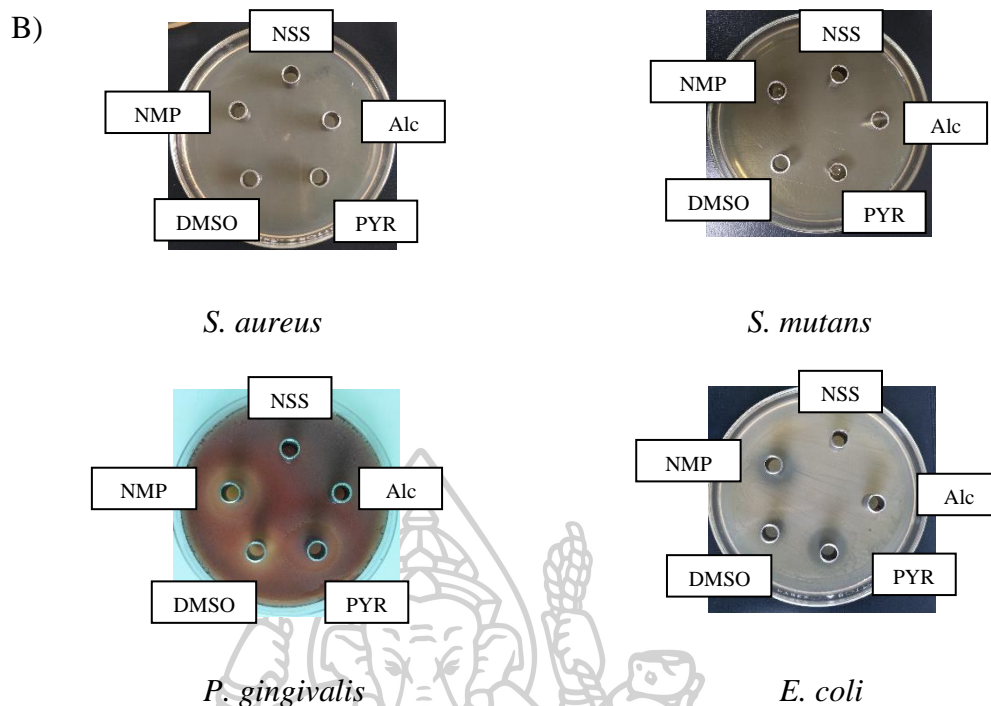
P. gingivalis

E. coli

Figure 17 A) Inhibition zone diameter of DH-loaded ISM containing different solvent and oil and B) Inhibition zone of solvents against *S. aureus*, *S. mutans*, *P. gingivalis* and *E. coli*

4.2 Rosin

4.2.1 Appearance of R-based liquid formulations

According to the solvents screening, physicochemical properties, and injectability results from ERS-based ISG and ISM formulation, the organic solvent which was possible for developing of further study was DMSO since the low viscosity properties affecting the ease of injection. Moreover, olive oil has a similar physicochemical property with camelia oil. It presented the advantages in antimicrobial activities owing to the less amount of unsaturated fatty acid resulting less stearic hindrance to release the drug form ISM formula. Therefore, the composition of R-based ISG and ISM formulation using DMSO as solvent and olive oil as external oil phase were presented in Table 14.

The R-based ISG formulations in DMSO were presented as clear yellowish solutions from the color of R. After mixing with V, all formulations presented a similar appearance to the free drug-loaded formulations. However, the phase separation occurred between the solvent and the oil after emulsifying the ISM. The 20 and 30% w/w R exhibited the separation within 5 min; the 40% w/w R presented the separation within 40 min, whereas the 50 and 60% w/w R presented good emulsion stability for longer than 60 min. Thus the 40-60% R were selected for ISM study.

Table 14 Composition formula of system generated from R containing selected solvent, O, GMS and V

Formulation	V	R	Solvent	O	GMS
20RV	1	20	79		
30RV	1	30	69		
40RV	1	40	59		
50RV	1	50	49		
60RV	1	60	39		
20RV ISM	0.5	10	39.5	42.5	7.5
30RV ISM	0.5	15	34.5	42.5	7.5
40RV ISM	0.5	20	29.5	42.5	7.5
50RV ISM	0.5	25	24.5	42.5	7.5
60RV ISM	0.5	30	19.5	42.5	7.5

4.2.2 Evaluation of R-base formulation composition

4.2.2.1 pH measurement

The pH values of the DMSO, ISG and ISM formulations were measured as shown in Table 15. DMSO was alkaline with a pH of 11.20, while ISG and ISM were more acidic (5.02–6.48) owing to abietic acid of R and abietic acid derivatives[39, 66], and HCl of V [65, 67]. Thus, the pH value decreased after adding increasing amounts of R in the presence of V. However, ISM had a slightly higher pH than ISG at the same concentration of R, as olive oil has a low a low acidic value of 0.8 and interferes with the diffusion of vancomycin HCl [74]. In general, V presented good pH stability of 3.0–5.7 [65, 67]. Therefore, the V-loaded R-based ISG and ISM formulations were appropriated for V stability. Moreover, these formulations are possible to use in periodontal pocket patient as mention.

Table 15 The pH of R-based ISG and ISM (n = 3)

Formulation	pH ± S.D.
20RV	5.89 ± 0.05
30RV	5.56 ± 0.06
40RV	5.17 ± 0.09
50RV	5.15 ± 0.08
60RV	5.02 ± 0.14
40RV ISM	6.48 ± 0.06
50RV ISM	6.46 ± 0.01
60RV ISM	5.93 ± 0.02

4.2.2.2 Viscosity and rheology

DMSO showed low viscosity at 3.53 cps, while ISG and ISM indicated increasing viscosity when the amount of R was increased as shown in Table 16. The 20-40RV and 40RV ISM formulations exhibited low viscosity (<50 cps), such as 7.49 ± 0.60, 16.57 ± 0.84, 30.64 ± 1.02, and 38.62 ± 1.33 cps, respectively. The 50RV and 50RV ISM formulations had medium viscosity (50–100 cps), such as 59.98 ± 1.77 and

61.11 ± 1.67 cps, while the 60RV and 60RV ISM formulations had high viscosity (>100 cps), (112.45 ± 0.98 and 108.35 ± 2.45 cps), respectively. In comparison, ISM revealed a higher viscosity than ISG in the 40 and 50% R formulations because the viscosity of olive oil is rather high at 60 cps at 25°C [4, 41]. However, at the present 60RV ISM showed a slight decrease in viscosity. Moreover, R concentration below 50% ISM and ISG revealed Newtonian flow of the rheological behavior as presented in Figure 18 except 60% of R which presented the shear thinning behavior in both ISG and ISM.

Table 16 The viscosity of R-based ISG and ISM (n = 3)

Formulation	Viscosity ± S.D. (cps)
DMSO	3.53 ± 0.08
20RV	7.49 ± 0.60
30RV	16.57 ± 0.84
40RV	30.64 ± 1.02
50RV	59.98 ± 1.77
60RV	112.45 ± 0.98
40RV ISM	38.62 ± 1.33
50RV ISM	61.11 ± 1.67
60RV ISM	108.35 ± 2.45
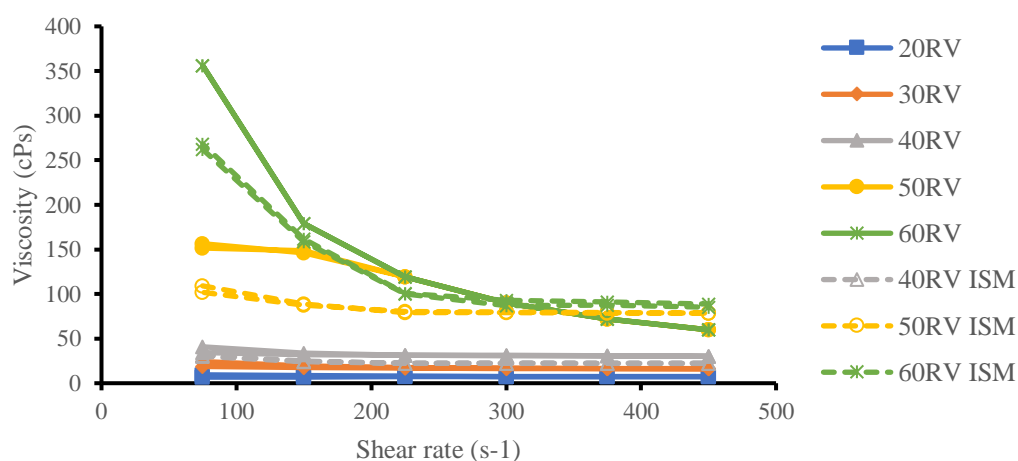
Figure 18 Rheology of V-loaded R based ISG and ISM

4.2.2.3 Injectability test

The injectability test was used to explain the expulsion ability of the formulation out of the syringe and needle while pressing the syringe plunger at the injection site [4, 41]. In this study, a 27 gauge needle was used as the common needle size for injecting drugs into the gum cavity [42]. The results showed that most of the ISG and ISM formulations had a lower injection force (<10 N), as presented in Table 17, which indicated that they were easy to inject except 60RV in which the needle detached during the experiment because of the high friction force between the formulation and the barrel [108]. However, when preparing the external phase to generate ISM, 60RV ISM was

the easiest to inject with a force of 16.83 N, as olive oil has a lubricating effect, which reduces the friction force [109]. In contrast, the injection forces of the 40RV ISM and 50RV ISM formulations were slightly higher than those of ISG due to the high viscosity of the olive oil which agrees with the viscosity results. Additionally, the work of injecting the formula also showed a similar trend as presented in Table 17 in which more work was required to inject a higher amount of R.

Table 17 The Injectability properties R-based ISG and ISM formulation (n = 3)

Formulation	Injectability Force (N)	Injectability AUC (N.sec)
20RV	1.10 ± 0.01	20.59 ± 0.42
30RV	2.73 ± 0.12	37.89 ± 2.24
40RV	3.10 ± 0.04	56.19 ± 0.57
50RV	7.98 ± 0.17	140.48 ± 5.29
60RV	N/A	N/A
40RV ISM	5.36 ± 0.02	92.24 ± 2.58
50RV ISM	8.31 ± 0.73	135.32 ± 3.75
60RV ISM	16.83 ± 1.14	272.89 ± 17.69

N/A = not available

4.2.2.4 Adhesion properties

A local drug delivery system for treating periodontal disease needs to be inserted into the gum cavity to eliminate bacteria. After insertion, the drug is removed by a chemical reaction and mechanical circulation of the saliva [110]. An adhesion test was performed to observe attachment between the formulation and the gum [4, 80]. The circular well of a 0.6% w/w agarose gel represented the periodontal pocket. After the formulation was injected into the well for 1 week, a spherical cylindrical probe was pressed into the setting formulation, which represented the force from chewing and saliva circulation. As shown in Table 18, the 20RV formulation presented the highest maximum force, owing to the fastest transformation of the formula *via* a solvent exchange mechanism [25, 111]. Moreover, increasing the R concentration reduced the maximum force for ISG and ISM because the hardened R prevented solvent exchange [25]. ISM showed a lower maximum force than ISG because the external phase interfered with solvent exchange [25]; thus, the formula was softer than ISG after transformation. ISM presented a higher adhesion force than the ISG, indicating that ISM have better attachment to the periodontal pocket than the ISG and the 40RV ISM formulation presented the highest force. The effect of R concentration in ISM showed a similar trend to maximum force because of less solvent exchange. Surprisingly, the adhesion force of the ISG was not different in the 40 to 60RV formulations. The remaining force after pressing the probe for 60 s revealed that a high concentration of R represented the low remaining force in both the ISG and ISM. After calculating the elasticity properties, all of the formulations had better plasticity properties than elasticity because the value of the elasticity/plasticity ratios were less than 1; thus, they could easily adapt to the specific shape of a patient's periodontal pocket [80].

Table 18 Adhesion properties of the Rosin based ISG and ISM formulations (n = 3)

Formulation	Adhesion properties			
	Maximum force (N)	Adhesion force (N)	Remaining force (N)	Elastic properties
20RV	3.786 ± 0.172	−0.026 ± 0.010	1.364 ± 0.244	0.36
30RV	3.579 ± 1.170	−0.002 ± 0.001	2.123 ± 0.773	0.59
40RV	0.856 ± 0.065*	−0.050 ± 0.001*	0.057 ± 0.026	0.07
50RV	0.737 ± 0.084*	−0.051 ± 0.001*	0.052 ± 0.003	0.07
60RV	0.420 ± 0.043*	−0.053 ± 0.002*	0.026 ± 0.005	0.06
40RV ISM	1.227 ± 0.329*	−3.4658 ± 0.517*	1.128 ± 0.350	0.91
50RV ISM	0.133 ± 0.077*	−2.010 ± 0.525*	0.003 ± 0.002	0.03
60RV ISM	0.060 ± 0.016*	−0.192 ± 0.019*	0.005 ± 0.001	0.08

* indicate a significant difference at 95% confidential interval between ISG and ISM maximum and adhesion force in adhesion properties by using independent t-test analysis.

4.2.2.5 Size of ISM

The diameters of ISM in the emulsions and microparticles were measured under the inverted microscope as presented in Table 19. The diameters of both forms were < 250 µm which is the actual size of microparticles [112]. The sizes of the 40RV, 50RV, and 60RV emulsions were 98.48 ± 16.11, 125.55 ± 4.75, and 137.80 ± 16.8 µm, respectively. The microparticles were smaller in diameter in the 40RV ISM, 50RV ISM, and 60RV ISM formations, such as 78.63 ± 12.97, 93.81 ± 10.53, and 118.32 ± 15.61, respectively, because the particles shrank due to the loss of solvent from the solvent exchange mechanism. Moreover, increasing the concentration of R increased the size of both forms as follows: 40% < 50% < 60% (w/w).

Table 19 The diameter of emulsion and microparticle form R-based ISM formulation (n=3)

Formulation	Diameter (µm)	
	Emulsion form	Microparticle form
40RV ISM	98.48 ± 16.11*	78.63 ± 12.97*
50RV ISM	125.55 ± 4.75*	93.81 ± 10.53*
60RV ISM	137.80 ± 16.84*	118.32 ± 15.61*

* Indicates a significant difference at 95% confidence interval between the size of ISM emulsion and microparticle form by using a paired t-test analysis.

4.2.2.6 Drug release

In this study, drug release was performed using the dialysis method, as illustrated in Figure 19. V dissolved in DMSO was used as an internal control. As results, V in DMSO released within 6 h, while both the ISG and ISM formulations delayed drug release by 7 days. The higher concentration of R resulted in a greater delay of drug release from the ISG and ISM, particularly in the 60% R. The 40RV ISM and 50 RV ISM exhibited a greater delay in drug release than ISG owing to the outer oil phase which retarded solvent exchange and drug release. Thus, these results agreed with the adhesion properties and transformation results. However, 60% R was not different in the ISG and ISM. The cumulative drug release of the 40–60% R formulations did not reach 100% in either the ISG or ISM because some of the drugs were trapped in the matrix and microparticles due to the blockage by hardening R. The low concentration region of R, including V in DMSO, 20RV, 30RV and 40 RV presented first-order release. In contrast, the 50RV, 60RV and ISM formulations presented with Higuchi's

release kinetics, as shown in Table 20, which means that the rate of drug diffusion from the ISG matrix and ISM was greater than matrix degradation [113]. Moreover, the ISG formulations presented a non-Fickian release mechanism, whereas all of the ISM formulations exhibited the Fickian release mechanism because the R relaxation time is much greater than the characteristic solvent diffusion time [114].
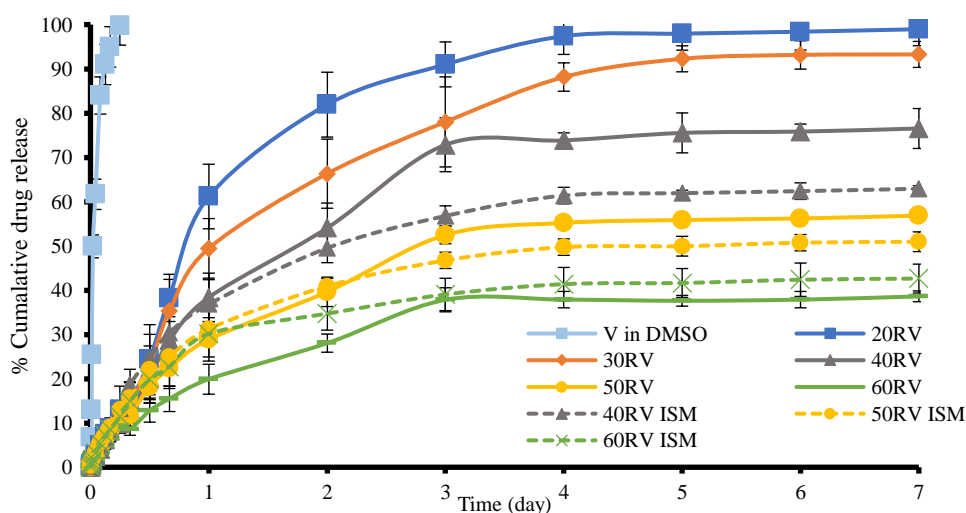
Figure 19 Release of V from DMSO, ISG, and ISM formulations containing rosin as the matrix using the dialysis method (n = 3)

Table 20 Comparison of the degrees of goodness-of-fit from curve fitting the release profiles of V released from ISG and ISM in PBS pH 6.8 using the dialysis membrane method for the different release models.

Formula	Zero order		First order		Higuchi's		Power law			Release
(%w/w)	cd	msc	cd	msc	cd	msc	cd	msc	n± S.D.	mechanism
V in DMSO	0.7061	0.9135	0.9850	3.9777	0.8905	1.9892	0.9089	2.0846	0.4035 ± 0.075	Fickian
20RV	0.8602	1.7970	0.9899	4.4740	0.9437	2.7598	0.9495	2.8144	0.5763 ± 0.075	Non-fickian
30RV	0.8991	2.1226	0.9947	5.1257	0.9615	3.1398	0.9727	3.4319	0.5947 ± 0.075	Non-fickian
40RV	0.8960	2.0923	0.9816	3.8771	0.9615	3.1384	0.9714	3.3842	0.5894 ± 0.075	Non-fickian
50RV	0.8860	2.0004	0.9235	2.4528	0.9772	3.6630	0.9787	3.6774	0.5408 ± 0.075	Non-fickian
60RV	0.8710	1.8772	0.8678	1.9058	0.9749	3.5668	0.9742	3.4882	0.5231 ± 0.075	Non-fickian
40RV ISM	0.8083	1.4811	0.8660	1.8920	0.9572	3.0330	0.9556	2.9443	0.4762 ± 0.075	Fickian
50RV ISM	0.7828	1.3560	0.7715	1.3585	0.9484	2.8475	0.9539	2.9061	0.4415 ± 0.075	Fickian
60RV ISM	0.7383	1.1698	0.6725	0.9987	0.9245	2.4661	0.9413	2.6643	0.4131 ± 0.075	Fickian

4.2.2.7 *In-vitro* weight loss

V-loaded R-based ISG presented greater weight loss than ISM formula (Table 21), owing to the outer oil phase preventing the formula from dissipating. Moreover, increasing the concentration of R also minimized the dissipating since the higher

viscosity resulting high intermolecular force. Therefore, 60RV ISM presented the lowest dissipating. The presence of the outer oil phase in ISM exhibited no significant difference in weight loss of both ISG and ISM at a 95% confidential interval.

Table 21 The degradation of V-loaded R based ISG and ISM formulation after drug release (n = 3)

Formulation	Weight loss (%)
20RV	53.93 ± 4.01
30RV	53.04 ± 1.94
40RV	25.54 ± 0.91
50RV	22.97 ± 3.49
60RV	7.21 ± 0.52
40RV ISM	15.75 ± 2.12
50RV ISM	13.79 ± 1.32
60RV ISM	4.15 ± 0.58

4.2.2.8 Antimicrobial activities

Typically, the localized drug delivery formulation has antimicrobial activities against pathogens to treat periodontal disease [115]. It has been reported that 1% V oral paste applied to periodontal patients reduces the plaque score and gingivitis [116]. In this study, V-loaded ISG and ISM were tested for their antimicrobial activities against *S. aureus*, *S. mutans*, *P. gingivalis,* and *E. coli* (Table 22 and Figure 20). NSS was used as the negative control, which developed no inhibition zone against any of the microbes. DMSO resulted in an inhibition zone against 4 microbes because a high concentration of DMSO leads to cell shrinkage [117]. VD also presented an inhibition zone, which was more effective than pure DMSO against 4 microbes because DMSO enhances drug transport into bacterial cells [40, 118]. Both ISG and ISM showed the inhibition zones against *S. mutans* and *P. gingivalis*. Increasing the amount of R exhibited less inhibition zone for killing bacteria due to delayed drug release. The ISG also developed an inhibition zone against *S. aureus*, whereas only the 40RV ISM formulation revealed antimicrobial activity. Moreover, the ISG formulation with a low concentration of R inhibited *E. coli*, while none of ISM formulations were effective.

Table 22 Inhibition zone diameters of NSS, DMSO, V-loaded ISG and the ISM formulations containing rosin as the matrix against *S. aureus*, *S. mutans*, *P. gingivalis*, and *E. coli* (n = 3)

Formula	Inhibition zone (mm)			
	S. aureus	*S. mutans*	*P. gingivalis*	*E. coli*
NSS	-	-	-	-
DMSO	12.67 ± 0.58	11.00 ± 0.00[a]	13.67 ± 1.15[d]	12.00 ± 0.00
VD	23.67 ± 0.58	22.67 ± 0.58[a,b,c]	23.00 ± 0.00[d,e,f]	13.67 ± 0.58
20RV	23.33 ± 0.58	22.00 ± 0.00[b]	18.33 ± 0.58[e]	12.33 ± 0.58
30RV	22.67 ± 1.15	18.67 ± 0.58[b]	18.00 ± 0.00[e]	11.33 ± 0.58
40RV	14.67 ± 0.58	14.33 ± 0.58[b]	14.67 ± 0.58[e]	-
50RV	11.67 ± 0.58	11.67 ± 0.58[b]	12.67 ± 0.58[e]	-
60RV	11.00 ± 0.00	11.00 ± 0.00[b]	11.67 ± 0.58[e]	-
40RV ISM	10.00 ± 0.00	15.00 ± 0.00[c]	13.67 ± 0.58[f]	-
50RV ISM	-	13.67 ± 0.58[c]	12.00 ± 0.00[f]	-
60RV ISM	-	12.67 ± 0.58[c]	11.67 ± 0.58[f]	-

- No inhibition zone; NSS = Normal saline solution; the superscripts a–f indicate a significant difference (p < 0.05) by using one-way ANOVA followed by an LSD post-hoc test.

Formula	Inhibition zone			
	S. aureus	*S. mutans*	*P. gingivalis*	*E. coli*
20RV				
30RV				
40RV				
50RV				
60RV				
40RV ISM				
50RV ISM				
60RV ISM				
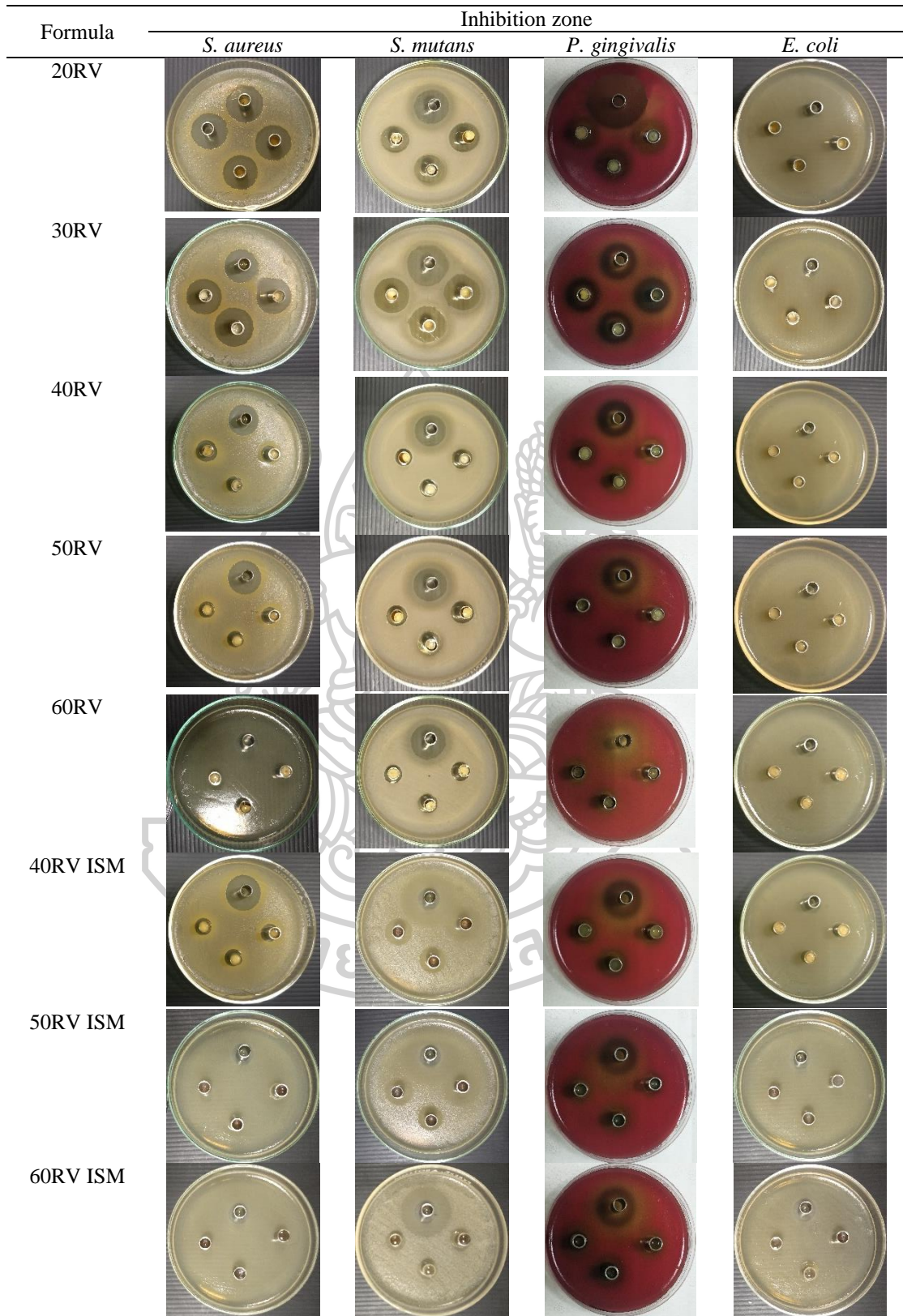
Figure 20 Inhibition zone diameters of V-loaded R based ISG and the ISM formulations against *S. aureus*, *S. mutans*, *P. gingivalis*, and *E. coli* using agar cup diffusion technique

Summary
part 1

In this study, three universal organic solvents using in medication were screened for developing the ISM formulation. DMSO and PYR presented the immiscible with oil that appropriated to generate emulsion form of ISM. In addition, both solvents could dissolve the model polymer and the drug. ERS was developed as matrix former for ISG and ISM formulations to deliver DH for local treating the periodontitis disease. Free-drug loaded ISG and ISM formula exhibited the pH 7.50-9.82 owning to alkaline properties of the solvents. However, the pH significantly decreased to 3.18-3.35 since the presented of DH which has the acidic properties nearly to the GCF pH values. ERS based ISG and ISM also revealed the lower viscosity and ease of injection of DMSO-based formulations made them more suitable as local ISG and ISM injection than PYR-based ones. Moreover, ISM showed advantages over ISG in injectability because of the lubricity effect from the external oil phase. ISM comprising olive oil and camellia oil as the external phase of emulsion exhibited similar results in easier injection, rapid phase transformation, and 7-days prolonged drug release. These DH-loaded ERS ISMs prolonged DH release and exhibited efficient antibacterial activity against periodontal pathogens. Rosin, the natural resin, were also developed as matrix former of ISG and ISM formulation comprising V as model drug by using DMSO as solvent and olive oil as external oil phase. V-loaded R based ISG and ISM formulations exhibited low pH 5.02-6.48 owing to abietic acid of R, abietic acid derivatives, and HCl of V. ISM presented slightly higher in pH due to the low acidic value of the olive oil the ease of injection with an injection force of less than 20 N. ISM exhibited less work of injection than ISG owing to the lubricity effect of the external oil phase. Their phase transformation was attained from solution and emulsion into a gel state and matrix comprising microparticles, respectively, after contact with an aqueous environment. The resin solution and emulsion droplets were hardened because of the precipitation of rosin. The obtained microparticles were significantly smaller in diameter than that of emulsion droplets because of the particle shrinkage from solvent loss during solvent exchange. Increasing the concentration of rosin enlarged the size of ISM. The 40RV ISM presented the highest adhesion force with the plasticity property of being easily adapted to an injection site such as the periodontal pocket. Furthermore, ISM illustrated more retardation of drug release than ISG owing to the presence of an external oil phase. Additionally, both ISG and ISM had antimicrobial activities against *S. mutans* and *P. gingivalis*, indicating the possibility for periodontal pocket drug delivery to increase the effectiveness of periodontitis treatment and reduce drug side effects. Although the materials of composition are safety for human used, the cytotoxicity should be considered test. Moreover, the clinical efficacy of the formulations should be further study.

Part 2
Transformation mechanism

4.3 Density of oils and solvents

Density is mass of unit volume of the material substance. Density is an essential measurement of how tightly matter is crammed together. It is the crucial factor affecting the physicochemical properties of the chemical substance such as the contact angle, surface tension and interfacial tension. In this study, the densities of the related solvents were measured by the densitometer at room temperature which the obtained values are shown in Table 23. PBS presented the density of 1.0035 g/cm^3 which was nearly the reverse osmosis RO water's density (1.0001 g/cm^3) and higher than the oils. PYR revealed the highest density (1.1061 g/cm^3) followed by DMSO (1.0935 g/cm^3) which were higher than that of the PBS solution.

Table 23 Density of oils and solvents (n=3)

Substance	Density ± S.D. (g/cm^3)
RO water	1.0001 ± 0.0005
PBS pH 6.8	1.0035 ± 0.0005
DMSO	1.0935 ± 0.0005
PYR	1.1061 ± 0.0000
Olive oil	0.9090 ± 0.0005
Camelia oil	0.9103 ± 0.0007

4.4 Contact angle of oils and solvents

Contact angle or wetting angle is determined from the angle of liquid drop in the dome shape place on the surface material. The angle formed between the surface and the line tangent to the edge of the drop of the liquid is called the contact angle [119]. In this study, the contact angle of the oil and solvents were measured on the glass slide surface by the goniometer drop shape analyzer as shown in Table 24 and Figure 21. RO water was measured as the control liquid. It presented the highest contact angle with 52.37° which revealed the hydrophobic property of the glass slide. In contrast, PBS which is the water based presented the rather low angle compared to the RO water due to the negative surface charge of silanol group as present in equation 6 [120]. DMSO and PYR, the polar aprotic solvents, exhibited the contact angle 26.69° and 24.79°, respectively which notably less than RO water about 2 times. However, their angle values were slightly higher than hydrophobic oils which olive oil and camelia oil exhibited the values of 22.38° and 23.52°, respectively.

$$SiOH \rightleftharpoons SiO^- + H^+ \tag{11}$$

Table 24 Contact angle of oils and solvents (n=6)

Substance	Contact angle ± S.D. (degree)
RO water	52.37 ± 2.58
PBS pH 6.8	32.24 ± 0.64
DMSO	26.69 ± 2.52
PYR	24.79 ± 1.12
Olive oil	22.38 ± 2.34
Camelia oil	23.52 ± 1.48

Figure 21 Contact angle of control group: RO water, solvents: PBS pH 6.8, DMSO and PYR, and oils: olive oil and camelia oil.

4.5 Surface tension of oils and solvents

Surface tension is the tendency of liquid surfaces at rest to shrink into the minimum surface area. At liquid–air interfaces, surface tension revealed the greater attraction of liquid molecules to each other (due to cohesion force) than to the molecules in the air (due to adhesion force) [121]. In this context, surface tension in the air at room temperature of control group: RO water, solvents, and oils were studied as presented their interfacial values in Table 25 and Figure 22. The RO water revealed the highest surface tension as 73.71 mN/m since the high intermolecular force from H-bond with the other forces [122] followed by PBS which revealed the 72.82 mN/m. DMSO presented higher surface tension than PYR owing to sulfoxide structure [123] which formed the H-bond and dipole-dipole intermolecular force, while PYR is a 5-membered lactam ring which resulted the less intermolecular force [124]. Notably, olive oil and camelia oil show the similar results as 31.68 and 30.77 mN/m, respectively due to the similar hydrophobic force of their components.

Table 25 Surface tension of oils and solvents (n=6)

Substance	Surface tension ± S.D. (mN/m)
RO water	73.71 ± 0.71
PBS pH 6.8	72.82 ± 0.21
DMSO	39.81 ± 0.58
PYR	35.61 ± 0.13
Olive oil	31.68 ± 0.26
Camelia oil	30.77 ± 0.23

RO water   PBS pH 6.8   DMSO

PYR   Olive oil   Camelia oil
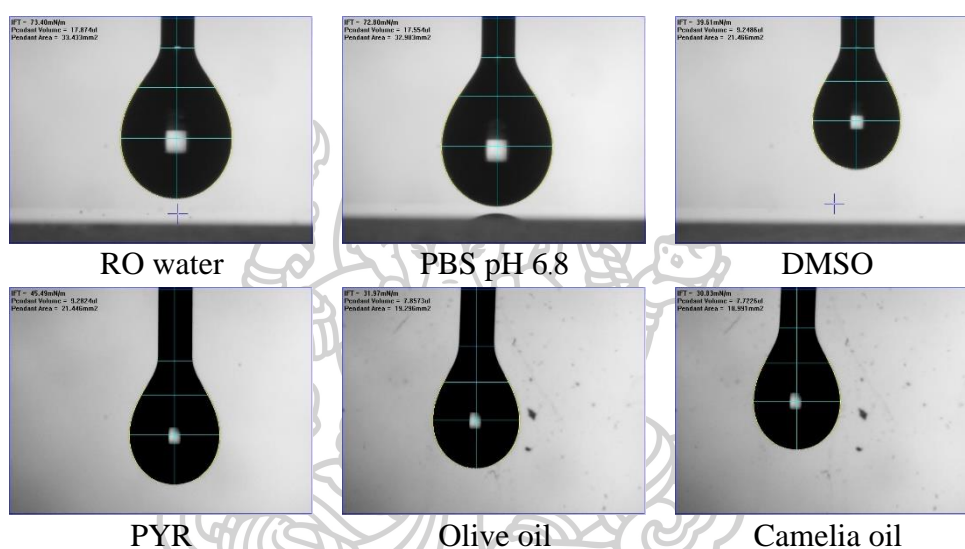
Figure 22 Surface tension in the air of control group: RO water, solvents: PBS pH 6.8, DMSO and PYR, and oils: olive oil and camelia oil.

4.6 Interfacial tension of oils and solvents

Interfacial tension is the force of attraction between the molecules at the interface of two fluids [125]. According to the previous ISM formulation, the polymer dissolving in selected organic solvent was emulsified with olive oil or camelia oil to formulate the emulsion form of ISM. For more clearly understanding of the emulsion form before the transformation process, the interfacial tensions between the selected solvent and the oil was observed using the goniometer drop shape analyzer as shown in Table 26 and Figure 23. RO water presented the highest interfacial tension in camelia oil which was 28.36 mN/m with the big drop shape because of the high polarity of water. The present of electrolyte in PBS resulting in less interfacial tension against the oil which conformed to the contact angle. Surprisingly, both polar organic solvents revealed the lower interfacial tension for 7 times against camelia oil and for 5 times against olive oil compared to the water because of their lower polarity. Therefore, DMSO and PYR illustrated the small drop shape in both oils.

Table 26 Interfacial tension of solvents against olive oil and camelia oil (n=6)

Solvent	Interfacial tension ± S.D. (mN/m)	
	Olive oil	Camelia oil
RO water	20.72 ± 0.05	28.36 ± 0.27
PBS pH 6.8	18.06 ± 0.11	24.23 ± 0.16
DMSO	4.20 ± 0.07	4.64 ± 0.02
PYR	3.44 ± 0.06	3.58 ± 0.01
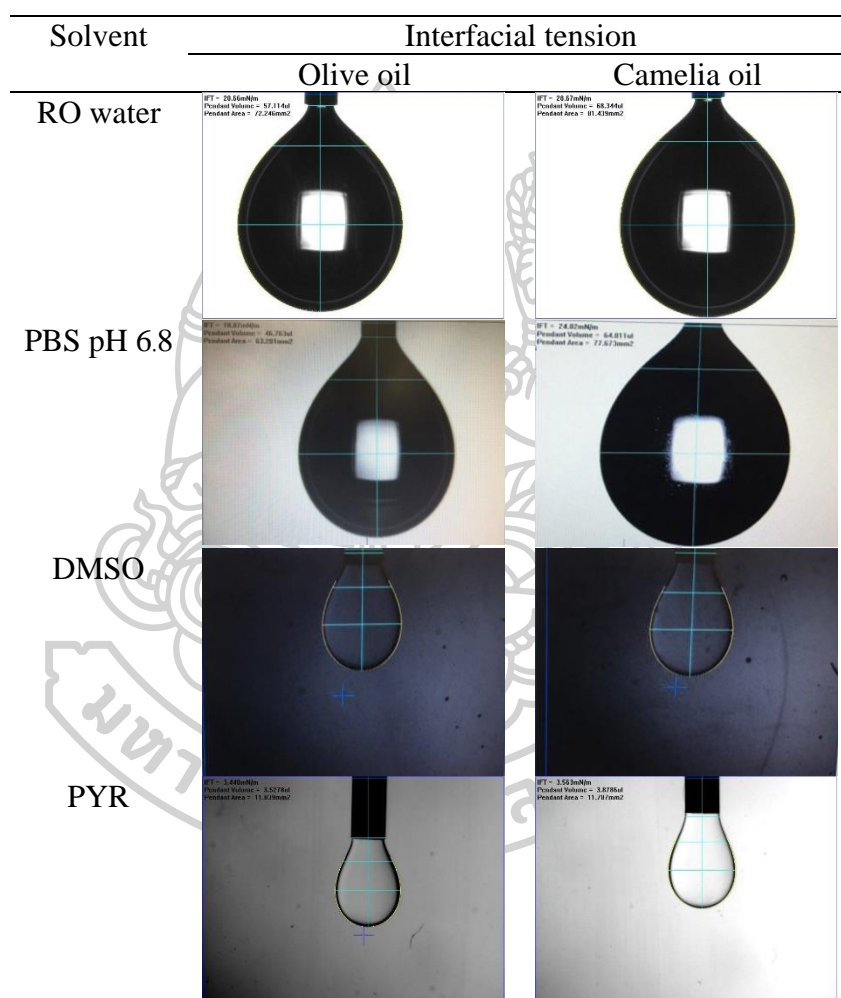
Figure 23 Droplet photograph from interfacial tension measurement of solvents against olive oil and camelia oil (n=6)

4.7 ERS-based ISG and ISM transformation

4.7.1 *In-vitro* ERS-based ISG and ISM formation

This test was performed to observe the transformation of the liquid formula into the solid-like, gel-like or microparticle by visual observation after injection them into PBS pH 6.8 owing to solvent exchange mechanism [8]. The transformation of ISG prepared using different solvents is presented in Fig. 24A. DH-loaded ISG showed the yellow color due to the color of DH. The surface of all formula suddenly turned into solid mass when contacted with PBS and slowly transformed into the gel matrix which exhibited greater opaque with white color. After 10 min, the free drug-loaded formula presented the degradation of the gel matrix whereas DH-loaded ISG remained the shape of the gel matrix similar to initial form. Moreover, DH-loaded ISG exhibited a slower transformation into solid than free-drug formula. These results indicated that the high viscosity of the formula prevented the degradation of the gel matrix and retarded the rate of transformation of the gel [126]. ISM prepared using different solvents and oils are presented in Figure 24B. DH-loaded ISM also showed the yellow color as ISG. After ISMs were injected into PBS, the surface of the formula rapidly turned into solid form and the appearance slowly changed from transparent solution into opaque with white color. Interestingly, some degradation occurred after 30 min since increasing turbidity of PBS was evident. However, ISM degradation was apparently less than ISG because the external oil phase prevented the diffusion of internal solvent and environmental water from the solvent exchange and protected the loss of matrix yield [74]. Owing to the high viscous after DH was incorporated, DH-loaded ISM showed the same trend with ISG for slower transformation into solid than free-drug formula. Moreover, both ISM and ISG containing PYR showed slower transformation than that comprising DMSO. In addition, ISM exhibited more retardation of transformation than ISG since the external oil phase performed as the barrier for water to diffuse into the gel.

For more clear understanding of ISM transformation, DH-loaded ISM fabricated using different solvents and oils were investigated profoundly for their transformation under the inverted microscope as presented in Figure 25. At the initial time, all formula appeared as an emulsion form with the transparent droplets of DH in solvent dispersed in the oil. After contacted with distilled water some droplets of formula became solidify which finally resulted in ERS phase separation into the spherical shape of microparticles [41, 42] and formula using PYR as solvent showed a slower transformation than that using DMSO as solvent. The logP of DMSO and PYR are -13.5 and -0.85 respectively [91, 127], which indicated that DMSO is more hydrophilicity than PYR leading to a fast solvent exchange with environmental water and thereafter rapid phase separation of polymer.

A

Formula	Time (min)				
	0	5	10	30	60
F1					
F2					
F3					
F4					

B

Formula	Time (min)				
	0	5	10	30	60
F5					
F6					
F7					
F8					
F9					
F10					
F11					
F12					

Figure 24 Transformation of free-drug and DH-loaded ISGs containing different
solvents (A); free-drug and DH-loaded ISM containing different solvents and oils (B)
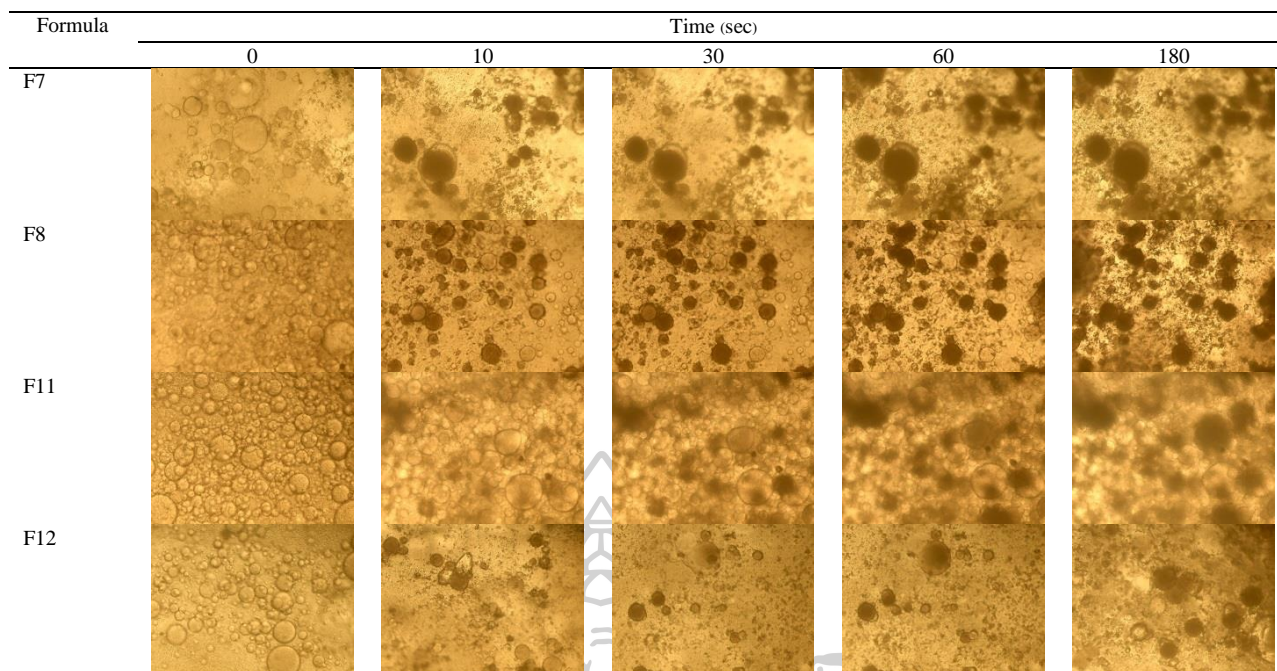
Formula	Time (sec)				
	0	10	30	60	180
F7					
F8					
F11					
F12					

Figure 25 Transformation of DH loaded ISMs in different solvent and oil under an inverted microscope

4.7.2 Rate of water diffusion into the ISG and ISM

When the solvent exchange occurred, the ISGs were transformed into the gel matrix and ISMs were transformed into microparticle due to polymer phase separation. DH-loaded ISM was selected as the model formulation for observing the diffusion rate and length of water diffusion into formulation. Figure 26 presented the visual images of ERS-based ISG and ISM transformation under the stereomicroscope at different times. The opaque ring suddenly appeared after filling ISM in the agarose gel well which represented the phase inversion zone between PBS and ISM and the opaque ring band was increased by time. For more clear vision of diffusion length in ISM formula, amaranth which is the water soluble red dye was added in the agarose gel. The diffusion of PBS with amaranth into ISM formulation illustrated as the red band as shown in Figures 26 of F7, F8, F11, and F12. The diffusion length of the occurred gel and microparticle matrix as shown in Figure 27 was slowly increased owing to barrier effect of the harden matrix and the hydrophobic oil which distance of diffusion length was increased as following F2>F4>F8>F7>F12>F11 indicating that the formulation comprising DMSO exhibited a more diffusion length than that using PYR as the solvent due to its higher polarity of DMSO and apparently less viscosity. Moreover, ISM containing camellia oil exhibited a larger diffusion length than another one because the low viscosity of this oil performed as the loose barrier, thus the water easily diffused into the formula. The diffusion length of ISG and ISM formulas was further calculated into the diffusion rate for a clearer understanding of water diffusion as presented in Figure 28. F4 presented the highest rate of diffusion at the early 5 min and slower by

the time owing to the harden gel matrix whereas F2 presented the slower rate than F4 in the early state. However, after the initial 5 min, ISG using DMSO as solvent exhibited the higher rate of diffusion than that using PYR owing to the high polarity with higher water affinity and less viscosity of DMSO. The diffusion rate of ISM was not different significantly in the early 5 min. The rates were slower by the time since the transformation into the microparticle form was occurred. The solid part interfered the diffusion of water resulting in a decrease in diffusion rate. After 5 min, the diffusion rates showed more clearly different which F8 presented the highest rate conforming with diffusion length, whereas F12 presented the slowest in diffusion rate due to the high viscosity and the camellia oil which has more unsaturated fatty acid than olive oil [102] interfered the water diffusion.
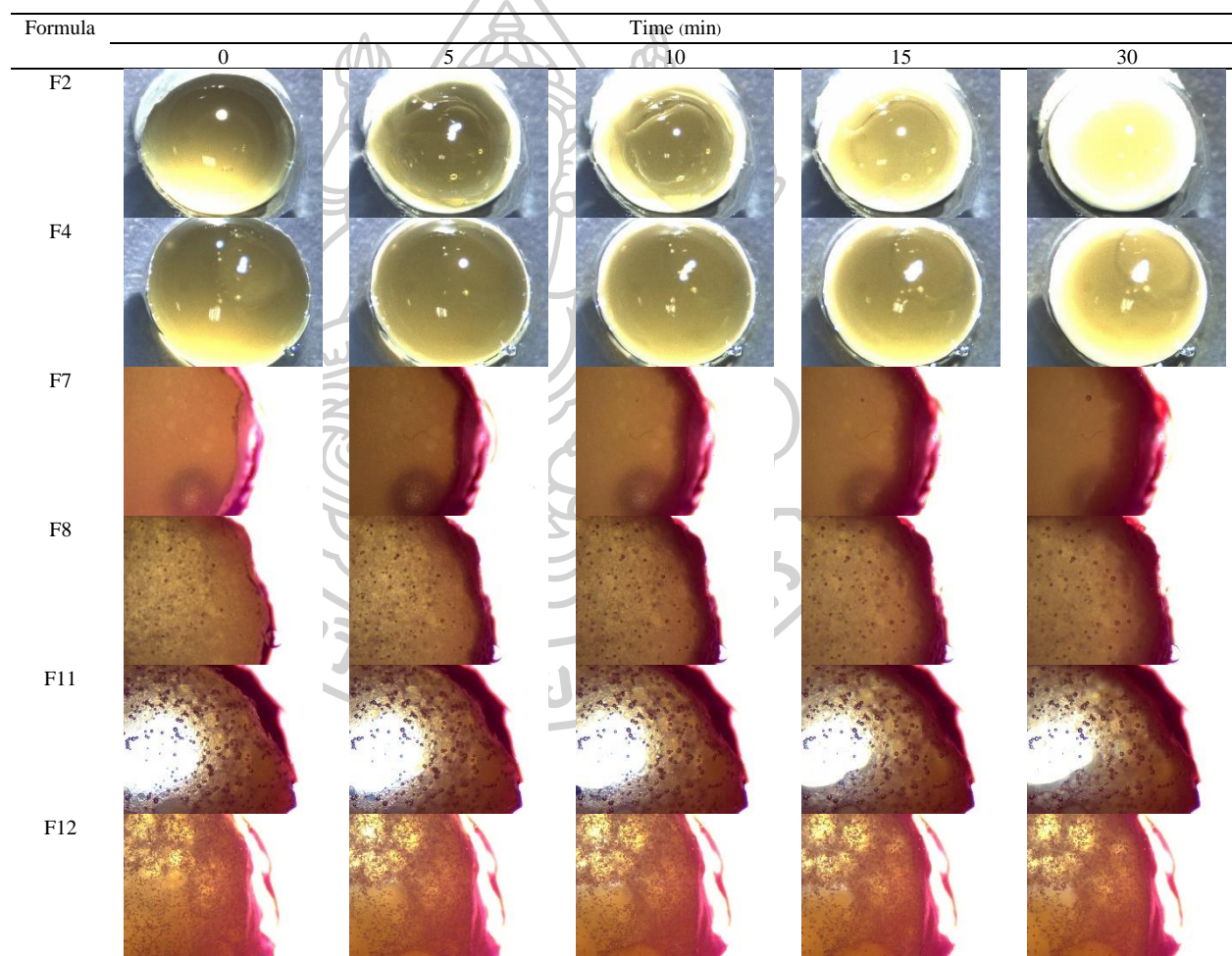
Figure 26 Macroscopic transformation of ERS from ISGs and ISMs under the stereomicroscope (10x) in 0, 5, 10, 20 and 30 min
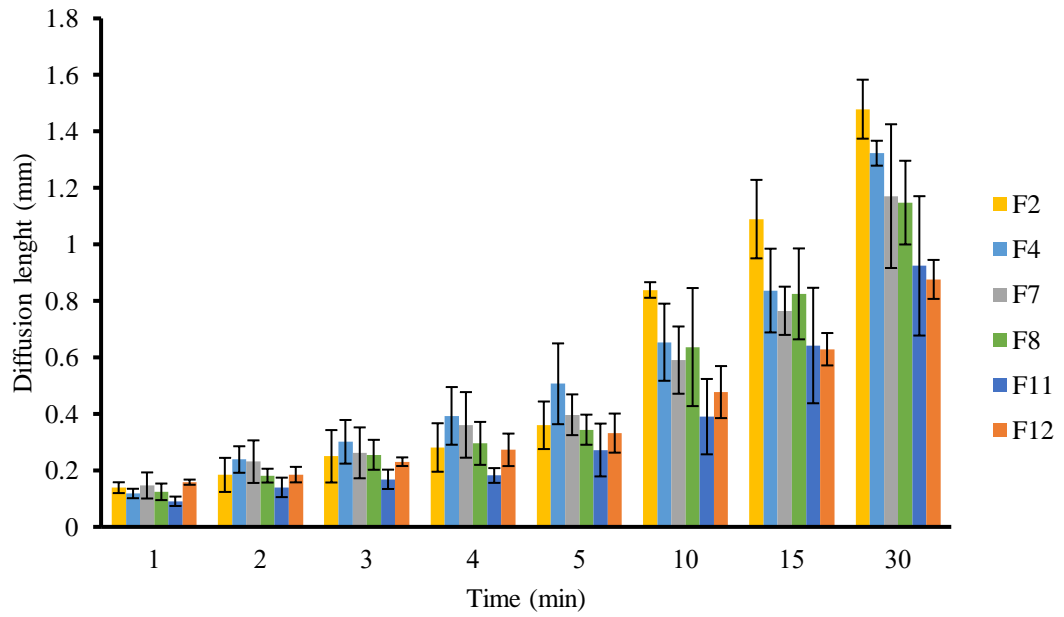
Figure 27 Diffusion length of ERS-based ISG and ISM formula at different time (n=3)
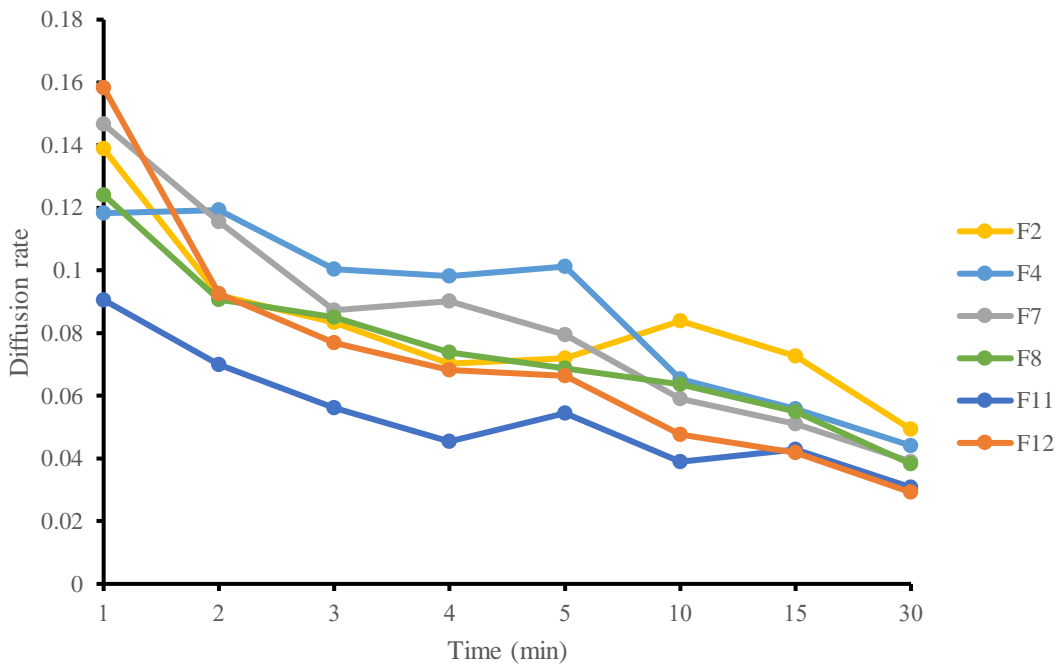
Figure 28 Diffusion rate of ERS-based ISG and ISM formula at different time

4.7.3 SEM morphology

The SEM micrograph of solidified free drug-loaded ISG and ISM were illustrated in Figure 29. The surface of F1 contained several pores and a rough surface whereas F3 showed a smooth surface. The cross-section of F1 showed more numerous pores than F3 indicated that DMSO modified the structures of ERS matrix into sponge-like topography owing to its high polarity leading to the phase separation between polymer and solvent [111]; thus, F3 presented as a dense ERS matrix. In the case of ISM, they exhibited as the spherical shape microsphere with an estimated diameter of 50 μm. They were smaller than that observed under the inverted microscope. The limitations of inverted-microscope was to adjust for focusing before dropping PBS hence some droplet of emulsion merged resulting in enlargement of microparticles. Moreover, some irregular shapes occurred owing to the explosion of microparticles during the freeze-dried process. From surface topography, F5 and F6 presented rough surface with small pore whereas F9 and F10 revealed smoother surface. The ISM prepared using DMSO as solvent showed more porous than that using PYR as solvent in a cross-sectional view which related to ISG topography which confirmed that DH was entrapped inside the microparticle and its release was retarded. Nevertheless, the DH-loaded formula was not determined for their SEM owing to the difficulty in drying after the drug release since some solvent still remained inside the remnants.
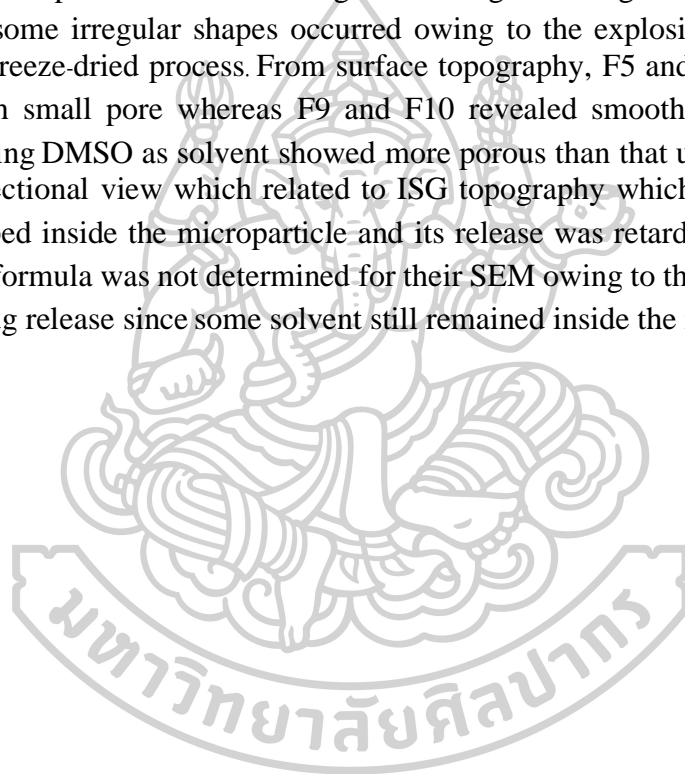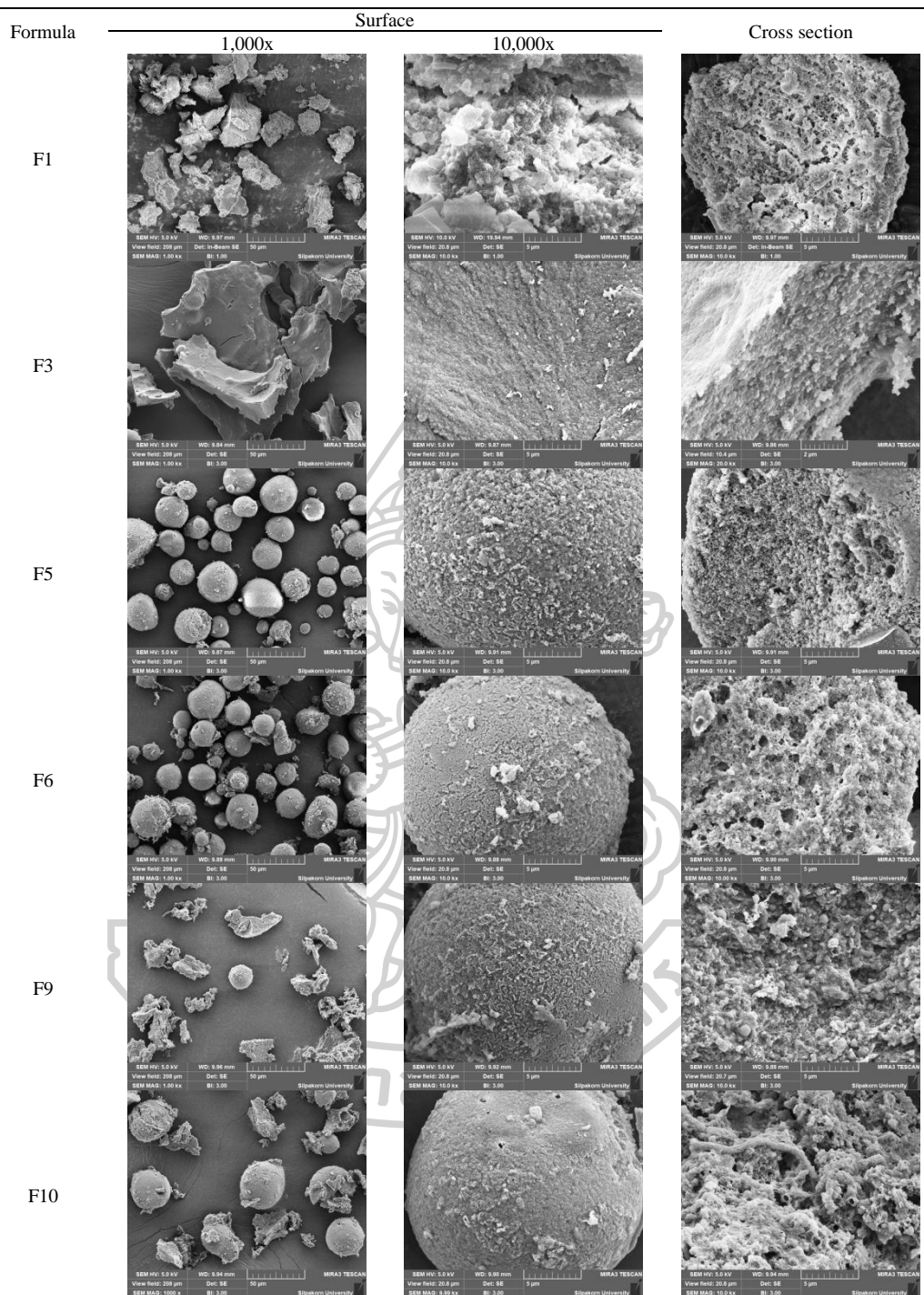
Figure 29 SEM micrograph of surface and cross-section of free drug-loaded ISGs containing different solvents and free drug-loaded ISMs prepared using different solvents and oil.

4.8 R-based ISG and ISM transformation

4.8.1 Density of R-based ISG formulation

The R-based ISG formulation exhibited the density between 1.0943-1.1097 g/cm^3 which slightly higher than neat DMSO and olive oil as presented in Table 27. According to the higher density than the oil, this result showed the possibility to perform the interfacial tension experiment against the oil.

Table 27 Density of oils and solvents (n=3)

Substance	Density ± S.D. (g/cm^3)
20 RV	1.0943 ± 0.0005
30 RV	1.0984 ± 0.0005
40 RV	1.1010 ± 0.0005
50 RV	1.1051 ± 0.0005
60 RV	1.1097 ± 0.0005

4.8.2 Contact angle of R-based ISG formulation

ISG is the polymeric solution containing the insoluble polymer which precipitated after contacting the water. As the internal phase of the ISM formulation, the external oil prevented the burst release and myotoxicity. For the clear understanding of the transformation mechanism of both ISG and ISM the contact angle was performed to explore the wettability of these formula. In this experiment, the glass slide was used as the hydrophobic surface to observe the angle. The solution comprising 20% w/w R showed the lowest contact angle followed by 30RV<40RV<50RV<60RV as presented in Table 28. Apparently, the R concentration less than 40% w/w revealed the lower contact angle than neat DMSO owing to the acidic pH inducing the higher charge density of silica glass resulting more adhesion force between glass slide and the formula [119]. However, the high concentration of R promoted more viscosity; thus their contact angle exhibited the high value than DMSO. Moreover, increasing the amount of R also enhanced the degree of contact angle of formulations which related to the viscosity results.

Table 28 Contact angle of V-loaded R-based ISG formulations (n=6)

Formulation	Contact angle ± S.D. (degree)
20RV	22.61 ± 2.30
30RV	24.25 ± 1.82
40RV	24.87 ± 0.60
50RV	26.87 ± 1.20
60RV	29.46 ± 1.93

Figure 30 Contact angle of V-loaded R-based ISG formulations

4.8.3 Surface tension of R-based formula

In this study, the surface tension of the R-based ISG formulation were investigated using the goniometer. The ISGs were expelled from the glass barrel through the blunt 18-gauge needle as much as possible before the drop, then held the liquid in drop shape position which attached to the needle. The surface tension between the liquid and the air were calculated as shown in Table 29. 20RV presented the low surface tension followed by 30RV<40RV<50RV which were less than DMSO since the high cohesion force of the resin. Surprisingly, 60RV presented the lowest surface tension owing to drop's weight. Therefore, the gravity force was strongly bringing the drop apart from the needle. By consideration of 20-50RV, increasing the amount of R exhibited the higher surface tension.

Table 29 Surface tension of V-loaded R-based ISG formulations (n=6)

Formulation	Surface tension ± S.D. (mN/m)
20RV	34.31 ± 0.19
30RV	34.71 ± 0.18
40RV	35.96 ± 0.58
50RV	36.56 ± 1.19
60RV	27.60 ± 2.19

| 20RV | 30RV | 40RV |
| 50RV | 60RV | |
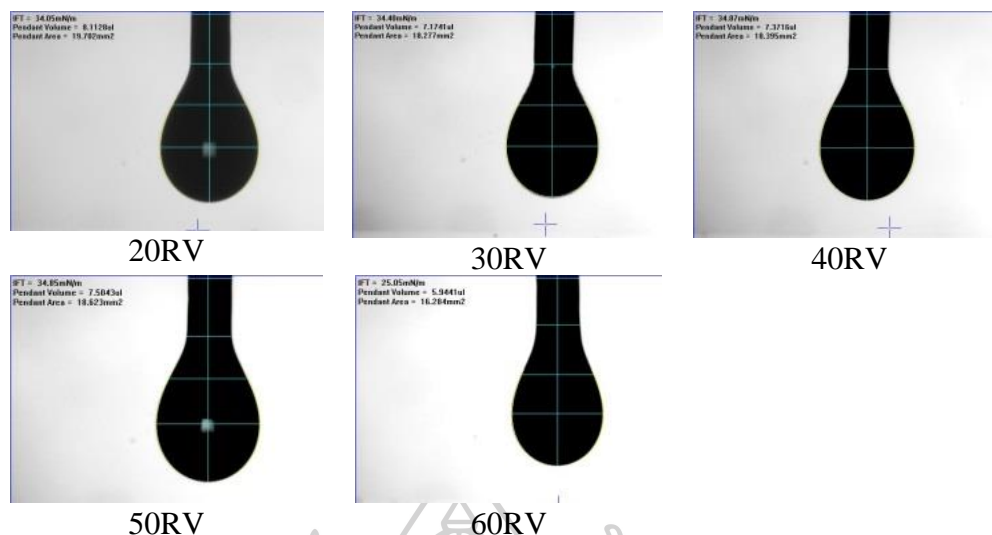
Figure 31 Surface tension of V-loaded R-based ISG formulations

4.8.4 Interfacial tension of R-based formula

The interfacial tension of R-based ISG formulation were measured against the olive oil as presented in Table 30. Increasing the concentration of R resulting in lower interfacial tension in 20-50 RV owing to the higher cohesion force of the resin and the surrounding oil pressure [4]. Although, 60RV contained low amount of DMSO, it exhibited the interfacial tension 1.07 which was higher than 40RV and 50RV. This investigation was related to the size of emulsion and microparticle forms since 60RV ISM presented the largest diameter in both forms. However, the outer oil phase containing 7.5% GMS could not be investigated due to the turbidity of GMS interfered the vision of the instrument.

Table 30 Interfacial tension of V-loaded R-based ISG formulation (n=6)

Formulation	Interfacial tension ± S.D. (mN/m)
20RV	2.02 ± 0.04
30RV	1.79 ± 0.03
40RV	1.02 ± 0.06
50RV	0.54 ± 0.01
60RV	1.07 ± 0.03

20RV 30RV 40RV

50RV 60RV
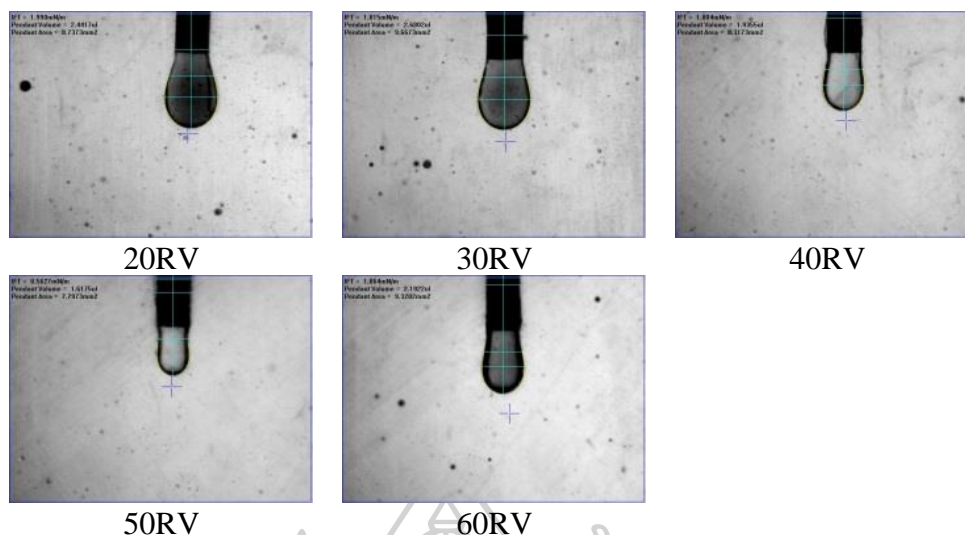
Figure 32 Interfacial tension of V-loaded R-based ISG formulations

4.8.5 *In-vitro* R-based ISG and ISM transformation

After injecting the formulation into PBS pH 6.8, the surface of all formulations suddenly turned into a gel-like and continued to be slowly transformed into an opaque solid matrix, which was whiter in color, as illustrated in Figure 33. The surface of the low R concentration solution was less and slower transformed into a solid than the high R concentration solution, owing to the presence of dense hydrophobic R molecules in high concentration solution precipitated in water and prevented the water diffusion [10]. ISM transformed slower than ISG because the external oil phase interfered the diffusion of water into the formulation [112]. The ISM transformation was performed under an inverted microscope to observe the microscopic transformation as presented in Figure 34. At the initial time, the formulation was in an emulsion form and the emulsion droplets hardened because the R precipitated after contact with PBS pH 6.8, [10, 11] and turned into microparticles. The 60RV ISM formulation showed a slightly slower transformation than the others because the high concentration of R prevented diffusion of water into the microparticles. To explain the transformation process, 0.003% sodium fluorescein-incorporated 0.6%w/w agarose gel was coated on glass slides to simulate the human gum cavity. The formulation was dropped beside the gel and observed the interfacial phenomena under the inverted microscope. The green color of sodium fluorescein from the PBS diffused into the brown color of the formulation and the ISG and ISM were transformed into a solid, as presented in Figure 35. The ISG formulations exhibited phase separation between the DMSO and R, as small droplets of DMSO were observed during the transformation process leading to phase separation of R [111]. Moreover, the phase separation also occurred in ISM in the internal droplets, which changed color from brown to light green. The PBS diffused through the outer oil phase owing to excess GMS. Then, the PBS attached to the outer shell of the internal droplets because the GMS was the birefringent layer [39] as a stabilizer to improve stability of the emulsion, as shown in Figure 35. Then, water diffused into the emulsion droplets

and the phase separation occurred, leading to the precipitation of R. The transformed solid microparticles were observed as a turbid green color.
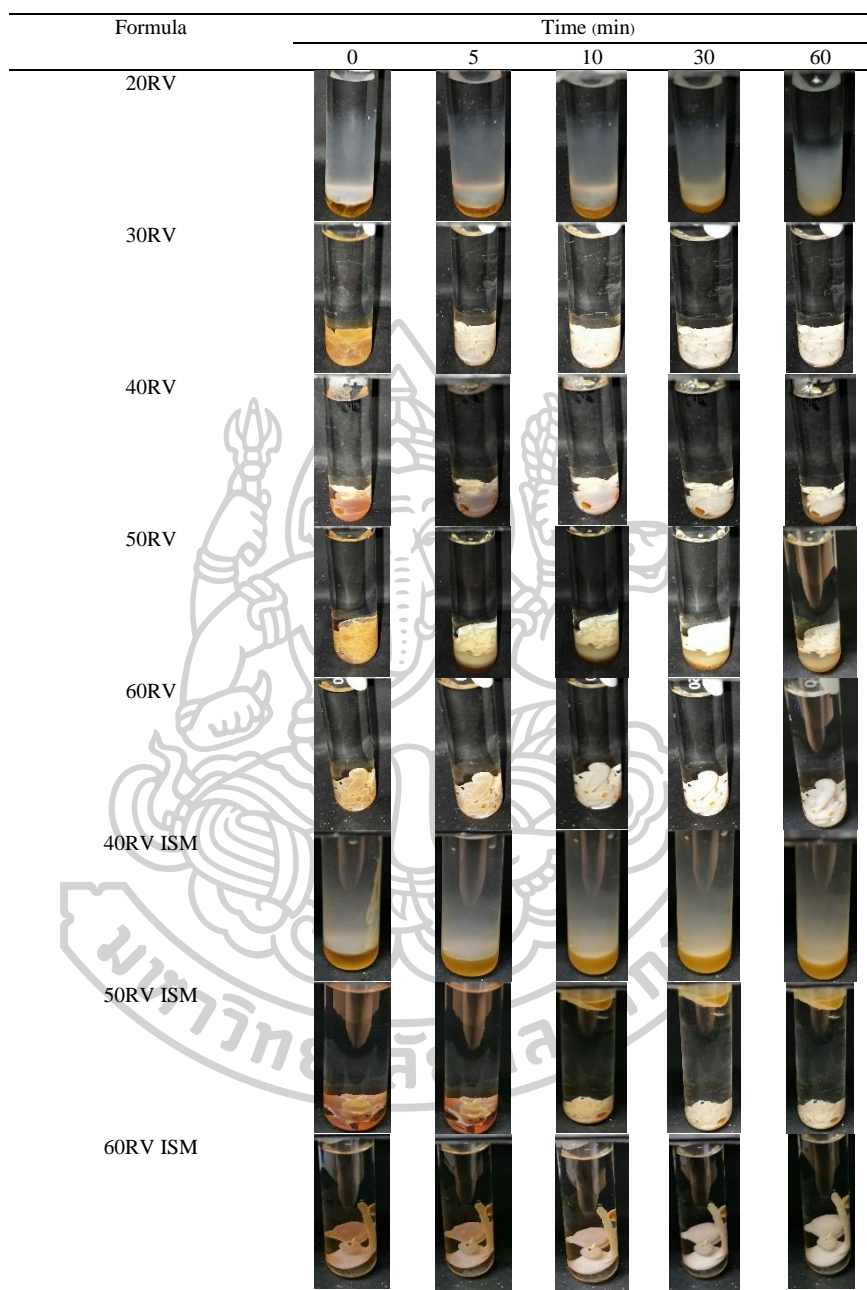
Figure 33 Macroscopic transformation of V-loaded R based ISGs and ISMs in PBS pH 6.8 at different times

Formula	Time (sec)				
	0	10	30	60	180
40RV ISM					
50RV ISM					
60RV ISM					
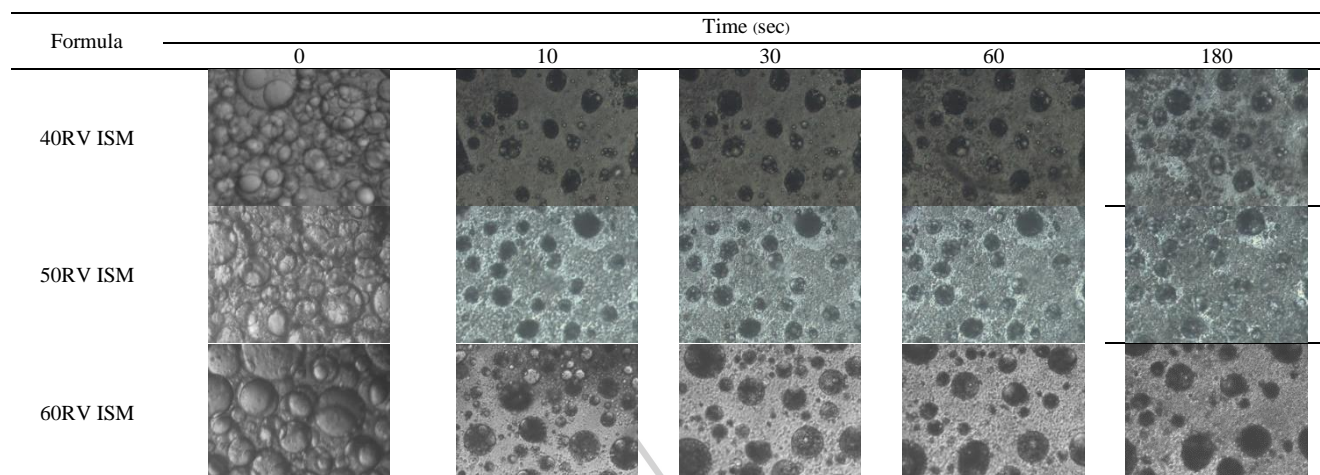
Figure 34 Microscopic transformation of V-loaded ISMs containing 40–60% (w/w) rosin under the inverted microscope.
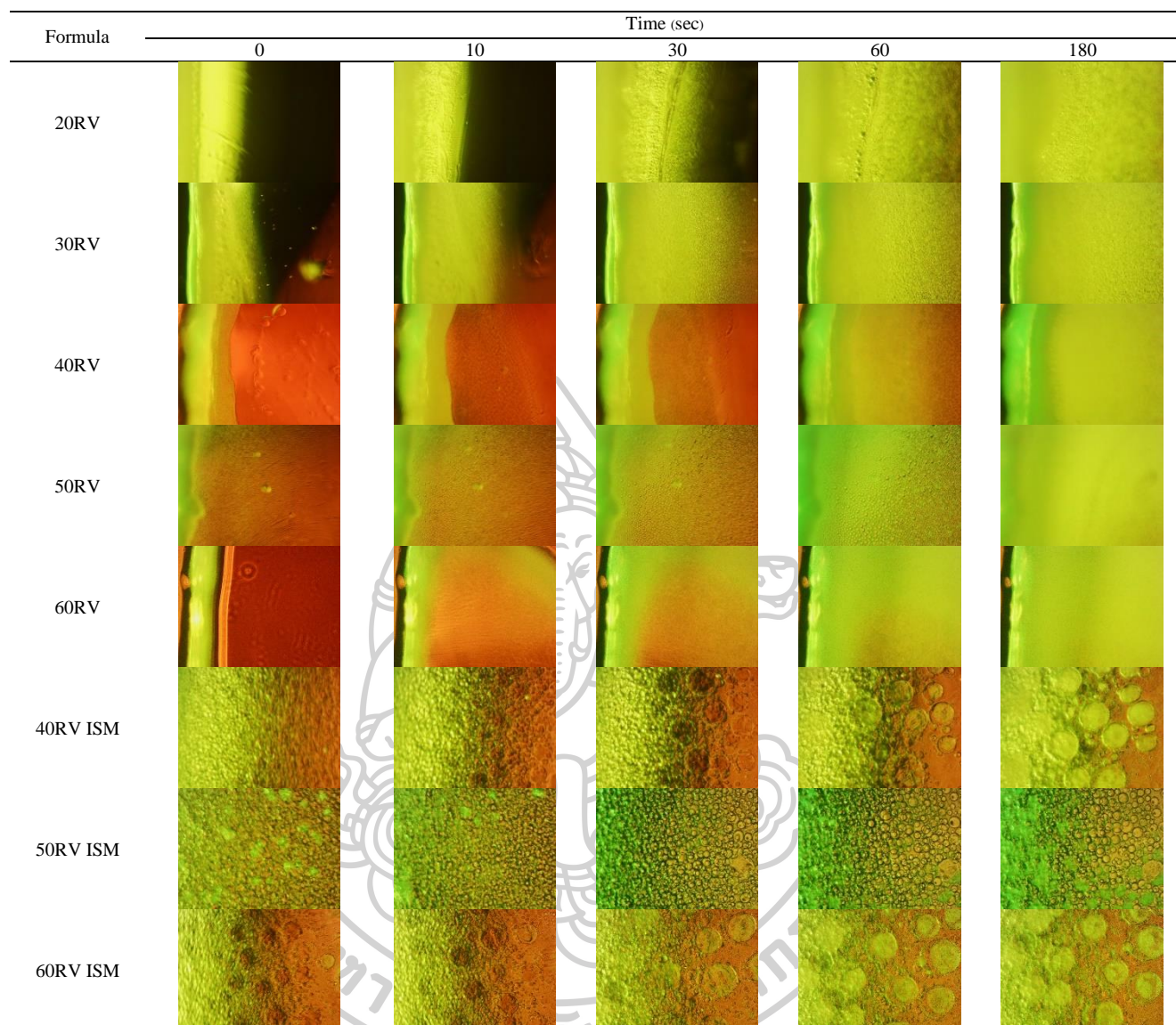
Figure 35 Microscopic transformation of V-loaded ISGs containing 20–60% (w/w) rosin and ISMs containing 40–60% rosin under the inverted microscope using 0.003% w/w sodium fluorescein in agarose gel as the gum cavity simulation system.

4.8.6 Rate of water diffusion into ISG and ISM

This study using SF green as a green color loaded in the R-based ISG, which also behaved as internal phase of ISM, for observing the water diffusion length and rate of each formulation as presented in Figure 36-38. The white opaque ring suddenly appeared after filling 20RV in the agarose gel well which represented the phase inversion zone between PBS and the formulation. The ring band was increased by time which was similar to the ERS-based formulation results. Increasing the concentration of R exhibited slower water diffusion owing to the interfering effect of the solidified resin that prevented water diffuse through the formulation. ISM which containing outer oil phase showed a less diffusion length which also similar to that of ERS formulations. The diffusion length of ISG and ISM formulas was further calculated into the diffusion rate in which 40RV presented the highest rate of diffusion at the early 5 min and slower by the time owing to the harden gel matrix while 20RV and 30RV presented the slower rate than 40RV in the early state because of the rapid transformation. However, after the initial 5 min, 20RV exhibited the higher rate than the others owing to the less viscosity. 40RV ISM also presented the highest diffusion rate compared to the other ISM which increasing the concentration of R resulted in the lower diffusion rate similar to that of ISG.

Formulation	Time (min)				
	0	5	10	15	30
20RV					
30RV					
40RV					
50RV					
60RV					
40RV ISM					
50RV ISM					
60RV ISM					
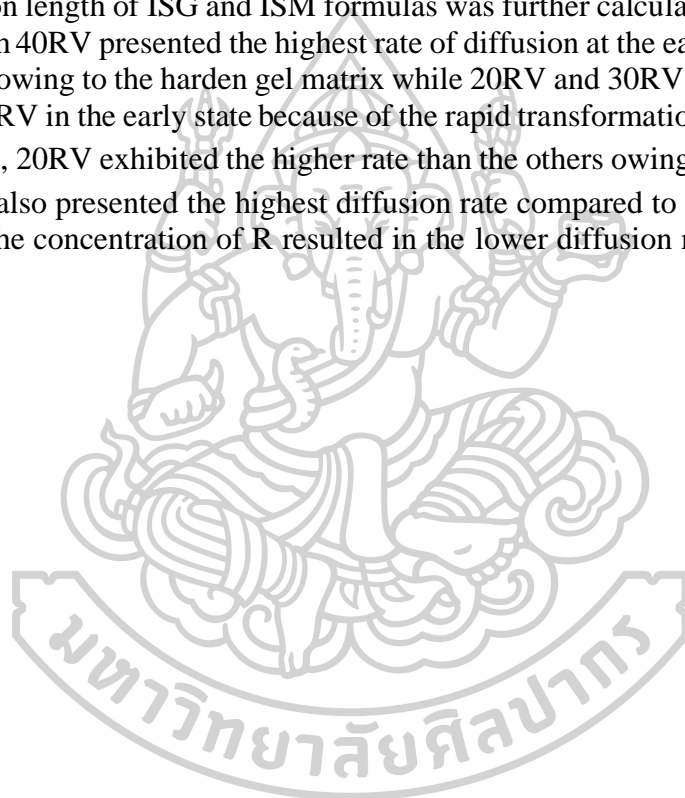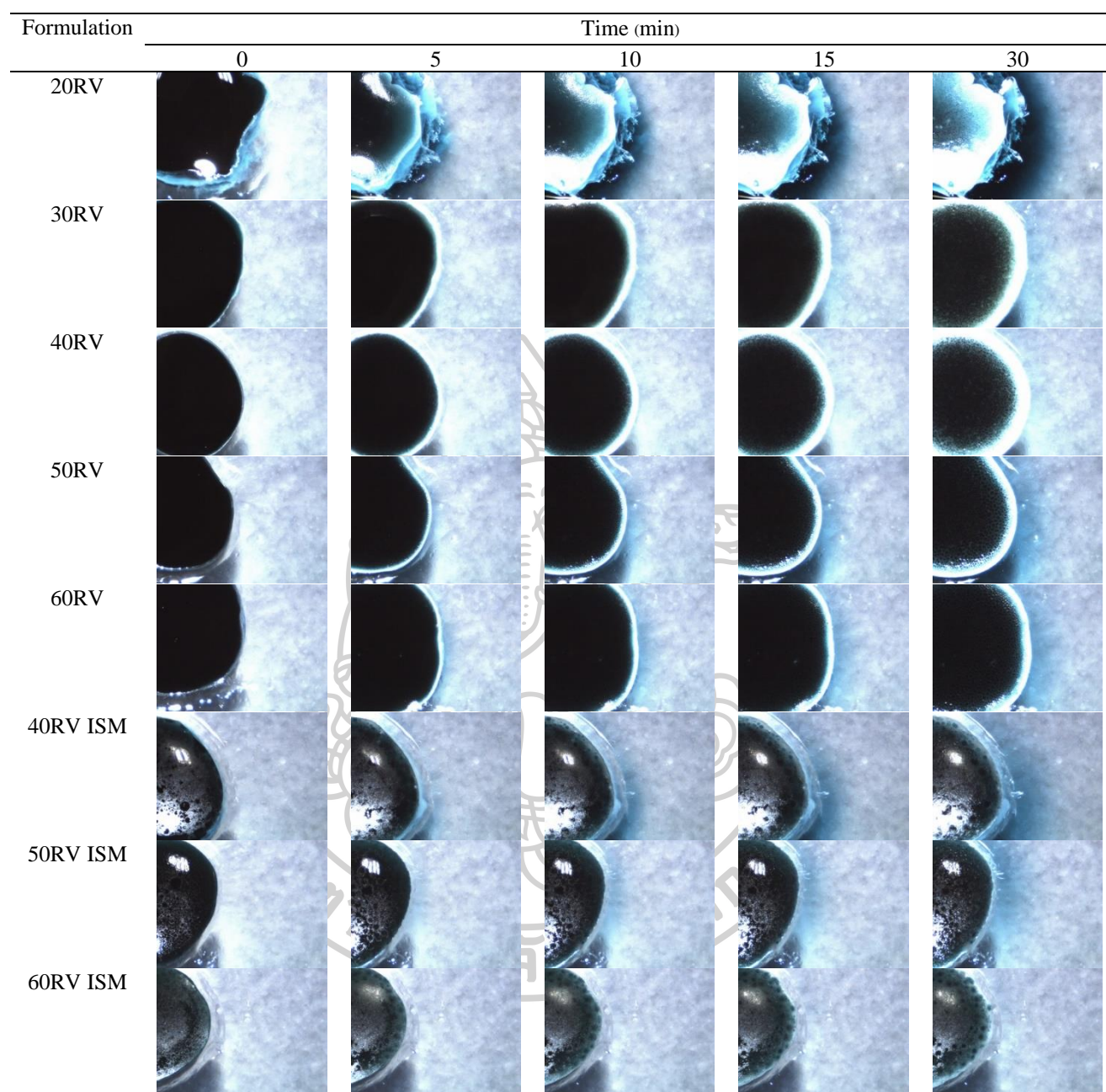
Figure 36 Macroscopic transformation of V-loaded R based ISGs and ISMs comprising 0.01% w/w SF green under the stereomicroscope (10x) in 0, 5, 10, 20 and 30 min
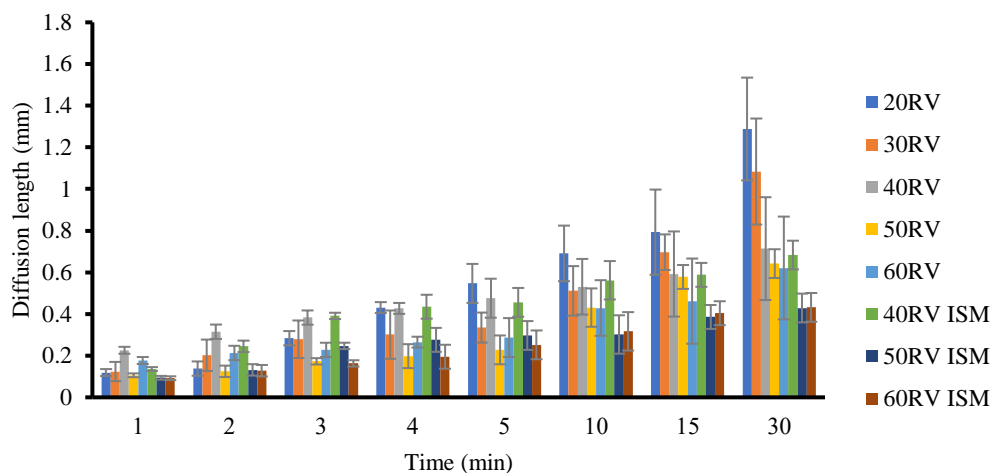
Figure 37 Diffusion length of ERS-based ISG and ISM formula at different time (n=3)
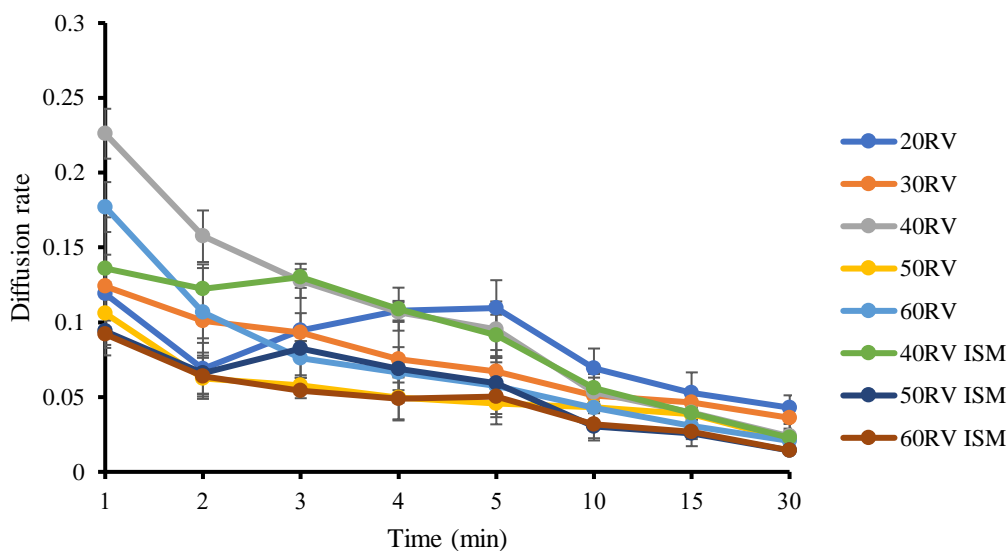
Figure 38 Diffusion rate of R-based ISG and ISM formula at different time

4.8.7 SEM morphology

The SEM micrographs of the V-loaded ISG formulations are presented in Figure 39A. The R had no pores at the surface, while the ISG formulations exhibited a porous structure, indicating that DMSO could change the structure of R precipitated matrix during transformation due to phase separation and leached out of this solvent. Increasing the concentration of R affected the size and uniformity of the pores. A high concentration of R promoted various pore sizes, which exhibited a rapid release during the initial phase followed by slower release. The small size of the pores trapped the drug inside; thus, the release profile did not reach 100%. The SEM micrographs of the ISM formulation revealed a spherical shape with a smooth surface as shown in Figure 39B

due to the GMS birefringent layer [39]. The cross-sectional photograph also revealed the porous structure, which was similar to the porous surface of R-based ISG transformation topography resulting in the drug release ability. These pores performed responsibility as the reservoir for the drug solution. Therefore, the drug releasing was sustained as illustrated in the cumulative drug releasing results.

B

Formula	Surface		Cross-section
	10,000x	30,000x	30,000x
40RV ISM			
50RV ISM			
60RV ISM			
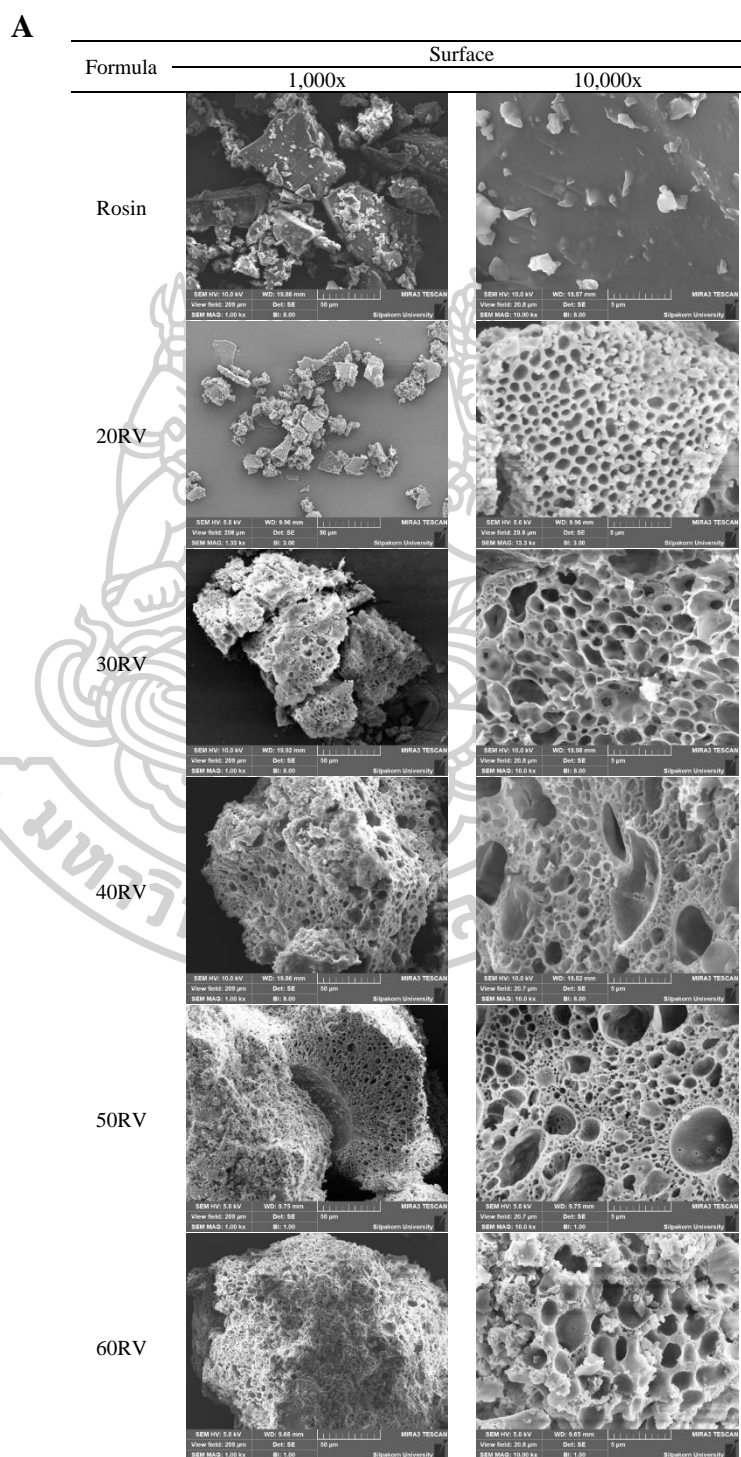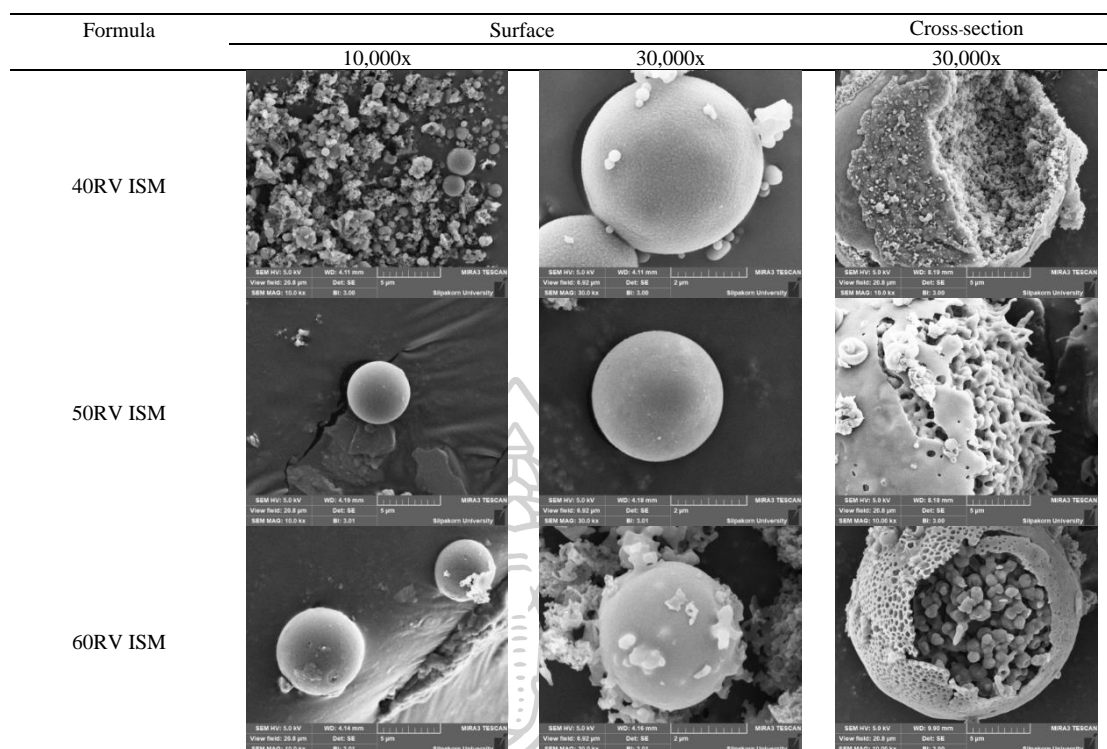
Figure 39 A. SEM micrographs of the surface of rosin and the ISG formulations containing V at 1,000× and 10,000×;

B. SEM micrographs of the surface and cross-section of the ISM formulations containing V at 10,000× and 30,000×.

4.9 Computer modeling

Nowadays, many aqueous-insoluble substances were demonstrated as the matrix forming agents of self-transformation systems due to their phase separation and precipitation properties into solid matrix mass after immersed in water. The solvent exchange mechanism related with the opposite diffusing direction between the environment water and solvent of the formulation used for developing the local matrix drug delivery systems. However, this mechanism is still unclarified profoundly. From the previous study, the major phenomenon which occurred during the phase transformation was the phase separation of the matrix former from the solvent. This phenomenon resulted in the matrix former aggregating and became a precipitated mass when contacting the water. Thus, the transformation process of the matrix former not only occurred from the solvent exchange mechanism but also had the phase separation of the matrix from the solvent. To be more clearly understanding, the computer modeling was applied to observe the initial phenomenon of phase separation during the solvent exchange process. Gaussian is one of the popular software used to calculate the binding energy between the substance and receptor [82]. In a previous study, the

Gaussian was used to predict the drug and various target interactions such as enzyme, ion-channel, nuclear receptor, and G-protein coupled receptor (GPCR) [82]. In this study, Gaussian software was used to find the optimized molecule configuration of the matrix former (abietic acid (A) and Eudragit RS (ERS)) and the drug (doxycycline (DH) and vancomycin (V)) and calculate the binding energy of the combined molecule in each gradient water environmental solvents.

4.9.1 The optimization configuration of drug, matrix former and combined structure

In this study, the initial structure of abietic acid and Eudragit RS were constructed by GuassView 6.0 program while the initial structure of DH and V were obtained from PubChem (CID 54685920) and RCSB protein data bank (PDB ID: 1aa5), respectively. These molecules were optimized at the DFT B3LYP/3-21G* level using Gaussian 09 in gas phase and their optimized structures were represented in Figure 40. Their single point energy calculations at the B3LYP/3-21G* level in DMSO, water and 50% DMSO in water were also performed.
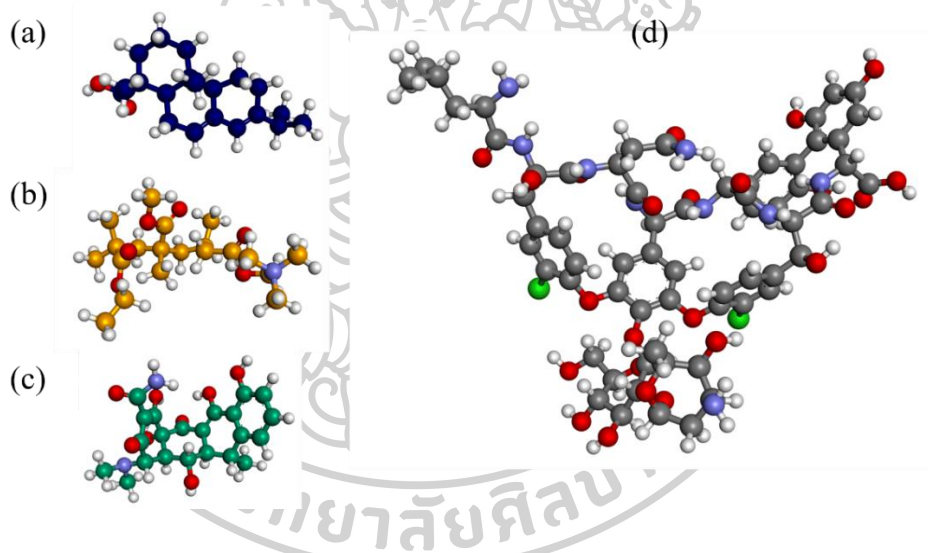
Figure 40 Structure of matrix forming agents and model drugs: (a) Abietic acid (A) (b) Eudragit RS (ERS) (c) doxycycline (DH) and (d) vancomycin (V)

The binding between the drug and matrix former: vancomycin (V) - abietic acid (A) and doxycycline (DH) - Eudragit RS (ERS) were predicted at B3LYP/3-21G* level in gas phase, followed by the single point energy calculations at the B3LYP/3-21G* level in DMSO, water and 50% DMSO in water. Due to the large size of vancomycin (V), V was divided into three parts as shown in Figure 41(a) and the possible binding between abietic acid and each part of vancomycin *via* hydrogen bonding interaction were predicted. Part 1, Part 2 and Part 3 of V could bind with 6, 4 and 3 molecules of abietic acid as shown in Figure 41(b), Figure 41(c) and Figure 41(d), respectively. Figure 41(e) represented that one molecule of vancomycin could bind with 13

molecules of abietic acid *via* hydrogen bonding between carboxylate group of abietic acid and hydroxyl and amine group of vancomycin.
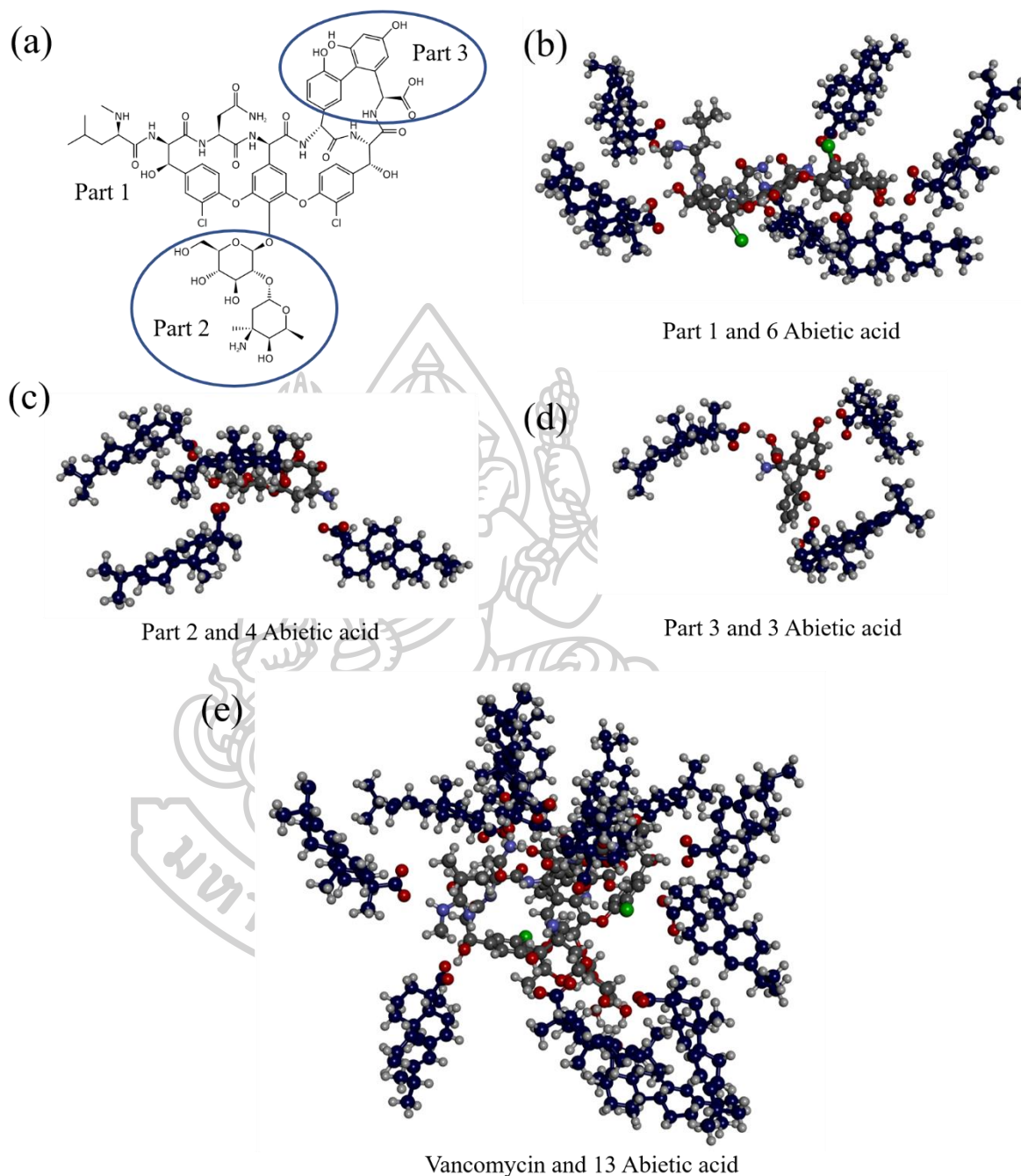
Figure 41 The possible binding between vancomycin and abietic acid *via* hydrogen bonding interaction

For doxycycline (DH) - Eudragit RS (ERS), the possible binding *via* hydrogen bonding interaction of one molecule of DH and one molecule of ERS was demonstrated in Fig. 42. It can be noticed that the carbonyl groups of ERS forms hydrogen bonds with hydroxyl and amine group of DH.
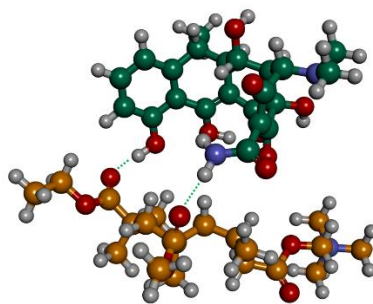
Figure 42 The possible binding between doxycycline (DH) - Eudragit RS (ERS)
via hydrogen bonding interaction

4.9.2 The Binding energy

The binding energy of vancomycin (V) - abietic acid (A) and doxycycline (DH) - Eudragit RS (ERS) in DMSO, water and 50% DMSO in water were calculated at the same level of theory using the equation shown below. For vancomycin (V) - abietic acid (A), the approximate binding energy of vancomycin and one molecule of abietic was obtained from the binding energy of part 1 divided by 6.

E-binding = E(complex) - E(substrate)   (12)

As can be seen in Table 31, the trend of binding energy value of AV was DMSO< 1:1 DMSO:water< water owing to the low polarity of abietic acid which easily dissolves in DMSO, thus the low energy was required to break the bond between A and V molecules for dissolving these two different molecules. After increasing the amount of water, the binding energy increased because of the effect of water-induced precipitation of abietic acid [10, 128]. The complex of vancomycin and abietic acid (Figure 41(e)) demonstrated an instability during the transformation. Thus, the molecules changed their position into more rigidity [8] which was the initial state of the precipitation process. Therefore, increasing the amount of water required more energy to break the intermolecular bond between the abietic acid and vancomycin.

Table 31 Binding energy of vancomycin (V) - abietic acid (A) and doxycycline (DH) - Eudragit RS (ERS) in different solvents calculated at the B3LYP/3-21G* level

	Binding energy (kcal/mol)	
Solvent	AV	ED
DMSO	-4.61	-11.43
DMSO:Water (1:1)	-4.59	6.23
Water	-4.58	6.15

The binding energy of the doxycycline (DH) - Eudragit RS (ERS) also exhibited the same trend as AV; the lowest binding energy was presented in the DMSO environment and increased upon the amount of water. Hence, the water-insoluble resin and polymer revealed that the binding energy increased due to the rigidity of the matrix former structure during the transformation process from liquid to solid form solvent-induced precipitation. The solvent that could dissolve the polymer typically used low energy to break the bond between the drug and polymer whereas the insoluble solvent required more energy [129, 130].

Summary
Part 2

For the clear understanding of the transformation process *via* solvent exchange mechanism of both ISG and ISM formulations, the contact angle, surface tension, interfacial tension, and the *in-vitro* transformation was determined and analyzed their obtained data. DMSO and PYR exhibited the less wettability than the oils against the hydrophobic glass slide. 20RV presented the lowest contact angle followed by 30RV<40RV<50RV<60RV where the R concentration below 40% w/w revealed the lower contact angle than neat DMSO owing to the acidic character of abietic acid and V. Moreover, increasing the amount of R also revealed the low wettability. 20RV presented the low surface tension followed by 30RV<40RV<50RV which were less than DMSO since the high cohesion force of the resin. Surprisingly, 60RV demonstrated the lowest surface tension. The interfacial tensions between the selected solvents and R-based ISGs were observed against the oil to simulate the emulsion form. Both polar organic solvents revealed the lower interfacial tension of 7 times against camelia oil and of 5 times against olive oil compared to the water because of their lower polarity. Increasing the concentration of R resulting in lower interfacial tension in 20-50 RV owing to the higher cohesion force of the resin and the surrounding oil pressure. Although, 60RV contained low amount of DMSO, it exhibited the interfacial tension higher than 40RV and 50RV. This investigation was related to the size of emulsion and microparticle form since 60RV ISM presented the largest diameter in both forms. The transformation of the liquid into the solid gel or microparticle were observed by visual in PBS pH 6.8. The surface of all formula suddenly turned into solid form when contacted with PBS and slowly transformed into the gel matrix. At the initial time, all formula is in emulsion form with the transparent droplets. After contacted with distilled water some droplets of formula became solidify which finally resulted in matrix former precipitation into the spherical shape of microparticles. DMSO is more hydrophilicity than PYR led to a fast solvent exchange with environmental water and thus rapidly precipitated. Furthermore, 0.003% sodium fluorescence comprised of 0.6%w/w agarose gel was used to investigate the route of water diffusion. Firstly, the PBS diffused through the outer oil phase owing to excess GMS. After that, the PBS attached to the outer shell of the internal droplets since GMS was the birefringent barrier layer which improve stability of the emulsion. Then, water diffused into the emulsion droplets and the phase separation occurred, leading to the precipitation of R which the transformed solid microparticles were observed as a turbid green color. Moreover, the water diffusion of ERS and R based ISG and ISM formulation were observed under the stereomicroscope at different times. The opaque ring suddenly appeared after filled ISG and ISM in the agarose gel well which represented the phase inversion zone between PBS and the formulations which the ring band was increased by time. Moreover, ERS-based ISM containing camellia oil exhibited a larger diffusion length than another one because of the low viscosity of the oil performed the loose barrier, thus the water easily diffuses into the formula. In the morphology study, DMSO exhibited the rough surface

and present more pores than PYR indicating that DMSO modified the matrix structures of ERS and R matrix from its leakage and drug release thereafter generated more pores in a matrix structure. ISM appeared as a spherical shape with a smooth surface whereas cross-sectional topography revealed its porous structure. R and ERS exhibited a similar trend of binding energy during the transformation process. The binding energy was increased in the presence of water because of the solvent-induced precipitation explaining the mechanism of transformation from liquid to solid form of the insoluble rosin and polymer. DMSO could dissolve the matrix former by employing low energy to break the bond between the drug and matrix former then required more energy in the presence of the water. The combined molecule presented an instability during the transformation process; thus, the molecules change the position into more rigidity, which water required more energy to break the bond. This phenomenon was an initial phase of the precipitation of the resin and polymer during the phase separation process *via* solvent exchange mechanism. From this research, the underlying transformation mechanism of ISG and ISM *via* solvent exchange mechanism was revealed. Phase separation between the solvent and the matrix forming agent occurred during the transformation process for both synthetic polymer and natural resin. In addition, the water diffusion route of ISM was also revealed since the excess GMS promoted the water invasion into the formulation. Computerized static modeling revealed the initial phase of this phenomenon. Nonetheless, this computerized static simulation should be studied more molecules of the drug and polymer by using the same ratio as the prepared formulation in further study or the dynamic modelling should be conducted with simulation for various environmental conditions.

CHAPTER 5
CONCLUSIONS

ERS, the synthetic copolymer of ethyl acrylate, methyl methacrylate, and low content of methacrylic acid ester with quaternary ammonium groups, was developed as matrix former for ISG and ISM formulation to deliver DH for local treatment of the periodontitis disease. Additionally, R which is the natural resin obtained from pines was also developed as a matrix former of ISG and ISM formulation comprising V as presented with schematic diagram in Figure 43. Both ERS and R-based formulations presented the acidic pH since DH and V are weak acid drugs. ERS and R-based ISM showed advantages over ISG in the lower viscosity and ease of injection because of the lubricity effect from the external oil phase. Notably, ISM exhibited a retardation of antibiotic drug release and had antimicrobial activities against *S. mutans* and *P. gingivalis*, indicating the possibility for periodontal pocket drug delivery for enhancement of the periodontitis treatment effectiveness and reducing drug side effects. DMSO presented the advantages over PYR owing to its lower viscosity for promoting the ease of injection which suitable for use with the dental needle. Although PYR has antimicrobial activity, the prepared system comprising DMSO as solvent presented more antimicrobial activity than that using PYR since the less viscosity of DMSO induced more drug diffusion into agar. However, the high viscosity of PYR also prevented the degradation of the formulation and resulted in a smaller microparticle size. Camelia oil and olive oil contain different amounts of unsaturated fatty acids for 88.2%, 86.3%, respectively. Thus, camelia oil has many bending structures than olive oil resulting in a high friction force. For this reason, the formulation comprising camellia oil required a higher injectability force and AUC than another. Olive oil was more viscous and promoted in the smaller size of microparticles, hence olive oil was suitable for developing the ISM formulation. The ERS-based formulation could not be observed the adhesion properties because the formula was fragile after 7 days whereas the R-based formulation could be observed. Increasing the R concentration reduced the maximum force for ISG and ISM because the hardened R prevented solvent exchange. Furthermore, ISM showed a lower maximum force than ISG since the external phase interfered solvent exchange; thus, the formula was softer than ISG after transformation. Notably, ISM presented a higher adhesion force than the ISG, signifying that ISM exhibited better attachment to the periodontal pocket than the ISG in which the 40RV ISM formulation presented the highest force. Furthermore, all of the R-based formulations had better plasticity properties than elasticity; therefore, they possibly adapt to the specific shape of a patient's periodontal pocket. The outer surface of all formulas suddenly turned into opaque solid form when contacted with PBS and continued slowly to transform into the gel matrix. For ERS-based and R-based ISM at the initial time, all formulations were in emulsion dosage form with the transparent droplets. After contact with distilled water, some droplets of formula became solidified

which finally resulted in matrix former precipitation into the spherical shape of microparticles which diameters less than 250 µm. The ISG formulations exhibited phase separation between the DMSO and R, as small droplets of DMSO were observed during the transformation process leading to precipitation of R. Moreover, the phase separation also occurred in ISM in the internal droplets. Firstly, the PBS diffused through the outer oil phase owing to an excess GMS. Subsequently, the PBS was attached to the outer shell of the internal droplets because GMS presented as the birefringent barrier layer and improved the stability of an emulsion. Then, water diffused into the emulsion droplets and the phase separation occurred, leading to the precipitation of R. To be more clearly understand the phase transition of resin and polymer from developed drug delivery systems, the computer modeling was applied to clarify the phenomenon of phase separation during the solvent exchange process. In this study, Gaussian software was used to find the optimized molecule configuration statically of the matrix former (R and ERS) and the antibiotic drugs (V and DH) and subsequently calculated the binding energy of the combined molecule in each gradient water environmental solvent. R and ERS exhibited a similar trend of binding energy during the transformation process. The binding energy was increased in the presence of water because of the solvent-induced precipitation, explaining the mechanism of transformation from liquid to solid state of the insoluble rosin and polymer. DMSO, which could dissolve the matrix former, used low energy to break the bond between the drug and matrix former then required more energy in the presence of the water. The combined molecule presented an instability during the transformation process; thus, the molecules changed their position into more rigidity while water required more energy to break the bond. This phenomenon was assumed as the initial phase of the precipitation of the resin and polymer precipitation during the phase separation process *via* the solvent exchange mechanism. The surface topography from SEM photographs of ERS-based ISG using PYR as solvent presented a smoother surface than that prepared using DMSO indicating that DMSO leakage affected the structures of ERS matrix presenting more pores owing to its high polarity provoking rapid solvent exchange and phase separation to generate sponge-like ERS matrix. ISM appeared as a spherical shape with an estimated diameter of 50 µm. Increasing the amount of R promoted nonuniformity of pore sizes, hence the initial rapid release occurred in high concentration R-based ISG followed by the slow release. The small size of the pores trapped the drug inside; thus, the release profile did not reach 100%. The SEM micrographs of the R-based ISM formulation also revealed a spherical shape with a smooth surface. However, their cross-sectional study revealed the porous or sponge-like structures similar to that of ISG.

From overall results, V-loaded 40% w/w R-based ISM and DH-loaded 30% w/w ERS-based ISM exhibited the appropriate physicochemical properties and efficient antimicrobial activities as the localized antimicrobial periodontal pocket targeting

which transformed into the microparticle *via* solvent exchange mechanism. DMSO presented the good properties used as the solvents owing to its polarity, less viscosity, and immiscibility with the oil for preparing into emulsion using GMS as emulsion stabilizer. Moreover, DMSO influenced the structures of the matrix to have more pores which entrapped the drug inside resulting in prolonged drug release. Olive oil and camellia oil presented similar properties as the outer phase of ISM emulsion. They were responsible as the outer barrier for reducing the burst release of the drug and retarded the drug release. In addition, the oil exhibited a lubricity effect and promoted ease of injectability of the formulation. The excess GMS in the outer oil phase provoked the water diffusion through the oil and reached the internal polymeric phase resulting in phase separation of matrix-forming agents. At the same time, the solvent also diffused out and brought the drug-releasing from the formulation. Additionally, both ISG and ISM had antimicrobial activities against *S. mutans* and *P. gingivalis*, indicating the possibility for periodontal pocket drug delivery to increase the effectiveness of periodontitis treatment and reduce drug side effects. Nonetheless, the safety of the developed ISMs should be further investigated such as cytotoxicity on gingival cells or animal model. In addition, the clinical study of their effectiveness should be also considered and conducted subsequently.
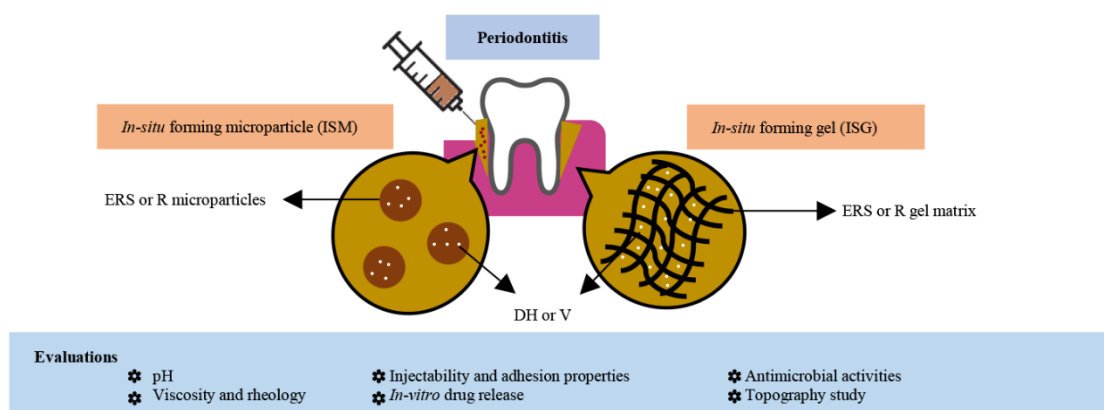
Figure 43 Schematic diagram for development of DH-loaded ERS and V-loaded R-based ISG and ISM formulations for periodontitis treatment *via* solvent exchange mechanism

APPENDIX
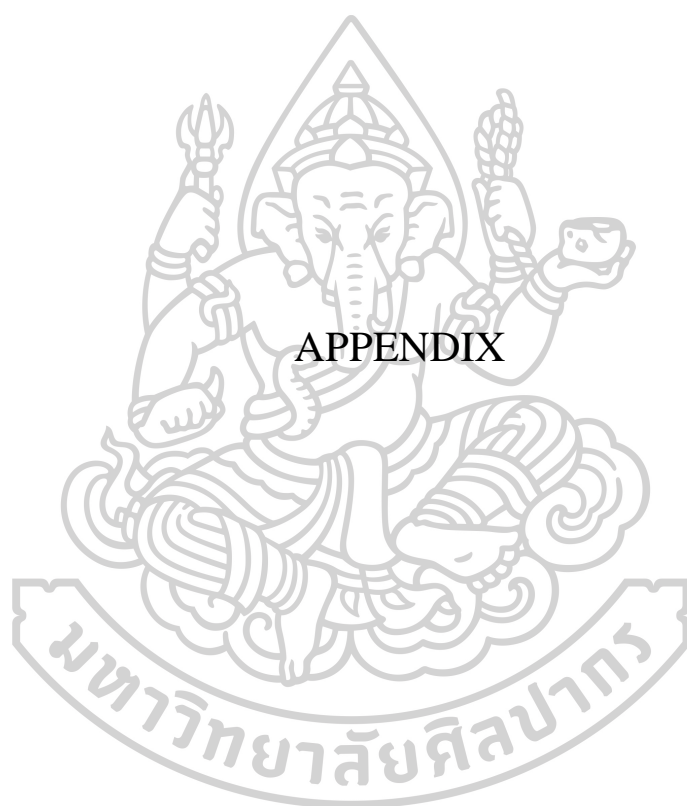
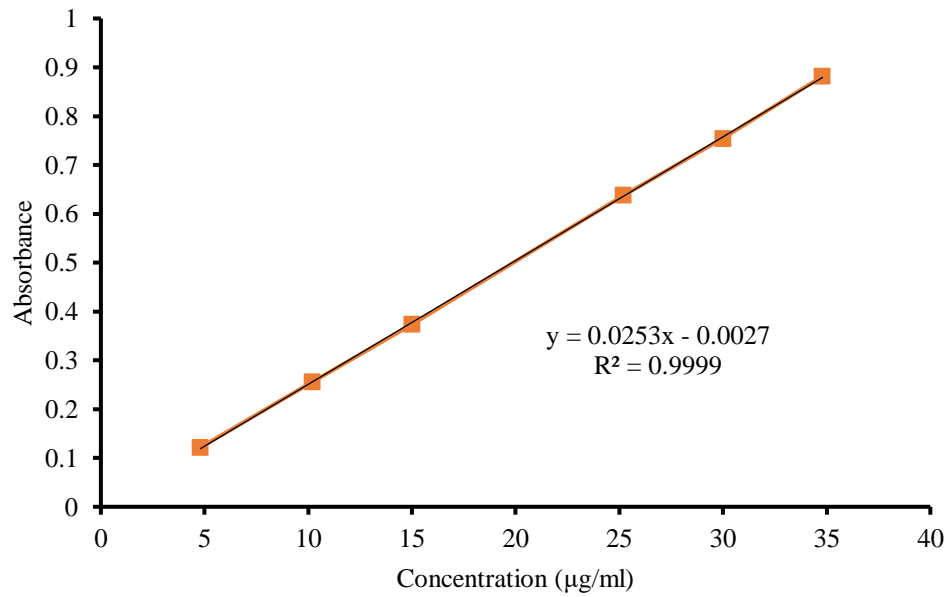**UV-Vis calibration curve for the *in-vitro* drug release study**

Figure 44 Calibration curve of doxycycline hyclate in phosphate buffer pH 6.8 (UV-Vis at 379 nm)
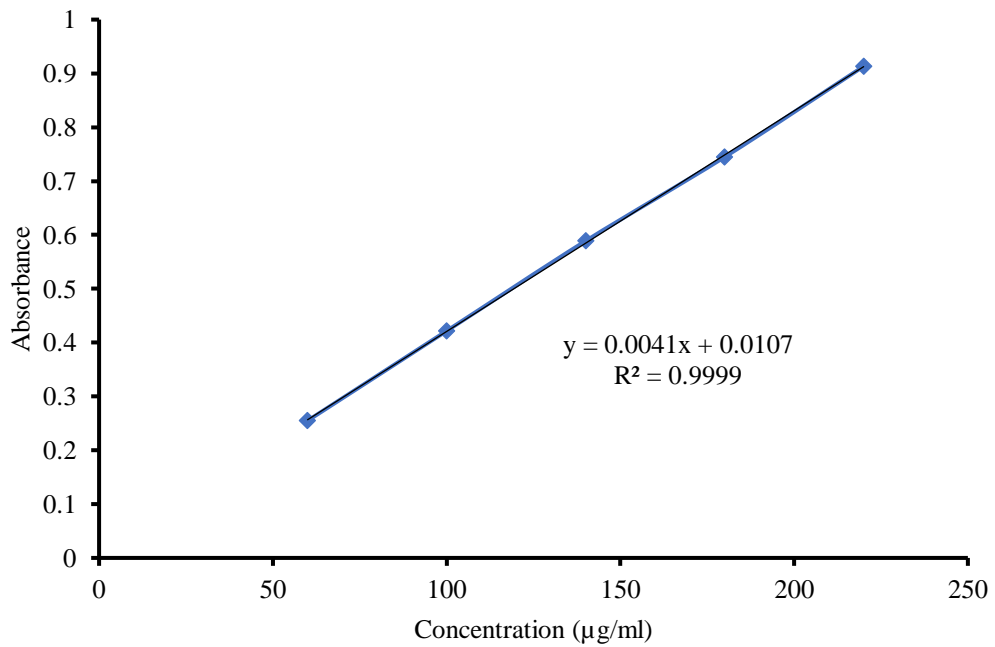

Figure 45 Calibration curve of vancomycin HCl in phosphate buffer pH 6.8 (UV-Vis at 280 nm)

REFERENCES

1. Macín-Cabrera S. Sanz-Alonso M. , Castrillón-Rivera L, Palma-Ramos A, Noguez-Méndez N, Quirino-Barreda C, Rubio-Martínez A. Non surgical periodontal treatment in patients with gingivalis and moderate periodontitis. Revista Odontológica Mexicana. 2015; 19(3): e151-e160.

2. Kopytynska-Kasperczyk A., Pastusiak M., Jarzabek B., Prochwicz W. Local delivery system of doxycycline hyclate based on ε-caprolactone copolymers for periodontitis treatment. International Journal of Pharmaceutics. 2015; 491(1-2): 335-344.

3. Javali M.A., Vandana K.L. A comparative evaluation of atrigel delivery system (10% doxycycline hyclate) Atridox with scaling and root planing and combination therapy in treatment of periodontitis: a clinical study. Journal of Indian Society of Periodontology. 2012; 16(1): 43-48.

4. Do M.P.,Neut C., Metz H., Delcourt E., Mäder K., Siepmann J., Siepmann F. In-situ forming composite implants for periodontitis treatment: How the formulation determines system performance. International Journal of Pharmaceutics. 2015; 486(1-2): 38-51.

5. Yapar E.A., İnal Ö., Özkan Y., Baykara T. Injectable in situ forming microparticle : a novel drug delivery system. Tropical Journal of Pharmaceutical Research. 2012; 11(2): 307-318.

6. Kranz H., Yilmaz E., Brazeau G.A., Bodmeier R. In vitro and in vivo drug release from a novel in situ forming drug delivery system. Pharmaceutical Research. 2008; 25(6): 1347-1354.

7. Thakral S., Thakral N.K., Majumdar D.K. Eudragit® : a technology evaluation. Expert Opinion on Drug Delivery. 2013; 10(1): 131-149.

8. Phaechamud T., Thurein S.M., Chantadee T. Role of clove oil in solvent exchange-induced doxycycline hyclate-loaded Eudragit RS in situ forming gel. Asian Journal of Pharmaceutical Sciences. 2018; 13(2): 131-142.

9. Satturwar P.M., Fulsele S.V., Dorle A.K. Evaluation of polymerized rosin for the formulation and development of transdermal drug delivery system: a technical note. AAPS PharmSciTech. 2005; 6(4): E649-654.

10. Pal O.P., Malviya R., Bansal V., Sharma P.K. Rosin an important polymer for drug delivery: a short review. International Journal of Pharmaceutical Sciences Review and Research. 2010; 3(1): 35-37.

11. Söderberg T.A., Gref R., Holm S., Elmros T., Hallmans G. Antibacterial activity of rosin and resin acids in vitro. Scandinavian Journal of Plastic and Reconstructive Surgery and Hand Surgery.1990; 24(3): 199-205.

12. Madan M., Bajaj A., Lewis S., Udupa N., Baig J.A. In situ forming polymeric drug delivery systems. Indian Journal of Pharmaceutical Sciences; 2009. 71(3): 242-251.

13. U.S. department of health and human service, National institutes of health. Periodontal (gum) disease cause, symptoms and treatments. 2013

14. Saini R., Marawar P.P., Shete S., Saini S. Periodontitis, a true infection. Journal of Global Infectious Diseases. 2009; 1(2): 149-150.

15. Könönen E., Gursoy M., Gursoy U.K., Periodontitis: a multifaceted disease of tooth-supporting tissues. Journal of Clinical Medicine. 2019; 8(8): 1135.

16. Kinane D.F., Stathopoulou P.G., Papapanou P.N., Periodontal diseases. Nature Reviews Disease Primers. 2017; 3(1): 17038.

17. Karasneh J.A., Ababneh K.T., Taha A.H., Al-Abbadi M.S., Ollier W.E.R. Investigation of the interleukin-1 gene cluster polymorphisms in Jordanian patients with chronic and aggressive periodontitis. Archives of Oral Biology. 2011; 56(3): 269-276.

18. Kim S.H., Kang S.R., Park H.J., Kim J.M., Yi W.J., Kim T.I., Improved accuracy in periodontal pocket depth measurement using optical coherence tomography. Journal of Periodontal & Implant Science. 2017; 47(1): 13-19.

19. Nazir M.A., Prevalence of periodontal disease, its association with systemic diseases and prevention. International Journal of Health Sciences. 2017; 11(2): 72-80.

20. Nazir S., Arain A.H., Mohsin A., Prevalence of gingival and periodontal diseases among a teaching hospital patients. Journal of the Pakistan Dental Asscociation. 2010; 19(4): 202-205.

21. สำนักทันตสาธารณสุข, รายงานผลการสำรวจสภาวะสุขภาพช่องปากระดับประเทศ ครั้งที่ 7 ประเทศไทย. 2555, กรมอนามัย.

22. Silva-Boghossian C.M., Neves A.B., Resende F.A.R., Colombo A.P.V. Suppuration-associated bacteria in patients with chronic and aggressive periodontitis. Journal of Periodontology. 2013; 84(9): e9-e16.

23. Sanz M. and Tonetti M.Periodontitis. European Federation of Periodontology.2019; https://youtu.be/oCplvAyrJBo [cited 2019 5 May 2019].

24. National institute of dental and craniofacial research. older adluts and oral health. 2020, National Institute of Dental and Craniofacial Research: Bethesda, Maryland, USA.

25. Phaechamud, T., Mahadlek J., and Chuenbarn T. In situ forming gel comprising bleached shellac loaded with antimicrobial drugs for periodontitis treatment. Materials & Design. 2016; 89: 294-303.

26. Prakasam, A., Elavarasu S.S., and Natarajan R.K. Antibiotics in the management of aggressive periodontitis. Journal of Pharmacy and Bioallied Sciences. 2012; 4(Suppl 2): S252-5.

27. Dong, W.Y., Körber M., López Esguerra V., Bodmeier R. Stability of poly(D,L-lactide-co-glycolide) and leuprolide acetate in in-situ forming drug delivery systems. Journal of Controlled Release. 2006; 115(2): 158-167.

28. Wang, L., Guan N., Jin Y., Lin X., Gao H., Subcutaneous vaccination with Porphyromonas gingivalis ameliorates periodontitis by modulating Th17/Treg imbalance in a murine model. International Journal of Immunopharmacology. 2015; 25(1): 65-73.

29. Rios H.F., Lin Z., Oh B., Park C.H., Giannobile W.V. Cell- and gene-based therapeutic strategies for periodontal regenerative medicine. Journal of Periodontology. 2011; 82(9): 1223-1237.

30. Chia H. and Wu B. Recent advances in 3D printing of biomaterials. Journal of Biological Engineering. 2015; 9(4): 1-14.

31. Subbarao K.C., Nattuthurai G.S., Sundararajan S.K., Sujith I., Joseph J., Syedshah Y.P., Gingival crevicular fluid: an overview. Journal of Pharmacy and Bioallied Sciences. 2019; 11(Suppl 2): S135-S139.

32. Bevilacqua, L., Biasi M.D., Lorenzon M.G., Frattini C., Angerame D. Volumetric analysis of gingival crevicular fluid and peri-implant sulcus fluid in healthy and diseased sites: a cross-sectional split-mouth pilot study. Open Dentistry Journal. 2016; 10:131-138.

33. Barros, S.P., Williams R., Offenbacher S., Morelli T., Gingival crevicular fluid as a source of biomarkers for periodontitis. Periodontol 2000. 2016; 70(1):53-64.

34. Kranz, H., Brazeau G.A., Napaporn J., Martin R.L., Millard W., Bodmeier R., Myotoxicity studies of injectable biodegradable in-situ forming drug delivery systems. International Journal of Pharmaceutics. 2001; 212(1): 11-18.

35. Phaechamud, T. and Setthajindalert O., Antimicrobial in-situ forming gels based on bleached shellac and different solvents. Journal of Drug Delivery Science and Technology. 2018; 46: 285-293.

36. Chantadee, T., Thammasut W., and Phaechamud T., Fluid properties and phase transition of antimicrobial eudragit RS/clove oil in situ forming depot. Materials Today: Proceedings, 2022.

37. Lertsuphotvanit, N., Santimaleeworagun W., Narakornwit W., Chuenbarn T., Mahadlek J., Chantadee T., Phaechamud T. Borneol-based antisolvent-induced in situ forming matrix for crevicular pocket delivery of vancomycin hydrochloride. International Journal of Pharmaceutics. 2022; 617:121603.

38. Mahadlek, J., Tuntarawongsa S., Senarat S. Phaechamud T. In situ solvent removal-based Eudragit®L/dimethyl sulfoxide forming gel for periodontal pocket drug delivery. Materials Today: Proceedings. 2022; 52: 2394-2399.

39. Voigt, M., Koerber M., and Bodmeier R., Improved physical stability and injectability of non-aqueous in situ PLGA microparticle forming emulsions. International Journal of Pharmaceutics. 2012; 434(1-2): 251-256.

40. Rungseevijitprapa, W. and Bodmeier R., Injectability of biodegradable in situ forming microparticle systems (ISM). European Journal of Pharmaceutical Sciences. 2009; 36(4): 524-531.

41. Haider, M., Elsayed I., Ahmed I.S., Fares A.R., In situ-forming microparticles for controlled release of rivastigmine: in vitro optimization and in vivo evaluation. Pharmaceuticals (Basel), 2021. 14(1): 66

42. Phaechamud, T., Chanyaboonsub N., and Setthajindalert O., Doxycycline hyclate-loaded bleached shellac in situ forming microparticle for intraperiodontal pocket local delivery. European Journal of Pharmaceutical Sciences. 2016; 93: 360-370.

43. Tuntarawongsa S., Lertsuphotvanit N., Mahadlek J., Phaechamud T. Beta-cyclodextrin-based in situ forming micro-particle for intra-periodontal pocket antimicrobial drug delivery. Materials Today: Proceedings. 2021; 47: 3430-3435.

44. Thu Rein S.M., Lwin W.W., Tuntarawongsa S., Phaechamud T., Meloxicam-loaded solvent exchange-induced in situ forming beta-cyclodextrin gel and microparticle for periodontal pocket delivery. Materials Science and Engineering: C. 2020; 117: 111275.

45. Wadher, K.J., Kakde R.B., and Umekar M.J., Formulation and evaluation of a sustained-release tablets of metformin hydrochloride using hydrophilic synthetic and hydrophobic natural polymers. Indian Journal of Pharmaceutical Sciences. 2011; 73(2): 208-215.

46. Singh, S., Sharma N., Arora S., Singla Y. An overview of multifaceted significance of eudragit polymers in drug delivery systems. Asian Journal of Pharmaceutical and Clinical Research. 2015; 8:1-6.

47. Porwal, A., Swami G., and Saraf S. Preparation and evaluation of sustained release microballoons of propranolol. Daru: Journal of Faculty of Pharmacy, Tehran University of Medical Sciences. 2011; 19(3): 193-201.

48. Abbaspour M. and garekani H.A. Preparation and characterization of ibuprofen pellets based on Eudragit RS PO and RL PO or their combination. International Journal of Pharmaceutics. 2005; 303: 88-94.

49. Niu, X., Liu Y., Song Y., Han J., Pan H. Rosin modified cellulose nanofiber as a reinforcing and co-antimicrobial agents in polylactic acid /chitosan composite film for food packaging. Carbohydrate Polymers. 2018; 183: 102-109.

50. Matthews, W.S., Bares J.E., Bartmess J.E., Bordwell F.G., Cornforth F.J., Drucker G.E., Margolin Z., McCallum R.J. McCollum G.J., and Vanier N.R, Equilibrium acidities of carbon acids. VI. Establishment of an absolute scale of acidities in dimethyl sulfoxide solution. Journal of the American Chemical Society. 1975; 97(24): 7006-7014.

51. Swanson B.N. Medical use of dimethyl sulfoxide (DMSO). Review Clinical and Basic Pharmacology. 1985; 5(1-2): 1-33.

52. Brobyn R.D. The human toxicology of dimethyl sulfoxide. Annals of the New York Academy of Sciences. 1975; 243: 497-506.

53. Marren K. Dimethyl sulfoxide: an effective penetration enhancer for topical administration of NSAIDs. Physician and Sportsmedicine. 2011; 39(3): 75-82.

54. Jacob, S.W. and Wood D.C. Dimethyl sulfoxide (DMSO) toxicology, pharmacology, and clinical experience. The American Journal of Surgery. 1967; 114(3): 414-426.

55. Jacob, S.W., Bischel M., and Herschler R.J., Dimethyl sulfoxide (dmso): a new concept in pharmacotherapy. Current Therapuetic Research-Clinical and Experiment. 1964; 6: 134-135.

56. Singhvi G. and Singh M., Review: In vitro drug release characterization models. International Journal of Pharmaceutical Studies and Research. 2011; 2: 77-84.

57. Jouyban, A., Fakhree M.A., and Shayanfar A., Review of pharmaceutical applications of N-methyl-2-pyrrolidone. Journal of Pharmacy and Pharmaceutical Sciences. 2010; 13(4): 524-35.

58. Godavarthy, S.S., Yerramsetty K.M., Rachakonda V.K., Neely B.J., Madihally S.V., Robinson Jr R.L., Gasem K.A.M. Design of improved permeation enhancers for transdermal drug delivery. Journal of Pharmaceutical Sciences. 2009; 98(11): 4085-4099.

59. Harreus A.L., Backes R., Eichler J.-O., Feuerhake R., Jäkel C., Mahn U., Pinkos R. and Vogelsang R. 2-Pyrrolidone. Ullmann's Encyclopedia of Industrial Chemistry. 2011.

60. Sasaki H., Kojima M., Nakamura J., Shibasaki J. Acute toxicity and skin irritation of pyrrolidone derivatives as transdermal penetration enhancer. Chemical & Pharmaceutical Bulletin. 1990; 38(8): 2308-2310.

61. Sasaki H., Kojima M., Mori Y., Nakamura J., Shibasaki J. Enhancing effect of pyrrolidone derivatives on transdermal penetration of 5-fluorouracil,

triamcinolone acetonide, indomethacin, and flurbiprofen. Journal of Pharmaceutical Sciences. 1991; 80(6): 533-538.

62. Srinath S., Management of periodontal disease with doxycycline: an update. International Journal of Pharmaceutical and Clinical Research. 2015; 7: 252-255.

63. Sandor G.K., Low D.E., Judd P.L., Davidson R.J. Antimicrobial treatment options in the management of odontogenic infections. Journal of the Canadian Dental Association. 1998; 64(7): 508-514.

64. Garrett S., Johnson L., Drisko C.H., Adams D.F., Bandt C., Beiswanger B., Bogle G., Donly K., Hallmon W.W., Hancock E.B., Hanes P., Hawley C.E., Kiger R., Killoy W., Mellonig J.T., Polson A., Raab F.J., Ryder M., Stoller N. H., Wang H. L., Wolinsky L.E., Evans G. H., Harrold C.Q., Arnold R.M., Southard G.L., et al., Two multi-center studies evaluating locally delivered doxycycline hyclate, placebo control, oral hygiene, and scaling and root planing in the treatment of periodontitis. Journal of Periodontology. 1999; 70(5): 490-503.

65. Gibson W.A., Antibiotics and Periodontal Disease: A selective review of the literature. The Journal of the American Dental Association. 1982; 104(2): 213-218.

66. Collins J.F. Effect of vancomycin on plaque after periodontal surgery. Journal of Dental Research. 1970; 49(6):1478-1480.

67. Kaslick R.S., Tuckman M.A., and Chasens A.I., Effect of topical vancomycin on plaque and chronic gingival inflammation. Journal of Periodontology. 1973; 44(6): 366-368.

68. Rams T.E., Feik D., Mortensen J.E., Degener J.E., van Winkelhoff A.J. Antibiotic susceptibility of periodontal Enterococcus faecalis. Journal of Periodontology. 2013; 84(7): 1026-1033.

69. DePaola P.F., Jordan H.V., and Soparkar P.M., Inhibition of dental caries in school children by topically applied vancomycin. Archives of Oral Biology. 1977; 22(3): 187-191.

70. Seçmeler Ö. and Galanakis C.M. Chapter 8 - Olive fruit and olive oil, in innovations in traditional foods, C.M. Galanakis, Editor. 2019, Woodhead Publishing.193-220.

71. Budiyanto A., Ahmed N.U., Wu A., Bito T., Nikaido O., Osawa T., Ueda M., Ichihashi M. Protective effect of topically applied olive oil against photocarcinogenesis following UVB exposure of mice. Carcinogenesis. 2000; 21(11): 2085-2090.

72. Shanbhag V.K.L. Oil pulling for maintaining oral hygiene - a review. Journal of Traditional and Complementary Medicine. 2016; 7(1): 106-109.

73. Singla N., Acharya S., Martena S., Singla R. Effect of oil gum massage therapy on common pathogenic oral microorganisms - a randomized controlled trial. Journal of Indian Society of Periodontology. 2014; 18(4): 441-446.

74. Phaechamud, T., Lertsuphotvanit N., and Praphanwittaya P., Viscoelastic and thermal properties of doxycycline hyclate-loaded bleached shellac in situ-forming gel and –microparticle. Journal of Drug Delivery Science and Technology. 2018; 44: 448-456.

75. Chaicharoenpong C. and Petsom A., Chapter 132 - Use of tea (Camellia oleifera Abel.) seeds in human health, in nuts and seeds in health and disease prevention,

Preedy V.R., Watson R.R., and Patel V.B., Editors. 2011, Academic Press: San Diego. 1115-1122.

76. Luo S.-Z., Hu X.-F., Pan L.-H., Zheng Z., Zhao Y.-Y., Cao L.-L., Pang M., Hou Z.-G., Jiang S.-T., Preparation of camellia oil-based W/O emulsions stabilized by tea polyphenol palmitate: Structuring camellia oil as a potential solid fat replacer. Food Chemistry. 2019; 276: 209-217.

77. Miura D., Kida Y., and Nojima H., Camellia oil and its distillate fractions effectively inhibit the spontaneous metastasis of mouse melanoma BL6 cells. Federation of European Biochemical Societies Letters. 2007; 581(13): 2541-2548.

78. Estevinho L.M., Carmen Salinero X.F., Mansilla J.P., Vela P., Saínz M.J., Vázquez-Tato M.P., Seijas J.A. Antimicrobial properties of camellia oleifera oil. in 16th International Electronic Conference on Synthetic Organic Chemistry (ECSOC-16). 2012.

79. Xiao, X., He L., Chen Y., Wu L., Wang L., and Liu Z., Anti-inflammatory and antioxidative effects of Camellia oleifera Abel components. Future Medicinal Chemistry. 2017; 9(17): 2069-2079.

80. Do, M.P., Neut C., Metz H., Delcourt E., Siepmann J., Mäder K., Siepmann F. Mechanistic analysis of PLGA/HPMC-based in-situ forming implants for periodontitis treatment. European Journal of Pharmaceutics and Biopharmaceutics. 2015; 94: 273-283.

81. Lin X., Li X., and Lin X., A review on applications of computational methods in drug screening and design. Molecules, 2020. 25(6): 1375.

82. Kalinin, S.V., et al., Gaussian process analysis of electron energy loss spectroscopy data: multivariate reconstruction and kernel control. Computational Materials. 2021; 7(1):154.

83. Friesecke G. and Theil F. Molecular geometry optimization, models, in encyclopedia of applied and computational mathematics. Engquist B., Editor. 2015. Springer Berlin Heidelberg: Berlin, Heidelberg. 951-957.

84. Blake R. The architecture of nuclear binding energy. Physics Procedia. 2011; 22: 40-55.

85. Dash S., Murthy P.N., Nath L., Chowdhury P.. Kinetic modeling on drug release from controlled drug delivery systems. Acta Poloniae Pharmaceutica. 2010; 67(3): 217-223.

86. 5 - Mathematical models of drug release, in strategies to modify the drug release from pharmaceutical systems, Bruschi M.L., Editor. 2015, Woodhead Publishing. 63-86.

87. Sarker Apu A., Pathan A., Kibria G., Jalil R.-U. In vitro release kinetic study of theophylline from Eudragit RS PO and Eudragit RL PO matrix tablets. Dhaka University Journal of Pharmaceutical Sciences, 2010. 8(1) 1-6

88. Zuo J., Gao Y., Bou-Chacra N., Löbenberg R., Evaluation of the DDSolver software applications. Biomed Research International. 2014; 2014: 204925

89. National center for biotechnology information. PubChem compound summary for CID 54685920, Doxycycline hydrochloride. https://pubchem.ncbi.nlm.nih.gov/compound/Doxycycline-hydrochloride. Accessed June 10, 2022.

90. Loll P.J., Bevivino A.E., Korty B.D., Axelsen P.H. Simultaneous recognition of a carboxylate-containing ligand and an intramolecular surrogate ligand in the crystal

structure of an asymmetric vancomycin dimer. Journal of the American Chemical Society, 1997. 119(7): 1516-1522.

91. National center for biotechnology information. PubChem compound summary for CID 679, Dimethyl sulfoxide. https://pubchem.ncbi.nlm.nih.gov/compound/Dimethyl-sulfoxide. Accessed June 10, 2022.

92. National center for biotechnology information. PubChem compound summary for CID 962, Water. https://pubchem.ncbi.nlm.nih.gov/compound/Water. Accessed June 10, 2022.

93. Blackstock J.C., CHAPTER 2 - The physical chemistry of aqueous systems. Guide to Biochemistry, Blackstock J.C., Editor. 1989, Butterworth-Heinemann. pp. 11-19.

94. Eggert F.M., Drewell L., Bigelow J.A., Speck J.E., Goldner M. The pH of gingival crevices and periodontal pockets in children, teenagers and adults. Archives of Oral Biology. 1991; 36(3): 233-238.

95. Galgut P.N., The relevance of pH to gingivitis and periodontitis. Journal of the International Academy of Periodontology. 2001; 3(3): 61-67.

96. Jantratid E., Strauch S., Becker C., Dressman J.B., Amidon G.L., Junginger H.E., Kopp S., Midha K.K., Shah V.P., Stavchansky S., Barends D.M. Biowaiver monographs for immediate release solid oral dosage forms: Doxycycline hyclate. Journal of Pharmaceutical Sciences. 2010; 99(4): 1639-1653.

97. Redelsperger I.M., Taldone T., Riedel E.R., Lepherd M.L., Lipman N.S., Wolf F.R. Stability of doxycycline in feed and water and minimal effective doses in tetracycline-inducible systems. Journal of the American Association for Laboratory Animal Science. 2016; 55(4): 467-474.

98. Phaechamud T., Jantadee T., Mahadlek J., Charoensuksai P., Pichayakorn W. Characterization of antimicrobial agent loaded Eudragit RS solvent Exchange-induced in situ forming gels for periodontitis treatment. AAPS PharmSciTech. 2017; 18(2): 494-508.

99. Karmakar G., Ghosh P., and Sharma B.K., Chemically modifying vegetable oils to prepare green lubricants. Lubricants. 2017; 5(4): 44.

100. Chantadee T., Santimaleeworagun W., Phorom Y., Phaechamud T. Mixed solvent-lauric acid solvent-exchange induced in situ forming gel. Key Engineering Materials. 2019; 819: 195-201.

101. Camargo, J.A., Sapin A., Nouvel C., Daloz D., Leonard M., Bonneaux F., Six J.-I., Maincent P. Injectable PLA-based in situ forming implants for controlled release of Ivermectin a BCS Class II drug: solvent selection based on physico-chemical characterization. Drug Development and Industry Pharmacy. 2013; 39(1): 146-155.

102. Wei W., Cheng H., Cao X., Zhang X., and Feng F. Triacylglycerols of camellia oil: composition and positional distribution of fatty acids. European Journal of Lipid Science and Technology. 2016; 118(8): 1254-1255.

103. Jose B.M., and Cubaud T., Role of viscosity coefficients during spreading and coalescence of droplets in liquids. Physical Review Fluids. 2017; 2(11): 111601.

104. Dave V.S., Fahmy R.M., Bensley D., Hoag S.W. Eudragit($^{\circledR}$) RS PO/RL PO as rate-controlling matrix-formers via roller compaction: Influence of formulation

and process variables on functional attributes of granules and tablets. Drug Development and Industrial Pharmacy. 2012; 38(10): 1240-1253.

105. Goto S., Kawata M., Nakamura M., Maekawa K., Aoyama T. Eudragit RS and RL (acrylic resins) microcapsules as pH insensitive and sustained release preparations of ketoprofen. Journal of Microencapsulation. 1986; 3(4): 293-304.

106. de Ménorval M.A., Mir L.M., Fernández M.L., Reigada R. Effects of dimethyl sulfoxide in cholesterol-containing lipid membranes: a comparative study of experiments in silico and with cells. PLoS One. 2012; 7(7): e41733.

107. Kern W.V., Steinke P., Schumacher A., Schuster S., von Baum H., Bohnert J.A. Effect of 1-(1-naphthylmethyl)-piperazine, a novel putative efflux pump inhibitor, on antimicrobial drug susceptibility in clinical isolates of Escherichia coli. Journal of Antimicrobial Chemotherapy. 2006; 57(2): 339-343.

108. McPherson J.S., Dixon S.A., Townsend R., Vandewalle K.S. Effect of needle design on pain from dental local anesthetic injections. Anesthesia Progress. 2015; 62(1): 2-7.

109. You D., Wang X., Cheng X., Jiang X. Friction modeling and analysis of injection process in squeeze casting. Journal of Materials Processing Technology. 2017; 239: 42-51.

110. Sholapurkar A., Sharma D., Glass B., Miller C., Nimmo A., Jennings E. Professionally delivered local antimicrobials in the treatment of patients with periodontitis-a narrative review. Dentistry Journal (Basel). 2020; 9(1): 1-19

111. Hellmann C., Treat N.D., Scaccabarozzi A.D., Razzell Hollis J., Fleischli F.D., Bannock J.H., de Mello J., Michels J.J., Kim J.-S. and Stingelin N. Solution processing of polymer semiconductor: Insulator blends—Tailored optical properties through liquid–liquid phase separation control. Journal of Polymer Science Part B: Polymer Physics. 2015; 53(4): 304-310.

112. Khaing E.M., Intaraphairot T., Chuenbarn T., Chantadee T., Phaechamud T. Natural resin-based solvent exchange induced in-situ forming gel for vancomycin HCl delivery to periodontal pocket. Materials Today: Proceedings. 2021; 47: 3585-3593.

113. Jain N., Lai P.C., and Walters J.D. Effect of gingivitis on azithromycin concentrations in gingival crevicular fluid. Journal of Periodontology. 2012; 83(9): 1122-1128.

114. Kugler, S., Ossowicz P., Malarczyk-Matusiak K., Wierzbicka E. Advances in Rosin-Based Chemicals: The latest recipes, applications and future trends. Molecules. 2019; 24(9): 1-52

115. Mathew M. and Gupta V.D. Stability of vancomycin hydrochloride solutions at various pH values as determined by high-performance liquid chromatography. Drug Development and Industrial Pharmacy. 1995; 21(2): 257-264.

116. Chantadee T., Santimaleeworagun W., Phorom Y., Chuenbarn T., Phaechamud T., Vancomycin HCl-loaded lauric acid in situ-forming gel with phase inversion for periodontitis treatment. Journal of Drug Delivery Science and Technology. 2020; 57: 101615.

117. Godet, M., Simar J., Closset M., Hecq J.-D., Braibant M., Soumoy L., Gillet P., Jamart J., Bihin B. and Galanti L. Stability of concentrated solution of vancomycin hydrochloride in syringes for intensive care units. Pharmaceutical Technology in Hospital Pharmacy. 2018; 3(1): 23-30.

118. de Oliveira M.A.L. Chapter 59 - Determination of olive oil acidity, in olives and olive oil in health and disease prevention, Preedy V.R. and Watson R.R., Editors. 2010, Academic Press: San Diego. pp. 545-552.

119. Marmur, A., Marmur A., Della C., Stefano V., Alidad S., Jaroslaw A., Drelich W. Contact angles and wettability: towards common and accurate terminology. Surface Innovations. 2017; 5: 1-24.

120. Behrens S.H., and Grier D.G., The charge of glass and silica surfaces. The Journal of Chemical Physics. 2001; 115(14): 6716-6721.

121. Hauner I.M., Deblais A., Beattie J.K., Kellay H., Bonn D. The dynamic surface tension of water. The Journal of Physical Chemistry Letters. 2017; 8(7): 1599-1603.

122. O'Connell J.P. and Prausnitz J.M. Intermolecular forces in water vapor. Industrial & Engineering Chemistry Fundamentals. 1969; 8(3): 453-460.

123. Pope D.C. and Oliver W.T. Dimethyl sulfoxide (DMSO). Canadian Journal of Comparative Medicine and Veterinary Science. 1966; 30(1): 3-8.

124. Russo S. and Casazza E. 4.14 - Ring-opening polymerization of cyclic amides (lactams). Polymer Science: A Comprehensive Reference, Matyjaszewski K. and Möller M., Editors. 2012, Elsevier: Amsterdam. 331-396.

125. Kronberg B., Holmberg K., and Lindman B. Surface and interfacial tension. Surface Chemistry of Surfactants and Polymers. Holmberg K. and Lindman B., Editors. 2014, John Wiley & Sons, Ltd.: United Kingdom. pp. 231-249.

126. Phaechamud, T., Mahadlek J., and Charoenteeraboon J. Texture and topography analysis of doxycycline hyclate thermosensitive systems comprising zinc oxide. Indian Journal of Pharmaceutical Sciences. 2013; 75: 385-392.

127. National center for biotechnology information. PubChem Compound Summary for CID 12025, 2-Pyrrolidinone. https://pubchem.ncbi.nlm.nih.gov/compound/2-Pyrrolidinone. Accessed June 10, 2022.

128. Satturwar P.M., Fulzele S.V., and Dorle A.K. Evaluation of polymerized rosin for the formulation and development of transdermal drug delivery system: A technical note. AAPS PharmSciTech. 2005; 6(4): E649-E654.

129. Ji, Y., Paus R., Prudic A., Lübbert C., Sadowski G. A Novel approach for analyzing the dissolution mechanism of solid dispersions. Pharmaceutical Research. 2015; 32(8): 2559-2578.

130. Wang, D., Yang D., Huang C, Huang Y, Yang D, Zhang H., Liu Q., Tang T., Gamal El-Din M., Kemppi T., Perdicakis B., Zeng H. Stabilization mechanism and chemical demulsification of water-in-oil and oil-in-water emulsions in petroleum industry: A review. Fuel, 2021; 286: 119390.

VITA

NAME   Tiraniti Chuenbarn

DATE OF BIRTH   27 April 1991

PLACE OF BIRTH   Ratchaburi, Thailand

PUBLICATION   1. Chuenbarn T., Phaechamud T. Bleached shellac in situ forming micro-particle fabricated with different oils as antibacterial delivery system for periodontitis treatment. Mater. Today. Proceedings 2021; 47(12): 3546-3553. https://doi.org/10.1016/j.matpr.2021.03.549
2. Chuenbarn T., Chantadee T., Phaechamud T., Doxycycline hyclate-loaded Eudragit® RS PO in situ-forming microparticles for periodontitis treatment. J. Drug Deliv. Sci. Technol., 2022; 71: 103294. https://doi.org/10.1016/j.jddst.2022.103294.
3. Chuenbarn T., Sirirak J., Tuntarawongsa S., Okonogi S., Phaechamud T.. Design and Comparative Evaluation of Vancomycin HCl-Loaded Rosin-Based In Situ Forming Gel and Microparticles. Gels. 2022; 8(4): 231. https://doi.org/10.3390/gels8040231